



Université du Québec
à Rimouski

**EFFETS DU CHANGEMENT GLOBAL SUR LES
PARTICULES EXOPOLYMÉRIQUES
TRANSPARENTES AU SEIN DE L'ESTUAIRE
MARITIME DU SAINT-LAURENT**

Mémoire présenté
dans le cadre du programme de maîtrise en océanographie
en vue de l'obtention du grade de maître ès sciences

PAR
© HOUSSEM GAALOUL

Novembre 2017

Composition du jury :

Christian Nozais, président du jury, Université du Québec à Rimouski

Gustavo Ferreyra, directeur de recherche, Université du Québec à Rimouski

Jean-Pierre Gagné, co-directeur de recherche, Université du Québec à Rimouski

Jonathan Gagnon, co-directeur de recherche, Université du Québec à Rimouski

Christine Michel, examinatrice externe, Pêches et Océans Canada

Dépôt initial Septembre 2017

UNIVERSITÉ DU QUÉBEC À RIMOUSKI
Service de la bibliothèque

Avertissement

La diffusion de ce mémoire ou de cette thèse se fait dans le respect des droits de son auteur, qui a signé le formulaire « *Autorisation de reproduire et de diffuser un rapport, un mémoire ou une thèse* ». En signant ce formulaire, l'auteur concède à l'Université du Québec à Rimouski une licence non exclusive d'utilisation et de publication de la totalité ou d'une partie importante de son travail de recherche pour des fins pédagogiques et non commerciales. Plus précisément, l'auteur autorise l'Université du Québec à Rimouski à reproduire, diffuser, prêter, distribuer ou vendre des copies de son travail de recherche à des fins non commerciales sur quelque support que ce soit, y compris l'Internet. Cette licence et cette autorisation n'entraînent pas une renonciation de la part de l'auteur à ses droits moraux ni à ses droits de propriété intellectuelle. Sauf entente contraire, l'auteur conserve la liberté de diffuser et de commercialiser ou non ce travail dont il possède un exemplaire.

REMERCIEMENTS

Je remercie mon superviseur Gustavo Ferreyra, et mes cosuperviseurs, Jonathan Gagnon et Jean-Pierre Gagné pour tout le temps qu'ils m'ont accordé durant ces quatres années de maîtrise. Leur disponibilité, leur patience et leur soutien fut une inspiration et m'a grandement aidé à toujours aller de l'avant malgré les problèmes rencontrés. Merci à l'équipe de la mission front 2013: Cédric Chavanne, Suzanne Roy, Julien Robitaille, Kevin Osterheld, Robin Accot et Habiba Bouakba. Merci à toute l'équipe de la mission acidification: Jory cabrol, Maurice Levasseur, Jean-Eric Tremblay, Chloé Martias et Qiang Chen. Un merci aux membres ayant participé à l'expérience en mésocosme: Marjolaine Blais, Gustavo Ferreyra, Michel Gosselin, Mohamed Lemlih, Claire Lix, Sonia Michaud, Alfonso Mucci, Michael Scarratt, Liliane St-Amand, Michel Starr et Gesche Winkler. Je remerci les techniciens: Steven Ouellet, Mathieu Babin, Pascal Rioux, Mélanie Simard, Nathalie Morin et Dominique Lavallée de m'avoir beaucoup aidé dans les travaux de laboratoire. Sans oublier Gilles Desmeules et Bruno Cayouette durant l'échantillonnage. Merci à l'administration de l'ISMER Brigitte Dubé, Marielle Lepage et Karine Lemarchand et spécialement Martine Belzile. Merci à Christian Nozais d'avoir accepté le titre de président du jury ainsi qu'à Christine Michel, évaluaterice externe de ce mémoire. J'aimerais remercier Québec-Océan, l'ISMER, le FRQNT. Merci à tous mes amis et spécialement Philippe Klotz. Finalement, je dédie ce mémoire à mes parents Mohamed Gaaloul et Saïda Kalaï.

RESUME

Ce mémoire étudie les particules exopolymériques transparentes (TEP, en anglais) au sein de l'estuaire maritime du Saint-Laurent (LSLE, en anglais). Il est composé de deux chapitres, l'un correspondant à une étude de terrain et le deuxième à un travail expérimental à l'aide d'un système de mésocosmes. Dans le premier de ces volets, la distribution spatiale de la concentration des TEP a été déterminée dans la couche de surface et la couche profonde de deux zones du LSLE: une zone de remontée des eaux profondes et une zone de front. La concentration moyenne des TEP dans la couche de surface des deux zones était $89,77 \pm 48,84 \mu\text{g}$ équivalent en gomme de Xanthan (XG eq, en anglais) par litre). Dans la couche profonde la concentration moyenne des TEP était égale à $33,59 \pm 21,12 \mu\text{g XG eq L}^{-1}$. La zone de remontée des eaux profondes était caractérisée par la dominance de matière organique d'origine terrestre, une concentration élevée en nutriments surtout en couche profonde, et un gradient des paramètres environnementaux situé au niveau de la tête du chenal Laurentien. Les TEP à ce niveau, ont montré aussi un gradient de concentration. La concentration des TEP la plus élevée était enregistrée au niveau de l'estuaire supérieur et du fjord du Saguenay. La zone de front était caractérisée par la rencontre entre une masse d'eau de caractère plus estuarien avec une masse d'eau de caractère plus océanique. Un flux vertical de la couche de surface vers la couche profonde semble aussi avoir été détecté par nos collaborateurs. Au niveau de la zone de front, les TEP ont montré de concentrations plus élevées au niveau de la masse d'eau de caractère estuarien. En outre, des concentrations exceptionnellement élevées en TEP ont été observées au niveau de la couche profonde de la zone de front. Aucune corrélation positive observée entre les TEP et les paramètres environnementaux des deux zones sauf les concentrations en carbone organique particulaire (POC, en anglais). Globalement, les concentrations en TEP étaient significativement ($p < 0.01$) et positivement corrélées au POC. Les TEP ont montré une contribution allant jusqu'à 82 % du POC du LSLE. Cependant, le principal contributeur au pool de POC de la couche de surface du LSLE variait entre les TEP, le phytoplacton et les détritus, dépendamment de la distribution spatiale. Comparées à d'autres environnements aquatiques, les ratios TEP/POC et TEP/chlorophylle *a* (chl *a*) du LSLE étaient parmi les plus élevées.

La partie expérimentale de cette recherche avait l'objectif d'évaluer les effets de l'augmentation de l'acidification et de la température sur les TEP du LSLE. Cinq valeurs de pH allant de 8,0 à 7,2 ont été testées dans deux niveaux de température (10 °C et 15 °C) durant un bloom de diatomés dominé par *Skeletonema costatum*. Nos résultats ont suggéré qu'une augmentation de l'acidité engendrée par l'augmentation de la concentration dissoute

en CO₂ résulte en un plus faible taux de croissance du phytoplancton et une augmentation du taux d'assimilation du CO₂ qui se manifeste en un ratio TEP/POC plus élevé. Une diminution de 0,2 unités du pH a entraîné une diminution moyenne de $0,03 \pm 0,07 \text{ d}^{-1}$ dans le taux de croissance spécifique du phytoplancton et une diminution moyenne de $86,28 \pm 19,61 \text{ } \mu\text{gC L}^{-1}$ et de $119 \pm 6,03 \text{ } \mu\text{gC L}^{-1}$ dans les concentrations des TEP et du POC enregistrés au maximum de la chl *a*, respectivement. Une diminution de 0,2 unité du pH a engendré une augmentation moyenne de $0,20 \text{ } \mu\text{g L}^{-1}$ dans la concentration totale en carbohydrates normalisée à la biomasse du phytoplancton enregistrés au maximum de chl *a*. L'augmentation de la température a eu un effet positif sur la biomasse phytoplanctonique, la concentration en carbohydrates et un effet négatif sur les ratios TEP/phytoplancton et TEP/POC. La hausse de la température a suggéré une accélération du taux de croissance du phytoplancton ce qui a induit une biomasse phytoplanctoniques plus élevée. Ceci a résulté en une concentration plus importante en monosaccharides dont la majorité a probablement demeurée dans la fraction dissoute en raison d'une température plus élevée qui a probablement ralenti ou bloqué la formation des TEP. L'effet de l'augmentation de la température et de l'acidification demeure uncertain, suggérant une adaptation du phytoplancton des régions côtières face à ces changements.

Mot clés: LSLE, TEP, POC, distribution spatiale, phytoplancton, pH et température

ABSTRACT

A study of transparent exopolymeric particles (TEP) in the Lower St-Lawrence estuary (LSLE) is presented in this work. It consists of two chapters, one corresponding to a field study and the second to experimental work using a mesocosm system. In the first of these components, the spatial distribution of TEP concentration was determined in the surface layer and the deep layer of an upwelling area and a front area of the LSLE. The mean TEP concentration in the surface layer of both areas was $89.77 \pm 48.84 \mu\text{g Xanthan gum equivalent (XG eq) per liter}$. In the deep layer, the mean TEP concentration was $33.59 \pm 21.12 \mu\text{g XG eq L}^{-1}$. The upwelling area was characterized by the dominance of organic matter of terrestrial origin, a high concentration of nutrients especially in the deep layer, and a gradient of the environmental parameters located at the head of the Laurentian trough. TEP at this level showed also a concentration gradient. The highest TEP concentrations were recorded in the higher estuary and the Saguenay fjord. Fronts detected in the front area were formed by the contact between an estuarine water mass and an oceanic water mass. TEP showed higher concentrations at the estuarine water mass than the oceanic water mass. In addition, high exceptional concentrations of TEP were observed at the deep layer of the front area. Overall, TEP concentrations showed no significant correlation with the environmental parameters except particulate organic carbon (POC) concentrations. TEP were significantly ($p < 0.01$) and positively correlated to POC. TEP exhibited a contribution of up to 82% of the POC in the LSLE. However, the main contributor to the POC of the surface layer varied between TEP, phytoplacton and detritus, depending on the spatial distribution. Compared with other aquatic environments, the LSLE presented within the highest TEP/POC and TEP/chlorophyll *a* ratios.

The experimental part of this research aimed to evaluate the effects of increased acidification and temperature on TEP in the LSLE. Five pH values ranging from 8.0 to 7.2 were tested in two temperature levels (10 °C and 15 °C) during bloom of the diatom *a Skeletonema costatum*. A decrease of 0.2 pH units resulted in an average decrease of $0.03 \pm 0.07 \text{ d}^{-1}$ in the phytoplankton specific growth rate and an average decrease of $86.28 \pm 19.61 \mu\text{gC L}^{-1}$ and of $119 \pm 6.03 \mu\text{gC L}^{-1}$ in the concentrations of TEP and POC recorded at maximum of chl *a*, respectively. However, our results have suggested that an increase in the acidity caused by the increase in the dissolved CO₂ concentration results in a lower phytoplankton growth rate and an increase in the CO₂ assimilation rate which might be manifested in a higher TEP/POC ratio. Moreover, a decrease of 0.2 pH units resulted in an average increase of $0.20 \mu\text{g L}^{-1}$ in the total carbohydrate concentration normalized to phytoplankton biomass. The increase of the temperature had a positive effect on

phytoplankton biomass, carbohydrate concentration and a negative effect on TEP/phytoplankton and TEP/POC ratios. The rise in temperature suggested an acceleration of the growth rate of phytoplankton which probably induced a higher biomass resulting in a higher concentration of monosaccharides. Mostly of these monosaccharides have probably remained in the dissolved fraction due to a higher temperature that may have decelerate the formation of TEP. The effect of increasing temperature and acidification remains uncertain suggesting the adaptation of phytoplankton from coastal regions to these global changes.

Key words: LSLE, TEP, POC, spatial distribution, phytoplankton, pH and temperature.

TABLE DES MATIERE

REMERCIEMENTS	vii
RESUME	viii
ABSTRACT.....	x
TABLE DES MATIÈRES.....	xii
LISTE DES FIGURES	xvi
LISTE DES TABLEAUX.....	vi
LISTE DES ABRÉVIATIONS	xx
INTRODUCTION GÉNÉRALE	1
1. CONTINUUM DU CARBONE ORGANIQUE DANS LES OCÉANS	1
2. DÉFINITION DES GELS MARINS	2
3. MÉCANISMES DE FORMATIONS DES GELS MARINS	2
4. LES PARTICULES EXOPOLYMÉRIQUES TRANSPARENTES.....	3
4.1. Origine et rôle.....	3
4.2. Caractéristiques physiques et chimiques des TEP	4
4.3. Interaction entre les TEP et des paramètres biologiques.....	5
5. PROBLÉMATIQUES ET OBJECTIFS.....	6
5.1. Distribution spatiale des TEP au sein de l'estuaire maritime du Saint-Laurent.....	6
5.1.1. Les TEP dans les estuaires	6
5.1.2. L'estuaire du Saint-Laurent, un réservoir important de carbone organique.....	7
5.1.3. Les TEP dans l'estuaire maritime du Saint-Laurent.....	8
5.2. Effet du changement global sur les TEP	9
SPRING SPATIAL DISTRIBUTION OF TRANSPARENT EXOPOLYMERIC PARTICLES WITHIN TWO KEY REGIONS OF THE LOWER ST-LAWRENCE ESTUARY: UPWELLING AND FRONT.....	12
RESUME.....	13

ABSTRACT.....	14
1.1. INTRODUCTION.....	15
1.2. MATERIAL AND METHODS.....	17
1.2.1. STUDY AREAS AND SEAWATER SAMPLING.....	17
1.2.2. ENVIRONMENTAL PARAMETERS MEASURMENTS.....	19
1.2.2.1. Salinity and temperature	19
1.2.2.2. Nutrients concentrations.....	19
1.2.2.3. Chlorophyll a.....	19
1.2.2.4. Determination of the pH.....	20
1.2.3. DETERMINATION OF TEP CONCENTRATION.....	21
1.2.4. PARTICULATE ORGANIC CARBON QUANTIFICATION AND STABLE ISOTOPES	21
1.2.5. PHYTOPLANKTON DENSITY	22
1.2.5.1. Phytoplankton carbon concentration estimation	23
1.2.6. BACTERIAL DENSITY	23
1.2.6.1. Bacterial carbon estimation.....	24
1.2.7. STATISTICAL ANALYSIS.....	24
1.3. RESULTS.....	25
1.3.1. ENVIRONMENTAL PARAMETERS.....	25
1.3.1.1. Salinity	25
1.3.1.2. Temperature	25
1.3.1.3. pH	25
1.3.1.4. Nutrients concentrations.....	26
1.3.1.5. Chlorophyll a.....	27
1.3.1.6. Stables isotopes	27
1.3.2. TRANSPARENT EXOPOLYMERIC PARTICLES.....	28
1.3.3. PHYTOPLANKTON DENSITY	29
1.3.4. BACTERIAL DENSITY	31
1.3.5. PARTICULATE ORGANIC CARBON	31
1.3.6. CARBON CONTRIBUTION ESTIMATION	32
1.4. DISCUSSION	35
1.4.1. TWO CONTRASTNG AREAS OF THE LSLE	35
1.4.2. TEP SPATIAL DISTRIBUTION IN THE UPWELLING AND THE FRONT AREAS	38
1.4.3. TEP AND POC CORRELATION.....	42
1.4.4. SPATIAL DISTRIBUTION OF THE CARBON CONTRIBUTION OF TEP TO POC	43

EFFECTS OF GLOBAL CHANGE ON TRANSPARENT EXOPOLYMERIC PARTICLES DURING A MESOCOSM SUB-ARCTIC DIATOM BLOOM.....	47
RESUME.....	48
ABSTRACT.....	49
1. 1. INTRODUCTION.....	50
1.2. MATERIAL AND METHODS	52
1.2.1. Experimental design	52
1.2.2. TEP CONCENTRATION DETERMINATION	55
1.2.4. PARTICULATE ORGANIC CARBON QUANTIFICATION	56
1.2.5. PHYTOPLANKTON DENSITY	56
1.2.6. BACTERIAL DENSITY	57
1.2.7. STATISTICAL ANALYSIS	58
1.3. RESULTS	58
1.3.1. TRANSPARENT EXOPOLYMERIC PARTICLES	60
1.3.3.1. Monitoring of TEP carbon concentration.....	60
1.3.3.2. Effect of pH decrease	61
1.3.3.3. Effect of temperature increase.....	61
1.3.3.3. Combined effect of pH decrease and temperature increase.....	61
1.3.2. PHYTOPLANKTON BIOMASS.....	62
1.3.2.1. Bloom developement	62
1.3.2.2. Effect of pH decrease	62
1.3.2.3. Effect of temperature increase	65
1.3.2.4. Combined effect of pH decrease and temperature increase.....	65
1.3.3. BACTERIAL BIOMASS	66
1.3.3.1. Monitoring of bacteria biomass.....	66
1.3.3.2. Effect of pH decrease	66
1.3.3.3. Effect of temperature increase	67
1.3.3.4. Combined effect of pH decrease and temperature increase.....	67
1.3.4. PARTICULATE ORGANIC CARBON	68
1.3.4.1. Temporal monitoring of POC.....	68
1.3.4.2. Effect of pH decrease	69
1.3.4.3. Effect of temperature increase	69
1.3.4.4. Combined effect of pH decrease and temperature increase	70
1.3.5. CARBOHYDRATE CHEMICAL COMPOSITION	71
1.3.5.1. Total carbohydrate concentration	71
1.3.5.2. Monosaccharide concentrations and contributions to the total carbohydrate	72
1.3.5.2.1. Glucose	73
1.3.5.2.2. Arabinose and mannose	73
1.3.5.2.3. Galactose.....	74
1.3.4.2.4. Fructose.....	76
1.3.4.2.5. Ribose	76
1.3.4.2.6. Xylose	77

1.4. DISCUSSION	77
1.4.1. PHYTOPLANKTON RESPONSE	77
1.4.2. BACTERIA RESPONSE.....	80
1.4.3. TRANSPARENT EXOPOLYMERIC PARTICLES RESPONSE.....	81
1.4.4. PARTICULATE ORGANIC CARBON RESPONSE.....	84
1.4.5. CARBOHYDRATE CHEMICAL COMPOSITION	88
CONCLUSION GÉNÉRALE	93
PERSPECTIVES	97
RÉFÉRENCES BIBLIOGRAPHIQUES.....	99

LISTE DES FIGURES

Chapitre 1

- Figure. 1** Map showing the geographical positions of the sampled stations in the area of upwelling (1, 2, 3 at the HLT (head of the Laurentian trough) zone, the HE (higher estuary), the Fjord (Fjord) and the LE (lower estuary)) and the area of front. First front (F1) was sampled at the two sides of the front (F1- and F1+), while the second front (F2) was sampled at the two sides (F2- and F2+) and the center (F1C1 and F1C2).....18
- Figure. 2** The means of isotopic ratios of $\delta^{15}\text{N}$ and $\delta^{13}\text{C}$ observed in surface layer (SL) and in deep layer (DL) of area 1 (A1) and area 2 (A2).27
- Figure. 3** Spatial distribution of transparent exopolymeric particles (TEP) in the areas 1 and the area 2. Green bars show data from the surface layer (SL) and black bars represent the deep layer (DL) measurements. Annotation: Fjd: fjord, HE: higher estuary and LE: lower estuary.....28
- Figure. 4** Spatial distributions of phytoplankton cell density in both, areas 1 (A1) and area 2 (A2). Three size classes of phytoplankton were considered: a) picophytoplankton ($< 0.2 \mu\text{m}$) (a), nanophytoplakton ($2-20 \mu\text{m}$) (b) and microphytoplankton ($>20 \mu\text{m}$) (c). Green bars represent data from the surface layer (SL), while black and white bars correspond to deep layer (DL). Annotation: Fjd: fjord, HE: higher estuary and LE: lower estuary.....30
- Figure. 5** Spatial distribution of particulate organic carbon (POC) concentrations ($\mu\text{g L}^{-1}$) in the area1 1 and the area 2. Green bars show data from the surface layer (SL) and black bars represent deep layer (DL). Annotation: Fjd: fjord, HE: higher estuary and LE: lower estuary.....32
- Figure. 6** Linear regression between particulate organic carbon (POC) and estimated POC (estim_POC) concentrations in the surface layer (SL) and the deep layer (DL) of both areas ($r= 0.81$; $P< 0.01$).....33
- Figure. 7** Spatial distribution of the relative contribution of the estimated carbon concentrations from phytoplankton (phyto_CC), bacteria (bact_CC), transparent exopolymeric particles (TEP_CC) and other organic matter (detritus_CC) to total

particulate organic carbon (POC) at the surface layer (a) and at the deep layer (b) of the area 1 and the area 2. Annotation: Fjd: fjord, HE: higher estuary and LE: lower estuary.....**33**

Figure. 8 linear regressions between data of transparent exopolymeric particles (TEP) and particulate organic carbon (POC) obtained at the surface layer (SL) and the deep layer (DL) of the upwelling area and the front area of the LSLE. Annotation: Int of conf: interval of confidence.....**43**

Chapitre 2

Figure. 1 Map showing the location of the mesocosm experiment in relation to the Lower St-Lawrence estuary.....**53**

Figure. 2 Experimental mesocosm design. Two temperature treatments with two levels (10 °C and 15 °C, respectively) and the acidification treatment with five pH levels. pH levels were decreased by 0.2 units. The first series of 10 °C is composed by blue circles, while 15 °C is displayed by orange circles. Each pH treatment is showed in one circle. One control mesocosm was added to each series.**54**

Figure. 3 Temporal pH monitoring within the mesocosms at 10°C (a) and 15°C (b) during all the days of the experiment. The targeted pH values are showed in the legend (pH was allowed to drift in the control mesocosms).....**59**

Figure.4 Temperature (°C) in each mesocosm during all the days of the experiment.....**59**
Figure. 5 Temporal development of chlorophyll *a* concentration within the mesocosms at 10°C (a) and 15°C (b) during the experiment.....**60**

Figure. 6 Temporal variation of carbon concentration (CC) corresponding to transparent exopolymeric particles (TEP) (a), phytoplankton (b), bacteria (c) and particulate organic carbon (POC) (d) at different levels of the pH treatment and control at 10 °C and 15 °C levels for the temperature treatment (a', b', c' and d').....**63**

Figure. 7 Variations of particulate organic carbon (POC) and transparent exopolymeric particles (TEP) as a function of pH decrease at maximum of chl *a*, at 10 °C and 15 °C.....**66**

Figure. 8 The variation in the specific growth rate estimated at different pH at 10 °C and 15 °C. At (t + 6) pH in the 10 °C control was equal to 8.1, while in the 15 °C, control pH displayed 8.4. Annotation: Sp gth rate: sepcific growth rate.....**67**

Figure. 9 Variation in maximum of phytoplankton (a) and maximum of nanoplankton biomass (b) observed at different pH and controls at 10 °C and 15 °C.**68**

Figure. 10 Linear regressions between estimated particulate organic carbon (POC), defined

as the converted biological carbon biovolume and POC at 10 °C and 15 °C. The dotted line corresponds to ($r= 1$). Annotation: estm POC: estimated POC.69

Figure. 11 Variations in the concentrations of transparent exopolymeric particles carbon concentration (TEP) versus the phytoplankton carbon concentration at maximum of chl *a*, at 10 °C and 15 °C. Annotation: phyto: phytoplankton.....71

Figure 12. Variations of total carbohydrate concentrations measured at different pH and controls at 10 °C and 15 °C during sampling days.....72

Figure. 13 Monosaccharide contribution (%) to the total carbohydrates pool present at different pH and controls at 10 °C and 15 °C. Notation: Ara: Arabinose; Man: Mannose; Glc: Glucose; Fru: Fructose; Rib: Ribose; Xyl: Xylose.....75

Figure. 14 Variations in the contribution (%) of transparent exopolymeric particles (TEP) normalized to particulate organic carbon (POC) versus CO₂ increase (pH decreasing gradient values) at maximum of chl *a*, at 10 °C and 15 °C.....87

Figure. 15 Variation in total carbohydrate concentration normalized to total biomass of phytoplankton and bacteria at maximum of chl *a*, at 10 °C and 15 °C. Annotation: phyto: phytoplankton; bact: bacteria; T.carb/biomass: Total carbohydrate/phytoplankton biomass.....90

LISTE DES TABLEAUX

Chapitre 1

Table. 1 Results of the T-test analysis among areas and among layers carried out on environmental parameters measured.....**26**

Table. 2 Results of the T-test analysis among areas and among layers carried out on transparent exopolymeric particle (TEP), microphytolankton ($>20\ \mu\text{m}$) nanophytoplankton (2-20 μm) picophytoplankton ($<0.2\ \mu\text{m}$), bacteria and particulate organic carbon (POC)..**30**

Table. 3 Average and range surface layer spring (May – Juin) values of transparent exopolymeric particles (TEP $\mu\text{g XG eq L}^{-1}$), particulate organic carbon (POC $\mu\text{g L}^{-1}$) and chlorophyll (a) (chl a ; $\mu\text{g L}^{-1}$) for estuarine and marine environments. Ratios of the mean values were estimated and are showed for TEP/POC and TEP/chl a . Annotation: nd: not determined.....**40**

Chapitre 2

Table. 1 Results of linear regressions (r^2 and P values) obtained between pH decrease and carbon concentrations of phytoplankton (phyto), transparent exopolymeric particles (TEP), particulate organic carbon (POC) and for maximum values recorded at 10 °C and 15 °....**64**

Table. 2 Linear regression coefficients, signification levels (P value) and slopes of the regression between each monosaccharide concentration and gradient of pH decrease during the sampling days at 10 °C and 15 °C experiments. Notation: max: maximum.....**78**

LISTE DES ABREVIATIONS

A1: area 1

A2: area 2

Bact_CC: bacteria carbon contribution

CAM: carbon assimilation mechanism

Chl *a*: chlorophyll *a*

Det_CC: detritus carbon contribution

DL: deep layer

DOC: dissolved organic carbon

EPS: exopolymeric substances

HLT: head of the Laurentian trough

HWM: heavy water mass

LSLE: Lower St-Lawrence estuary

LWM: light water mass

POC: particulate organic carbon

Phyto_CC: phytoplankton carbon contribution

SL: Surface layer

TEP: Transparent exopolymeric particules

TEP_CC: transparent exopolymeric particles carbon contribution

XG: Xanthan gum

INTRODUCTION GENERALE

1. CONTINUUM DU CARBONE ORGANIQUE DANS LES OCÉANS

Certaines estimations de la production primaire de l'océan global ont montré que la productivité du phytoplancton ($45 - 50 \times 10^{15}$ de carbone (C) an^{-1}) est similaire à la productivité des plantes terrestres ($45 - 68 \times 10^{15}$ de carbone par an^{-1}) (Longhurst *et al.*, 1995). Le phytoplankton assure 75 % de la production de l'océan global (Falkowski et Raven, 2013). Cette production existe sous forme de cellules phytoplanctoniques ou sous forme de molécules organiques. Ces molécules incluent entre autres, les polysaccharides et les protéines. La dynamique de cette matière dans les océans est contrôlée par des cycles biogéochimiques à travers lesquels, la production primaire est exportée sous forme particulaire de la couche de surface vers tous les niveaux trophiques. La sédimentation de cette matière est précédée par un processus d'agrégation de ces composés organiques incluant la collision et l'agglomération des molécules et des particules de taille colloïdale. Ceci permet le passage de la matière de l'état dissous (quelques molécules) à l'état particulaire (résultant de l'agrégation des particules submicrométriques) pour donner naissance à des gels marins formés d'un réseau tridimensionnel (Wells et Goldberg, 1992, Kepkay, 1994). Ainsi, le carbone organique dissout (DOC, en anglais) peut s'assembler pour produire du carbone organique particulaire (POC, en anglais) tel que les macro-gels marins. Ces gels sont capables d'échanger de façon réversible entre le DOC et le POC (Verdugo *et al.*, 2004). Cet assemblage de matériaux forme des particules qui peuvent sédimerter et éventuellement séquestrer le carbone organique dans l'océan profond. La dissolution et la reminéralisation des gels marins ont des implications importantes sur la productivité de l'océan global et le cycle du carbone de notre planète.

2. DÉFINITION DES GELS MARINS

Le DOC représente dans les océans $\sim 700 \times 10^{15}$ g C organique (Verdugo., 2012). Selon des études réalisées par Benner *et al.* (1992), Stordal *et al.* (1996) et Chin *et al.* (1998), 25 % de cette biomasse ($\sim 150 \times 10^{15}$ g C) s'agrège pour former les micro-gels et 10 % forment les macro-gels marins (soit $\sim 15 \times 10^{15}$ g C ~ 25 fois la biomasse de tous les organismes marins). Ils sont très abondants dans les cultures de phytoplancton. Par définition, les gels marins sont des hydrogels de taille supérieure à 0,2 μm ou à 0,4 μm et constitués par plusieurs réseaux tridimensionnels de polymères et d'eau de mer (Verdugo *et al.*, 2004). Ces polymères proviennent principalement de substances exopolymériques (EPS, en anglais) secrétées par les cellules phytoplanctoniques ou bactériennes. Ils sont riches en molécules organiques ayant des poids moléculaires élevés (10 à 30 KDa) (Wotton, 2004). Sur le plan opérationnel, ces gels sont visualisés après coloration avec un colorant spécifique. De nombreuses études ont montré leur omniprésence et leur importance d'une part, dans la dynamique des cycles biogéochimiques du carbone (ex. Mari, 1999 ; Engel et Passow, 2001) à travers leur processus d'agrégation et de sédimentation (Beauvais *et al.*, 2006; Engel, 2009) d'autre part, dans le réseau trophique marin (Mari and Rassoulzadegan, 2004) et même dans la dynamique des nutriments (Quiroz *et al.*, 2006).

3. MÉCANISMES DE FORMATIONS DES GELS MARINS

Les études sur les gels marins ont suggéré trois mécanismes de formation différents. Premièrement, les gels marins peuvent être libérés directement par le phytoplancton sous forme d'exsudats particulaires (Kiørboe et Hansen, 1993) ou par lyse cellulaire (Long et Azam, 1996). Ce mode de formation se base sur le fait que des cellules phytoplanctoniques peuvent secréter un mucus particulaire qui favorise la formation d'agrégats cellulaires (mucilage) (Kiørboe et Hansen, 1993). Ce mode dépend principalement de l'espèce. Deuxièmement, les gels marins résultent probablement de l'agrégation de polymères selon un processus physique décrit par une théorie de coagulation (Jackson, 1995; Burd et Jackson, 2009). Le processus d'agrégation dans cette théorie dépend, d'abord, de

l'abondance et de la taille des polymères. Ensuite, l'intensité des processus hydrodynamique du milieu (ex. la probabilité de rencontre entre les polymères augmente en fonction de la turbulence) (Jackson, 1995; Burd et Jackson, 2009). Enfin, les gels peuvent être formés par assemblage spontané du DOC pour produire de plus larges particules (Chin and Orellana, 1998; Verdugo *et al.*, 2004). Dans ce cas, l'assemblage peut être contrôlé soit par un processus physique quand les molécules sont assez proches pour interagir ensemble (ex. les ponts hydrogènes, la force de Van der Waals, lien hydrophobe/hydrophile) soit par processus chimique (ex. liaison covalente).

4. LES PARTICULES EXOPOLYMÉRIQUES TRANSPARENTES

4.1. Origine et rôle

Parmi les gels marins récemment identifiés et largement étudiés, il ya les gels marins transparents riches en polysaccharides, ils se distinguent par leur teneur en sucres acides. Ces gels sont appelés les particules exopolymériques transparentes (TEP, en anglais). Les TEP résultent de l'agrégation de plusieurs réseaux de polymères de polysaccharides secrétés principalement par le phytoplancton ou par les bactéries. Les TEP ont une composition en monosaccharides ressemblant à celle des EPS provenant de phytoplancton (Ding *et al.*, 2009). Dans ce cadre, les monosaccharides prédominants dans les EPS (fucose, arabinose et rhamnose) ont aussi été observés dans les TEP (Myklestad et Haug, 1972; Zhou *et al.*, 1998). De plus, des études ont montré que les bactéries utilisent les TEP comme une matrice pour leur colonisation (Azam et Malfatti, 2007; Bar-Zeev *et al.*, 2012). Le pourcentage des bactéries attachées aux TEP varie en moyenne entre 0,5 % et 25 % des bactéries totales du milieu (Passow et Alldredge, 1994; Mari et Kiørboe, 1996).

Les TEP jouent un rôle clé dans l'export et le transfert du carbone. En premier lieu, l'exportation du carbone se réalise à travers le processus de sédimentation verticale. La détermination du taux de sédimentation des TEP a fait l'objet de plusieurs études. Dans ce contexte, il a été montré que le flux maximal coïncide avec le maximum de sédimentation de la fraction totale du POC enregistré durant la fin des floraisons de phytoplancton

(Passow *et al.*, 2001). Le taux de sédimentation des TEP dans l'eau de mer est généralement variable entre 7 et 70 mgC m⁻² jour⁻¹. Il peut atteindre 490 mgC m⁻² jour⁻¹ (Passow *et al.*, 2001; Engel et Passow, 2001). De plus, une faible partie de ces particules sera enfouie progressivement dans les sédiments et ainsi soustraite du cycle du carbone. De ce fait, les TEP favorisent la séquestration du carbone dans l'océan profond (« pompe biologique ») (Mari, 1999; Engel et Passow, 2001; Mari *et al.*, 2001). En deuxième lieu, le transfert de carbone se fait en augmentant le flux du carbone entre le phytoplancton et les niveaux trophiques supérieurs. (Passow, 2001). Dans le cadre du transfert de carbone, l'agrégation du picophytoplancton et du nanophytoplancton dans les TEP forme de plus grosses particules. Ainsi, ces groupes de phytoplancton deviennent incorporables par les euphausiacés (Passow and Alldredge, 1999; Mari and Rassoulzadegan, 2004).

4.2. Caractéristiques physiques et chimiques des TEP

Sur le plan opérationnel, les TEP sont des particules retenues sur un filtre de porosité 0,2 µm ou 0,4 µm avec la capacité d'être colorées par le colorant Alcian Blue à pH acide de 2,5 (Alldredge *et al.*, 1993). Leur concentration est exprimée en équivalent en gomme de Xanthan (XG eq, en anglais). La concentration des TEP varie entre 100 et 1500 µg XG eq L⁻¹ dans les régions côtières (Passow, 2002a) et entre 28 et 140 µg XG eq L⁻¹ au large des océans (Engel, 2004). Durant les floraisons phytoplanctoniques, la concentration des TEP atteint de plus fortes valeurs (Passow, 2002a). Leur abondance varie de 10³ à 10⁸ particules L⁻¹ (Mari et Burd, 1998). Les TEP se caractérisent par un coefficient d'adhésion très importants. Selon Passow (2002b), l'agrégation des TEP n'est pas sélective. Toute particule présente dans l'eau de mer peut y être incorporée. Ainsi, les TEP peuvent atteindre des dimensions de quelques centaines de microns. Elles peuvent former des micro-environnements qui représentent un support d'attachement pour le carbone organique et le carbone inorganique (Passow *et al.*, 2001; Mecozzi *et al.*, 2001). Les TEP présentent un rapport carbon/azote (C/N) largement supérieur au rapport C/N de Redfield et variant entre 20 (Mari, 1999) et 26 (Engel et Passow, 2001). La teneur en carbone organique des TEP est du même ordre de grandeur que celle du phytoplancton (Mari, 1999; Engel et Passow,

2001). Le contenu en carbone organique des TEP a été estimé à un facteur de 75 % de la concentration totale des TEP déterminée par la méthode colorimétrique (Engel et Passow, 2001). Cependant, ce facteur est dépendant des espèces. Engel, (2004) a estimé une proportion de 63 % de carbone organique dans les agrégats de TEP dans une étude qui regroupe un grand nombre d'échantillons et avec une variété d'espèces importante. Par contre, le rapport TEP/POC a été estimé dans ces deux études avec des valeurs proches de $18 \pm 9\%$. La structure chimique des TEP possède des caractéristiques qui permettent de limiter leur désagrégation (Tanaka, 1992). On distingue, la présence de ponts ioniques entre des cations, tels que Ca^{2+} et Mg^{2+} et des groupements sulfates (OSO_3^-) ou des monomères acides (Engel, 2009; Verdugo, 2012; Passow, 2000; Verdugo et Saintschi, 2010; Passow, 2012). Les micro-gels qui en résultent se maintiennent ensemble par des interactions hydrophobes pour produire des TEP (Bar-Zeev *et al.*, 2011; Verdugo, 2012; Villacorte *et al.*, 2013). La distribution verticale des TEP est reliée à la productivité primaire et la concentration en nutriments. Elle montre des concentrations élevées dans la couche euphotique et plus faibles dans les couches sous-jacentes (Passow, 2000). Cette perte de masse résulte des effets combinés de l'activité bactérienne, de la fragmentation des particules, de leur solubilisation, de leur ingestion ou de leur dégradation (respiration) au cours de leur chute vers les profondeurs marines.

4.3. Interaction entre les TEP et des paramètres biologiques

Ils existent plusieurs paramètres qui peuvent influencer la dynamique des TEP. En premier lieu, la concentration et la composition chimique des précurseurs des TEP varient en fonction de la disponibilité en nutriments (Staats *et al.*, 2000; Underwood *et al.*, 2004), de la lumière (Smith et Underwood, 2000), de l'espèce (Claquin *et al.*, 2008) et de son état physiologique (Kahl *et al.*, 2008) ainsi que par le broutage (Corzo *et al.*, 2000). Dépendamment de l'espèce, la production des précurseurs des TEP peut être synchronisée avec l'activité photosynthétique ou durant une situation de stress provoquée par une limitation des éléments nutritifs (Claquin *et al.*, 2008). Par exemple, une sécrétion importante de précurseurs de TEP, durant une situation de limitation en silicates, a été

expliquée par un débordement de carbone organique quand les cellules de phytoplancton sont capables de réaliser la photosynthèse et non la division cellulaire, dans (Engel, 2000). Elle a aussi été expliquée par une lyse cellulaire, suite à des attaques virales à la fin des floraisons (Staats *et al.*, 2000; Underwood *et al.*, 2004). Plusieurs facteurs environnementaux ont un effet sur la dynamique des TEP et leurs précurseurs. Tel que expliqué, la disponibilité de certains cations (ex. Ca^{2+} et Mg^{2+}) (Mari et Robert, 2008) et l'intensité des processus hydrodynamiques qui jouent un rôle central dans le contrôle de la formation des TEP (Beauvais *et al.*, 2006; Stoderegger et Herndl, 1999). De même, le coefficient d'adhésion des TEP augmente avec l'augmentation de la salinité de l'eau, ce qui résulte en la formation de plus larges particules qui sédimentent plus rapidement (Mari *et al.*, 2012; Wetz *et al.*, 2009). Par contre, l'augmentation des radiations ultraviolettes réduit la concentration de ces particules par photolyse (Orellana et Verdugo, 2003). Finalement, la température et le pH de l'eau semblent aussi avoir un effet sur les TEP. La baisse du pH provoque une réduction de la taille des gels marins à travers le processus de condensation (Passow, 2012). À son tour, l'augmentation de la température accélère la formation des gels marins. Cela résulte de l'accélération du taux de croissance ou de l'atteinte d'un équilibre entre la production et la sécrétion de carbone par les cellules (Claquin *et al.*, 2008).

5. PROBLÉMATIQUES ET OBJECTIFS

5.1. Distribution spatiale des TEP au sein de l'estuaire maritime du Saint-Laurent

5.1.1. Les TEP dans les estuaires

Des études récentes de la matière particulaire dans les environnements estuariens ont montré l'importance des TEP et de leurs précurseurs dans le cycle du carbone des estuaires (Mari *et al.*, 2012; Wetz *et al.*, 2009; Wurl et Holmes, 2008). Par exemple, les TEP constituent une biomasse importante dans le pool du POC d'un estuaire situé en Caroline-du-nord, et qui décharge en moyenne $7,80 \times 10^9 \text{ gC an}^{-1}$ de DOC dans l'océan Atlantique. 17 % de cette biomasse de DOC est constituée de polysaccharides acides qui

représentent les précurseurs des TEP (Thornton, 2009). De plus, au sud de l'Asie et dans le détroit de Singapour, les TEP sont abondantes dans la micro-couche de surface (Wurl et Holmes, 2008). Dans la même étude, le taux d'enrichissement des TEP dans la micro-couche de surface à partir de la couche sous-jacente était de l'ordre de 0,39 à 2,43 ($1,31 \pm 0,52$, en moyenne) dans l'océan et de 0,29 à 9,72 ($1,77 \pm 3.03$, en moyenne) dans l'estuaire. Au cours d'une étude d'une période d'un an, Wetz *et al.* (2009) ont montré que les TEP représentent 16 % du pool du carbone organique total de l'estuaire Neuse en Caroline-du-nord. En plus, la concentration des TEP était corrélée au pH, la température, la turbulence et la salinité de l'eau de l'estuaire (Wetz *et al.*, 2009). Aussi, selon les travaux de Sun *et al.* (2012), les concentrations en cations Ca^{2+} sont positivement corrélées à la concentration en TEP. Enfin, Mari *et al.* (2012) a démontré, par une expérience au laboratoire, l'augmentation des propriétés d'adhésion des TEP en fonction de l'augmentation de la salinité, ce qui implique qu'il y aura de plus grosses particules dans la partie la plus saline d'un estuaire; ce qui influencera la sédimentation des TEP (Mari *et al.*, 2012).

5.1.2. L'estuaire du Saint-Laurent, un réservoir important de carbone organique

L'estuaire du Saint-Laurent s'étend sur 350 km, de la limite d'intrusion du sel au niveau de l'île d'Orléans jusqu'à Pointe-des-monts. Il fait partie d'un large écosystème situé sur la côte Est du Canada. Cet écosystème relie les grands lacs de l'Amérique du Nord à l'océan Atlantique. Il est composé du fleuve, de l'estuaire et du golf du Saint-Laurent. Le fleuve Saint-Laurent est le plus grand fleuve de l'Amérique du Nord ayant un bassin versant de $1\ 320\ 000\ \text{km}^2$. À travers l'estuaire, le fleuve Saint-Laurent injecte en moyenne $12\ 500\ \text{m}^3\ \text{s}^{-1}$ d'eau douce dans le golf du Saint-Laurent (Gilbert *et al.*, 2005). Ce volume représente la moitié des apports d'eau douce de la côte atlantique de l'Amérique du Nord et $\approx 1\%$ de l'apport global de la planète. La décharge de ce volume établit une forte et persistante circulation de surface dans l'estuaire. Le fleuve Saint-Laurent décharge chaque année entre $1,29$ et $1,72 \times 10^{12}\ \text{g}$ de DOC et $240 - 370 \times 10^9\ \text{g}$ de POC (Pocklington et Tan, 1987). L'export net de DOC de l'estuaire vers le golf du Saint-Laurent est du même ordre ($1,96 \times 10^{12}\ \text{gC}$) que la décharge du fleuve Saint-Laurent. Cependant, le flux du POC hors

de l'estuaire (128×10^3 C) représente moins que la moitié du POC déchargé par le fleuve. Ainsi, l'estuaire du Saint-Laurent représente un réservoir important de POC. La concentration estivale en POC dans la couche de surface de l'estuaire du Saint-Laurent dans le même ordre de grandeur que celle des régions les plus productives de l'océan global (ex. durant la période de forte remontée des eaux profondes de la côte nord-ouest de l'Afrique) (El-Sabh, 1990). Avec une production primaire de $6,62 \times 10^{12}$ gC an⁻¹, l'estuaire du Saint-Laurent est classé parmi les systèmes les plus productifs de la planète (El-Sabh, 1990). Therriault et Levasseur (1985) ont estimé à 134 gC m⁻² an⁻¹ la production primaire de la partie centrale de l'estuaire du Saint-Laurent, ce qui est légèrement au-delà de la moyenne de production de l'océan global.

5.1.3. Les TEP dans l'estuaire maritime du Saint-Laurent

Seul le travail de Annane *et al.* (2015) est disponible sur les TEP dans l'estuaire maritime du Saint-Laurent (LSLE, en anglais). Cette étude présente la variabilité saisonnière de la distribution verticale des TEP au sein du LSLE. La concentration des TEP a montré une grande variabilité autant sur l'échelle temporelle que verticale. Les concentrations étaient significativement dépendantes de la saison et de la couche d'eau. Les TEP présentaient significativement de plus fortes concentrations dans la couche de surface reliée aux floraisons saisonnières du phytoplancton (Annane *et al.*, 2015). Ce qui suggère que les TEP dans le LSLE provenaient principalement des sécrétions phytoplanctoniques. Durant les deux floraisons, la biomasse était dominée par diatomées (particulièrement par *Skeletonema costatum* suivie par *Thalassiosira* sp. et *Chaetoceros* sp.). Au printemps, les concentrations étaient faibles ($11,25$ µgC L⁻¹), tandis qu'en été et en automne les concentrations des TEP ont augmenté et ont atteint un maximum de 1161 µgC L⁻¹ (Annane *et al.*, 2015). La détermination de la contribution des TEP au pool du POC du LSLE a montré que les TEP étaient la deuxième source de carbone particulaire dans la couche de surface après le phytoplancton (41% pour les TEP et 54% pour le phytoplancton) (Annane *et al.*, 2015). Dans la couche intermédiaire froide et la couche profonde, les TEP présentaient de plus faibles contributions durant l'été et l'automne. Exceptionnellement

pendant le printemps, les TEP dans ces deux couches montraient de fortes contributions au POC, probablement expliquées par une forte concentration de la fraction colloïdale des TEP (entre 0,2 et 0,7 µm) reliée à la dynamique de la saison. Néanmoins, le travail de Annane *et al.* (2015) a été réalisé au niveau d'une unique station située dans le LSLE (IML-4; 48°40' N, 68° 35' W). Les interprétations étaient basées sur un seul point géographique de l'estuaire et aucune donnée n'était disponible sur la distribution spatiale des TEP dans le LSLE. Alors, le premier objectif de ce travail consiste à fournir les premières mesures de la distribution spatiale des TEP dans deux régions clefs du LSLE: une zone de remontée des eaux profondes et une zone de front. La variabilité spatiale de la contribution des TEP au POC de le LSLE sera estimée.

5.2. Effet du changement global sur les TEP

Dans le cadre actuel du changement climatique planétaire causé par les activités anthropiques le CO₂ accumulé dans l'atmosphère entre en contact avec les molécules d'eaux. Cette réaction libèrent des ions H⁺ et ainsi acidifie l'eau de mer. La hausse du CO₂ atmosphérique de 280 ppm à 400 ppm depuis l'ère préindustrielle, a mené à la diminution du pH des océans de 0,1 unité. On s'attend à ce que le pH diminue encore de 0,3 à 0,4 unité d'ici l'année 2100 si l'utilisation des énergies fossiles continue au rythme actuel (Caldeira et Wickett, 2003). L'augmentation de la concentration en CO₂ affecte plusieurs processus tels que la production primaire (Rost *et al.*, 2008; Egge *et al.*, 2009), la calcification (Rost *et al.*, 2008), la production de matériel extracellulaire (Engel, 2002), le taux de croissance (Feng *et al.*, 2008) et la fixation de l'azote (Rost *et al.*, 2008). Par ailleurs, l'acidification des océans semble aussi affecter la vitesse de sédimentation des agrégats marins (Armstrong *et al.*, 2002). Il a été montré que chez le phytoplancton, l'assimilation du CO₂ augmente avec l'accroissement de la concentration en CO₂ atmosphérique, ce qui cause une augmentation de la production de particules marines telles que les TEP (Riebesell *et al.*, 2007). Cela entraînera une accélération et une amplification du flux du POC de la surface vers le fond (Engel, 2005; Riebesell *et al.*, 2007). Par opposition, d'autres études ont montré qu'il n'existe pas de corrélation entre les fortes concentrations de CO₂ et la production des TEP

(Egge *et al.*, 2009). Mari, (2008) a constaté que les TEP formées à de faibles valeurs de pH (7,3) possèdent une plus grande taille et une plus grande flottabilité que celles produites à des valeurs élevées de pH (8,1). Ceci suggère qu'à faibles pH, les particules marines auront tendance à rester dans la couche de surface au lieu de sédimenter. Par contre, Engel *et al.* (2014) ont montré que de fortes concentrations en CO₂ n'affectent pas la formation abiotique des TEP chez *Emiliania huxleyi*.

L'augmentation de la température moyenne des eaux de surface devrait atteindre entre 1,8 et 4 °C à la fin du 21^{ème} siècle dépendamment de l'émission des gaz à effet de serre dans l'atmosphère (Solomon, 2007). L'augmentation de la température engendrera une hausse de la stratification des masses d'eau, une augmentation du niveau des océans (2,5 mm an⁻¹) et une diminution de la couverture de glace Arctique et Antarctique (Stammerjohn *et al.*, 2012). De plus, des changements sont prévus dans la circulation océanique, les précipitations et le flux d'eau douce vers les océans. Concernant le phytoplancton, une température plus élevée peut représenter un stimulant pour la croissance ou le métabolisme ou seulement un stress dépendamment des espèces (Claquin *et al.*, 2008). D'autre part, l'augmentation de la température entraînera une hausse de la production des TEP. Cet effet est dépendant de l'espèce. Trois diatomées (*Skeletonema marinoi*, *Nitzschia fraudulenta* et *Thalassiosira pseudonana*) et deux espèces du genre *Isochrysis* ont montré des effets significatifs de la température sur la production des TEP (Claquin *et al.*, 2008). Néanmoins, la même étude a montré que l'augmentation de la température n'affecte pas la production des TEP chez *Emiliania huxleyi* et *Lepidodinium chlorophorum* (Claquin *et al.*, 2008). Enfin, l'effet combiné de l'augmentation de la température et du CO₂ résulte en une diminution du taux de croissance (testé chez *Emiliania huxleyi*), de l'augmentation de la sécrétion du DOC et de la production des TEP et (Borchard *et al.*, 2011). D'autre part, Chen *et al.* (2015) ont montré qu'à certaines valeurs de pH et de température, la formation des gels marins est bloquée. De plus, l'effet d'agrégation des particules de TEP ainsi que leur sédimentation semble diminuer (Seebah *et al.*, 2014; Mari, 2008). En d'autres termes, les changements climatiques semblent altérer les réponses physiologiques des communautés de phytoplancton, ainsi que la dynamique du

carbone organique de la zone euphotique et l'exportation vers l'océan profond (Passow et Carlson, 2012). Cependant, les études scientifiques réalisées semblent parfois se contredire d'un scénario expérimental à un autre. Dans ce contexte, le deuxième objectif de cette étude sera de évaluer à travers une expérience en mésocosmes, l'effet d'un scénario de changement global sur les TEP dans le LSLE.

CHAPITRE 1

SPRING SPATIAL DISTRIBUTION OF TRANSPARENT EXOPOLYMERIC PARTICLES WITHIN TWO KEY REGIONS OF THE LOWER ST-LAWRENCE ESTUARY: UPWELLING AND FRONT

RESUME

La distribution spatiale de la concentration des TEP a été déterminée dans la couche de surface et la couche profonde de deux zones de l'estuaire maritime du Saint-Laurent (LSLE, en anglais): une zone de remontée des eaux profondes et une zone de front. La concentration moyenne des TEP dans la couche de surface des deux zones était $89,77 \pm 48,84 \mu\text{g}$ équivalent en gomme de Xanthan (XG eq, en anglais) par litre). Dans la couche profonde la concentration moyenne des TEP était égale à $33,59 \pm 21,12 \mu\text{g XG eq L}^{-1}$. La zone de remontée des eaux profondes était caractérisée par la dominance de matière organique d'origine terrestre, une concentration élevée en nutriments surtout en couche profonde, et un gradient des paramètres environnementaux situé au niveau de la tête du chenal Laurentien. Les TEP à ce niveau, montraient aussi un gradient de concentration. La concentration des TEP la plus élevée était enregistrée au niveau de l'estuaire supérieur et du fjord du Saguenay. Au niveau de la zone de front, les TEP ont montré de concentrations plus élevées au niveau de la masse d'eau de caractère estuarien que la masse d'eau de caractère océanique. En outre, des concentrations de fond exceptionnellement élevées en TEP ont été observées au niveau de la couche profonde de la zone de front. Globalement, les concentrations en TEP étaient significativement ($p < 0.01$) et positivement corrélées aux concentrations en carbone organique particulaire (POC, en anglais). Les TEP ont montré une contribution allant jusqu'à 82 % du POC du LSLE. Cependant, le principal contributeur au pool de POC de la couche de surface du LSLE variait entre les TEP, le phytoplacton et les détritus, dépendamment de la distribution spatiale. Comparées à d'autres environnements aquatiques, les ratios TEP/POC et TEP/chlorophylle a du LSLE étaient parmi les plus élevées.

Mots clefs: LSLE, TEP, POC et distribution spatiale

ABSTRACT

The spatial distribution of the transparent exopolymeric particles (TEP) concentration was determined in the surface layer and the deep layer of an upwelling area and a front area of the lower St-Lawrence estuary (LSLE). The mean TEP concentration in the surface layer of both areas was $89.77 \pm 48.84 \mu\text{g Xanthan gum equivalent (XG eq) per liter}$. In the deep layer, the mean TEP concentration was $33.59 \pm 21.12 \mu\text{g XG eq L}^{-1}$. The upwelling area was characterized by the dominance of organic matter of terrestrial origin, a high concentration of nutrients especially in the deep layer, and a gradient of the environmental parameters located at the head of the Laurentian trough. TEP at this level showed also a concentration gradient. The highest TEP concentrations were recorded in the higher estuary and the Saguenay fjord. In the front area, TEP showed higher concentrations at the estuarine water body than the oceanic water body. In addition, high exceptional concentrations of TEP were observed at the deep layer of the front area. Overall, TEP concentrations were significantly ($p < 0.01$) and positively correlated with particulate organic carbon (POC) concentrations. TEP showed a contribution of up to 82% of the POC in the LSLE. However, the main contributor to the POC of the surface layer of our study varied between TEP, phytoplacton and detritus, depending on the spatial distribution. Compared with other aquatic environments, the LSLE presented within the highest TEP/POC and TEP/chlorophyll *a* ratios.

Key words: LSLE, TEP, POC and spatial distribution

1.1. INTRODUCTION

The magnitude of the vertical flux in aquatic environments, and then their ability to export organic matter, is resolved by the density and sinking characteristics of large organic particles (marine gels) (Alldredge and Silver, 1988; Jackson and Burd, 1998). The class of ubiquitous transparent exopolymeric particles (TEP) (Alldredge *et al.*, 1993) proved to have an important role in mechanisms regulating aggregation and sedimentation in marine (Passow *et al.*, 2001) and estuarine systems (Mari, 2008; Wetz *et al.*, 2009; Annane *et al.*, 2015). TEP are formed by coagulation of polysaccharides chains (Mopper *et al.*, 1995; Zhou *et al.*, 1998; Engel and Passow, 2001). TEP carbon to nitrogen ratio (C:N) is beyond the Redfield ratio (C:N \approx 6.6; Redfield *et al.*, 1963). Moreover, TEP presents enhanced coagulation efficiency due to their high coefficient of stickiness (Mopper *et al.*, 1995; Engel, 2000). TEP are the link between DOC and POC as a carbon continuum. They influence the biogeochemical composition of marine gels by a non-selective enrichment of carbon (Verdugo *et al.*, 2004). Thereby, it has been shown that TEP are significantly correlated to phytoplankton species and density (Ding *et al.*, 2009), bacteria density (Azam and Malfatti, 2007), nutrients concentrations (Underwood *et al.*, 2004) and POC (Passow, 2002b). In addition, TEP were significantly correlated to salinity (Mari *et al.*, 2012), temperature (Claquin *et al.*, 2008) and pH (Passow, 2012) as well as turbulence conditions (Perdrotti *et al.*, 2010). However, TEP interactions with the environmental parameters are dependent on the aquatic environment.

The lower St-lawrence estuary (LSLE) represents a very important reservoir of organic matter. The St-Lawrence river discharges $1.29 - 1.72 \times 10^{12}$ g of dissolved organic carbon (DOC) and $240 - 370 \times 10^9$ g of particulate organic carbon (POC) each year (Pocklington and Tan, 1987). However, the net export of the dissolved organic carbon (DOC) from the LSLE to the Gulf of St-Lawrence is in the same order (1.96×10^{12} gC) as the St-Lawrence river discharge. While the POC flux out of the LSLE (128×10^9 gC), represents less than half the POC discharged by the St-Lawrence River (Pocklington and Tan, 1987; Gearing and Pocklington, 1990; Pocklington, 1988). However, particles carried in the higher St-

Lawrence estuary are mainly deposited at the head of the LSLE. Consequently, the LSLE retains an important part of the POC discharged from the river to the estuary. Moreover, primary production in the LSLE is mainly consumed/sedimented in the respective zone or very inefficiently exported downstream (Therriault and Levasseur, 1985). Nevertheless, in the LSLE only the seasonal variation of TEP is available (Annane *et al.*, 2015), showing high concentrations (up to 1548 µg XG eq L⁻¹ during summer). It represented the second most important contributor to POC pool of the SL (Annane *et al.*, 2015). In addition, the LSLE presents more oceanic features. The water column in the LSLE is well stratified and it has two layers with different origins and time of residence. In winter, a relatively fresh and cold surface layer (SL) lies on top of a warmer and saltier layer. With the onset of spring, the SL warms up faster and a three-layer system gradually develops. A SL relatively warm and fresh, a cold intermediate layer and a deep layer (DL) warmer and saltier than the cold intermediate layer. During the runoff period, the SL in the LSLE is a mixture of fresh water recently discharged and the upper layer of the previous winter. However, the DL originates from the slower advection of north Atlantic waters mixed with Labrador waters mainly coming from the Cabot Strait through the Laurentian channel. Furthermore, the LSLE presents area of upwelling and area of front. A noticeable upwelling area is located at the head of the Laurentian trough (HLT) where the DL waters rise to the surface due to a strong bathymetry gradients and high variability of tidal currents (Ingram, 1975 and 1983). A front area is a relative strait zone between two distinct water masses, usually light (warm, fresh) and heavy (cold, salty). Fronts are characterized by an upward or downward curving of the pycnocline, such that the pycnocline intersects with the surface or the bottom (Mooers *et al.*, 1998). This gives a strong density gradient in the cross frontal direction which generates strong vertical velocities (Hoskins and Bretherton, 1972; Mahadevan and Tandon, 2006). There are several frontal areas in the LSLE. They are generated in the upwelling area as a result of the presence of distinct water masses (Ingram, 1975). Fronts were also recorded in the Bic and Pointe-des-Monts areas. A persistent quasi-permanent cold front was detected near the estuary-gulf boundary (Tang, 1980).

Therefore, the primary aim of this study is: 1) to give first data on the spatial distribution of TEP in the upwelling area and front area of the LSLE and to analyse TEP interactions with biological parameters measured. The second purpose is: 2) to estimate TEP carbon contribution to the POC pool of the LSLE. Two hypothesis will be tested: 1) TEP concentrations are correlated to the biological parameters considered of the upwelling area and the front area. 2) TEP has a relevant contribution to the POC pool of the upwelling area and the front area.

1.2. MATERIAL AND METHODS

1.2.1. STUDY AREAS AND SEAWATER SAMPLING

Two oceanographic cruises were performed in 2013 at the Lower St-Lawrence estuary (LSLE) (Québec, Canada) onboard the R/V *Coriolis II* from 13rd to 17th of May and from 10th to 15th of June, respectively. Samples were collected from the surface layer (SL) and the deep layer (DL) of two different areas of the estuary. First, the area 1 (A1) was situated on the upper limit of the LSLE, at the level of Tadoussac and the mouth of the Saguenay fjord. It represented a part of the region that separates the higher St-Lawrence estuary with typical depths of 20-50 m from the LSLE with typical depths of 300-350 m (Fig. 2). During sampling, A1 that was represented by a geographical horizontal transect along the steeply depth increase of the threshold of the head of the Laurentian trough (HLT) (307 m, 262 m and 168 m, respectively at stations 1, 2 and 3, Fig. 2). More three stations were sampled around the HLT zone: 1) On the lower limit of the higher estuary, 2) on the mouth of the Saguenay fjord and 3) further off the lower estuary. The second area (A2) was located at the level of Pointe-aux-Outardes and Métis-sur-Mer. A2 extended over the transverse axis of the LSLE. Two fronts were detected onboard. The first front (F1) was recorded at 14 May 2013 at the south shore of the area, while the second one (F2) was observed at 15 and 17 May 2013 at the north shore. Samples were taken from the less dense (-) and the densest (+) water masses of both fronts (F1-, F2- and F1+, F2+).

respectively). Moreover F2 belonged for 3 days that makes us capable of sampling, two more stations at the center of F2 (F2C1 and F2C2). Seawater sampling was performed using a SBE 32 Caroussel water sampler with 12 bottles of 12 L each. The sampler was equipped with calibrated probes of conductivity, temperature and depth Seabird SBE-911. Sampling was performed at two different layers of the LSLE: 1) at the surface layer (SL) (between 0.5 and 10 m depths depending on station). 2) The deep layer (DL) (between 56 and 345 m depending on station). In order to detect and record fronts, we used wind data from Maurice Lamontagne Institute buoy, IML-4 (48.66° N, 68.58° W).

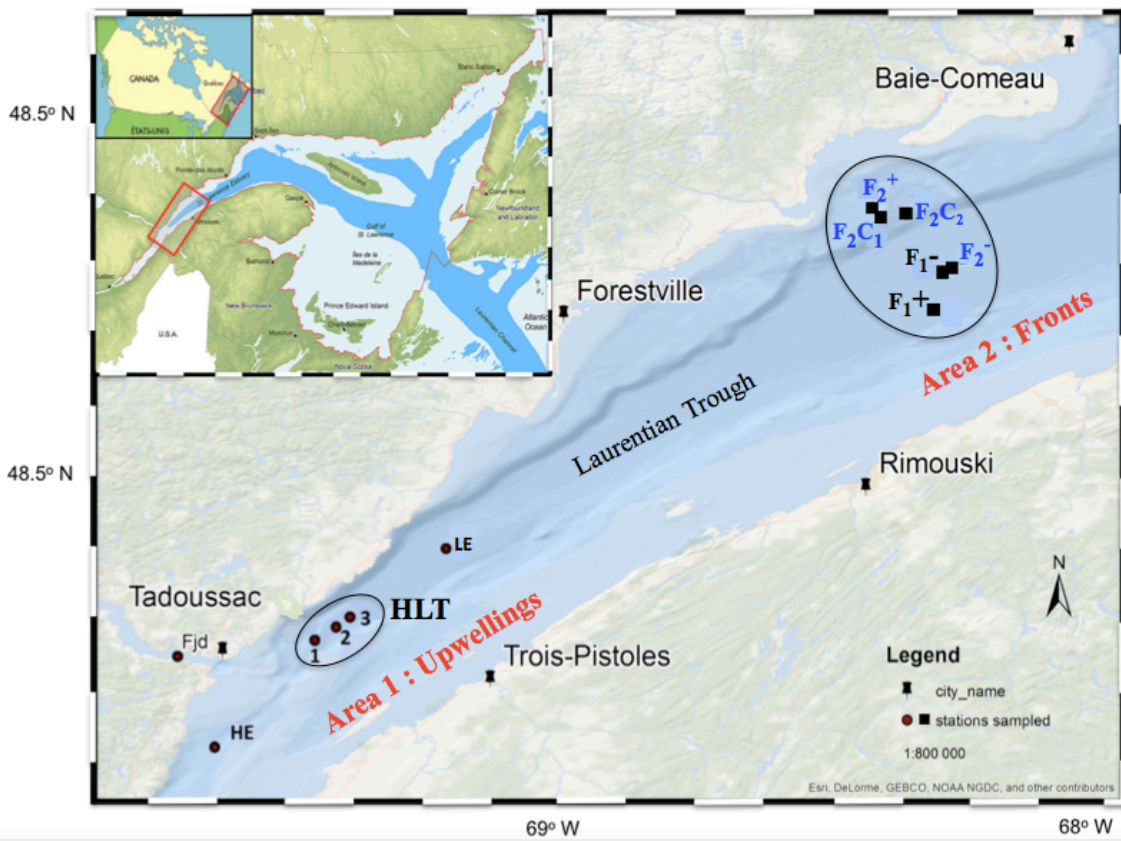


Figure. 1 Map showing the geographical positions of the sampled stations in the area of upwelling (1, 2, 3 at the HLT (head of the Laurentian trough) zone, the HE (higher estuary), the Fjord (Fjord) and the LE (lower estuary)) and the area of front. First front (F1) was sampled at the two sides of the front (F1- and F1+), while the second front (F2) was sampled at the two sides (F2- and F2+) and the center (F1C1 and F1C2).

It was downloaded from the St-Lawrence Global Observatory-SLGO, (<http://slgo.ca>, 2014) with a 15-minute temporal resolution. The hourly water level was obtained from the Rimouski station #2985 of Fisheries and Oceans Canada. Furthermore, an EIVA ScanFish II modulating instrument was used to record these fronts. It was towed behind the ship with a horizontal speed of 3.8 m s^{-1} and a vertical speed of 0.76 m s^{-1} . The ScanFish allowed detecting the difference in density of the two seawater masses forming fronts as well as to identify movements of the fronts caused by tidal currents.

1.2.2. ENVIRONMENTAL PARAMETERS MEASURMENTS

1.2.2.1. Salinity and temperature

The determination of the salinity and temperature characterization was carried out using data collected onboard.

1.2.2.2. Nutrients concentrations

Seawater samples of 12 mL were pre-filtered through Acrodisc syringue filters with $0.8 \mu\text{M}$ Versapor membranes and stored at -80°C in previously (10 %) acid-cleaned and dried polycarbonate cryogenic vial. Concentrations of nitrate plus nitrite ($\text{NO}_3^- + \text{NO}_2^-$), nitrite (NO_2^-), phosphate (PO_4^{3-}), and silicic acid (Si(OH)_4) were measured with a SEAL Technicon AutoAnalyzer II (AA3). Analyses were performed following an automated procedure based on the colorimetric method adapted from: Grasshoff *et al.* (2009).

1.2.2.3. Chlorophyll *a*

Chlorophyll *a* (chl *a*) was measured by the fluorometric method described by Holm-Hansen *et al.*, (1965) (from Parsons *et al.*, 1984). Duplicate 100 mL samples were filtered onto GF/F (2.5 cm) filters, quickly frozen in liquid nitrogen and stored at -80°C until extraction. The biomass was ground with a glass rod prior to be extracted with 10 mL of 90 % acetone. Chl *a* extracts were then read with a Trilogy (7200-000 model) Cie

Turner Designs fluorometer, calibrated with spinach (Sigma # C 57530) and acidification for phaeopigments correction (EPA Method 445.0).

1.2.2.4. pH

The measurements of pH were carried out only in the A1. Measurements of pH were performed following the protocol described by Mucci *et al.* (2011). Water samples for pH measurements were collected as soon as the rosette was onboard. Volumes of 125 or 250 mL were transferred into glass bottles leaving no headspace. Bottles were sealed with a ground-glass stopper and were immersed in a constant temperature bath ($25.0^{\circ} \pm 0.05^{\circ}\text{C}$) until thermal equilibrium was reached. Within one hour (h), pH was measured on board using a Hewlett-Packard UV-Visible diode array spectrophotometer (HP-8453A) and a 5-cm quartz cell. The indicators used were: Phenol red (Robert-Baldo *et al.*, 1985) and m-cresol purple (Clayton and Byrne, 1993). The absorbance at the wavelengths of maximum absorbance of the protonated and deprotonated indicators was measured and recorded. Tris(hydroxymethyl)-aminomethane buffers was used for a similar procedure before and after each set of samples measurements. The pH of the samples and buffers was calculated using equation from Byrne (1987):

$$\text{pH} = \text{pK}_{\text{HL}} + \text{Log}_{10}[(R - 2^{e_{\text{HL}}} / 1^{e_{\text{HL}}}) / (2^{e_{\text{L}}} / 1^{e_{\text{HL}}} - R_1 e_{\text{HL}} / 1^{e_{\text{HL}}})]$$

Where $\text{pH} = -\log_{10}[\text{H}^+]$, $\text{pK}_{\text{HL}} = -\log_{10} K_{\text{HL}}$ and K_{HL} is the dissociation constant of the indicator. R is the ratio of the absorbances at wavelengths 1 and 2 ($R = A_2/A_1$). $1^{e_{\text{HL}}}$ and $2^{e_{\text{HL}}}$ are the molar absorptivities of the protonated indicator at wavelengths 1 and 2. $2^{e_{\text{L}}}$ and $1^{e_{\text{HL}}}$ are the molar absorptivities of the deprotonated indicator at wavelengths 1 and 2.

1.2.3. DETERMINATION OF TEP CONCENTRATION

Transparent exopolymeric particle (TEP) concentrations were measured using the colorimetric method described in Passow and Alldredge (1995). Triplicate seawater

samples of volume ranging between 70 and 100 mL were filtered onboard onto a 0.2 µm polycarbonate membrane filter (Whatman Nucleopore) at low pressure (<10 mbar) using a vacuum pump. Once the volume of seawater is fully filtered, 500 µL of Alcian Blue solution was passed through the filters in order to stain the retained TEP. Excess of Alcian Blue was eliminated with 1 mL of deionized water. Filters were stored at -80 °C until analysis. In the land-based laboratory, filters were immersed in 6 mL of 80 % sulfuric acid solution continuously stirred with an orbital agitator (BUNSEN AO-400) during 2 h. The absorbance of the solution was determined spectrophotometrically at 787 nm. A virgin filter stained with Alcian Blue was used as a blank and are subtracted from the absorptions of the samples. The absorbance of the Xanthan gum at the same wavelengths was used for the calibration of the Alcian Blue absorption (5 dilutions). TEP colorimetric concentration was expressed in xanthan gum equivalent per liter ($\mu\text{g XG eq L}^{-1}$), which was calculated using equation from Passow and Alldredge (1995):

$$\text{TEP} = (\text{E}_{787} - \text{C}_{787}) * (\text{V}_t) * f_x$$

Where E_{787} is the absorption of the sample, C_{787} is the absorption of the blank, V is the volume filtered in liter and f_x is the calibration factor in microgram. TEP carbon concentration was estimated from the conversion factor of 0.63 presented by Engel (2004), which used more data collected from different locations and considering different plankton species:

$$\text{TEP } (\mu\text{g C L}^{-1}) = 0.63 * \text{TEP } (\mu\text{g XG eq L}^{-1})$$

1.2.4. PARTICULATE ORGANIC CARBON QUANTIFICATION AND STABLE ISOTOPES

Triplicate water samples varying between 250 mL to 500 mL were filtered on board onto pre-combusted (450 °C during 4 h) Whatman GF/F (25 mm) filters. Then, filters were preserved at -80 °C. In the laboratory, filters were freeze-dried and encapsulated in tin foil. Particulate organic carbon (POC) and particulate organic nitrogen (PON) concentrations were measured using an elemental analysis COSTECH system 4010 equipped with an

auto-sampler zero blank, connected to a mass spectrometer DeltaPlus XP ThermoScientific. Isotopes were measured with continuous flow isotope ratio mass spectrometry analysis. Caffeine and *Nannochloropsis* sp. were used as standards to quantify carbon and nitrogen, respectively. Standards used for $\delta^{15}\text{N}$ were Mueller Hinton Broth and caffeine, while for $\delta^{13}\text{C}$ standards used were *Nannochloropsis* sp., Muller Hinton Broth and caffeine. Standards were analyzed on every sequence of 36 samples or less and were weighed with a *Mettler Toledo (Mx5 model, Dispersion Laboratory)* microbalance. Isotopic ratios are expressed as the usual notation δ in parts per mil (‰) using the equation of (Fry 2006a):

$$\delta\text{HX} = [\text{R}_{(\text{sample})}/\text{R}_{(\text{standard})} - 1] * 1000$$

Standard errors for $\delta^{13}\text{C}$ and $\delta^{15}\text{N}$ were 0.2 and 0.4, respectively.

1.2.5. PHYTOPLANKTON DENSITY

Three phytoplankton size classes were considered in this study: picophytoplankton ($< 0.2 \mu\text{m}$), nanophytoplankton ($2-20 \mu\text{m}$) and microphytoplankton ($>20 \mu\text{m}$). Two duplicate samples of 5 mL and 12 mL were collected and immediately preserved with, respectively, 20 μL and 96 μL of glutaraldehyde 25% (final concentration of 0.1 %), and stored at -80 °C until analysis. In the laboratory, cell counts were performed depending on cell size: 5 mL samples were used for enumeration of picophytoplankton and nanophytoplankton classes, while 12 mL samples were used for microphytoplankton enumeration. Moreover, nanophytoplankton and picophytoplankton total cell numbers were determined following Belzile *et al.* (2008) adapted from Marie *et al.* (1997) and Lebaron *et al.* (1998). Each sample was thawed and immediately mixed with a vortex. 1 μL of a 10 μm beads solution was added. 1 mL of each sample was pipetted in tubes and were analyzed by flow cytometry with a Beckman Coulter Epics Altra cytometer. Microphytoplankton cell numbers were determined using a portable benchtop flow cytometer (CytoSense analyser CS-2009-27) equipped with a solid-state laser beam (Coherent Saphyre, 488 nm, 15 mW). 1 mL of 1:10 Tris-EDTA 10x (pH 8) solution was

used as a buffer and 200 µL of standard beads (10 µm) suspension were added for calibration. Sample intake speed was set at 5 µL min⁻¹. Nanophytoplankton density was estimated using both methods described, in order to verify and adjust the variability between both methods.

1.2.5.1. Phytoplankton carbon concentration estimation

Phytoplankton carbon biomass was expressed using a conversion factor based on carbon to biovolume (C:V) equations following Menden-Deuer and Lessard (2000). Two algorithms were used: the first considered the carbon estimation of taxonomically diverse phytoplankton groups excluding diatoms, as:

$$\text{Picogramm of carbon cell}^{-1} = 0.216 \times \text{volume}^{0.939}$$

The second relationship focused on diatoms, as:

$$\text{Picogramm of carbon cell}^{-1} = 0.288 \times \text{volume}^{0.811}$$

In our study phytoplankton carbon concentration was estimated following two steps. First, diatom density contribution to every phytoplankton size class was identified and subtracted from each group of every size class. Second, diatom carbon concentration was estimated using the second relationship, while carbon concentration of non-diatom cells was expressed using the first relationship. Determination of the total number of diatoms was performed using the Cytoclus 3 software (a software related to the CytoSense analyser instrument). Total carbon concentration of picophytoplankton, nanophytoplankton and microphytoplankton were calculated using the sum of diatom and non-diatom phytoplankton of every size category.

1.2.6. BACTERIAL DENSITY

On board, duplicate of 5 mL subsamples pre-filtered on 200 µm were fixed with 50 µL of glutaraldehyde (0.5 % final concentration), kept in the dark at 4 °C for 30 min and

then stored at -80°C until analysis. Bacterial density was determined by flow cytometry following the protocol of Belzile *et al.* (2008), adapted from Marie *et al.* (1997) and Lebaron *et al.* (1998) and using the nucleic acid stain SYBER Green I. In the laboratory, 200 μL of each sample were pipetted and stained with 0.3 μL of SYBR-Green I (0.1% final concentration; Molecular Probes Inc. # S-7585) for 15 min in the dark to optimize the staining. 800 μL of Tris-EDTA 10x buffer pH 8 were added to each sample to insure a stable pH and avoid coincidence of several particles in the laser beam. As an internal standard, 1 μL of a solution of 1 μm Polysciences Fluoresbrite beads was added. Samples were analyzed with an Epics Altra flow cytometer (Beckman Coulter) fitted with a 488 nm laser operated at 15 mW. Each sample was run twice following a flow rate of 60 $\mu\text{L min}^{-1}$ for bacteria counts and discrimination according to their size and nucleic acid content.

1.2.6.1. Bacterial carbon estimation

The bacterial carbon concentration was calculated using a conversion factor of bacterial cell to biomass factor equal to 30 fg carbon cell $^{-1}$ (Fukuda *et al.*, 1998).

1.2.7. STATISTICAL ANALYSIS

In order to compare average values distribution of all variables measured in this study, two samples parametric student's T-tests were carried out. The objective of this parametric analysis was to determine if a significant difference existed among layers and among areas. Among layers, difference was tested between SL and DL of each pooled area data. In turn, the differences between areas were tested for A1 and A2 for the SL and then the DL data. The variance of each variable's data was different from each other. Homoscedasticity was verified using test of Levenne and Bartlett. Normality of variables was tested using Shapiro-Wilk test. In the case where normality and/or homoscedasticity were not met, data were transformed (logarithmic, x^2 or $1/x$). To analyze the correlation between POC and the sum of the carbon estimation of total phytoplankton, bacteria and TEP, linear regressions were performed. Statistical analyses were carried out using XLstat-Base software.

1.3. RESULTS

1.3.1. ENVIRONMENTAL PARAMETERS

1.3.1.1. Salinity

Surfaec layer (SL) salinity displayed 23.61 ± 3.55 PSU and 25.74 ± 0.32 PSU, on average of respectively area 1 (A1) and area 2 (A2). T-test results showed no salinity significant difference among areas (Table. 1). At the DL, salinity showed 32.92 ± 2.05 PSU and 33.28 ± 1.04 PSU, on average of respectively A1 and A2. Variability tested among layers showed a significantly ($P < 0.01$) saltier deep layer (DL) waters rather than the surface layer (SL) (Table. 1).

1.3.1.2. Temperature

The SL temperature displayed 5.66 ± 1.35 °C and 4.61 ± 0.26 °C, on average of respectively A1 and A2. SL temperature had no significant difference among areas (Table. 1). At the DL, temperature values displayed 2.87 ± 1.20 °C and 0.92 ± 0.36 °C, on average of respectively A1 and A2. DL temperature was significantly ($P < 0.01$) higher in the A1 rather than A2. Among layers, the SL was significantly ($P < 0.01$) warmer than the DL temperature (Table. 1).

1.3.1.3. pH

The mean values of pH measurements recorded at the SL and the DL of A1 were equal to 7.94 ± 0.06 and 7.58 ± 0.10 , respectively. Measurements of pH performed in the A1 displayed a significant ($P < 0.01$) more acidic value at the DL rather than the SL (Table. 1).

	Among areas				Among layers			
	Surface layer		Deep layer		Area 1		Area 2	
	T-value	P-value	T-value	P-value	T-value	P-value	T-value	P-value
salinity	0.24	0.81	-0.44	0.65	4.41	< 0.01	-16.91	< 0.01
temperature	1.85	0.09	4.2	0.02	3.75	< 0.01	10.05	< 0.01
pH	-	-	-	-	1.01	< 0.01	-	-
nitrates	-0.09	0.38	1.78	0.02	-1.64	0.03	0.80	0.43
silicates	0.00	0.96	1.63	0.01	1.33	0.01	0.78	0.45
phosphates	2.78	0.01	-1.31	0.03	-2.51	0.02	-2.43	0.03
chl a	2.71	0.02	6.52	< 0.01	-4.66	< 0.01	-3.92	< 0.01
$\delta^{13}\text{C}$	-8.98	< 0.01	-11.59	< 0.01	0.00	0.99	-4.75	< 0.01
$\delta^{15}\text{N}$	2.55	0.02	5.48	0.01	-1.60	0.13	-2.73	0.02

Table. 1 Results of the T-test analysis among areas and among layers carried out on environmental parameters measured. Annotation: chl *a*: chlorophyll *a*.

1.3.1.4. Nutrients concentrations

The SL mean concentrations of nitrates were $12.90 \pm 4.39 \mu\text{g L}^{-1}$ and $11.14 \pm 6.19 \mu\text{g L}^{-1}$ in the A1 and and the A2, respectively. The SL silicates concentration showed $23.95 \pm 6.89 \mu\text{g L}^{-1}$ and $27.26 \pm 14.05 \mu\text{g L}^{-1}$ in the A1 and the A2, respectively. At the SL, nitrates and silicates concentrations exhibited no significant difference among areas. Significantly ($P < 0.05$) highest nitrates and silicates concentrations were recorded at the DL of A1 (Table. 1). On average values, nitrates and silicates displayed at the DL of A1, $18.39 \pm 6.27 \mu\text{g L}^{-1}$ and $35.67 \pm 16.27 \mu\text{g L}^{-1}$, while they showed $12.41 \pm 5.79 \mu\text{g L}^{-1}$ and $21.48 \pm 13.86 \mu\text{g L}^{-1}$, at the DL of A2, respectively. In turn, SL phosphates concentrations values displayed $0.27 \pm 0.17 \mu\text{g L}^{-1}$ and $1.59 \pm 1.16 \mu\text{g L}^{-1}$, on average of respectively A1 and A2, while, at the DL average phosphates concentrations were $0.13 \pm 0.04 \mu\text{g L}^{-1}$ and $1.25 \pm 0.54 \mu\text{g L}^{-1}$, respectively in A1 and A2. Phosphates concentrations displayed, among areas, significant ($P < 0.05$) higher concentrations were recorded in the A2 rather than the A1 (Table. 1). Moreover, among layers phosphates was significantly higher at the SL rather than the DL of both areas (Table. 1).

1.3.1.5. Chlorophyll *a*

The average concentrations of chlorophyll (chl *a*) at the SL of A1 and A2 were, respectively, $0.90 \pm 0.84 \mu\text{g L}^{-1}$ and $4.25 \pm 1.50 \mu\text{g L}^{-1}$, whereas in the DL, averages of chl *a* concentrations were $0.17 \pm 0.04 \mu\text{g L}^{-1}$ and $1.15 \pm 1.32 \mu\text{g L}^{-1}$, respectively. Among areas, chl *a* was significantly higher in the A2 rather than the A1 at both the SL and the DL (Table. 1). Chl *a* concentrations, were significantly ($P < 0.01$) higher at the SL rather than the DL of both areas.

1.3.1.6. Stables isotopes

The average values of $\delta^{13}\text{C}$ and $\delta^{15}\text{N}$ stable isotopic ratios are shown in Fig. 2. $\delta^{13}\text{C}$ displayed $-28.15 \pm 1.38 \text{‰}$ and $-28.15 \pm 1.53 \text{‰}$, on average values at the SL and the DL of A1, respectively. $\delta^{15}\text{N}$ displayed $17.29 \pm 4.71 \text{‰}$ and $11.87 \pm 6.79 \text{‰}$, on average of $\delta^{14}\text{N}$ at the SL and the DL of A1, respectively. Among layers, variability of the isotopic ratios depended on area. In A1, they showed no significant difference, whereas a significant ($P < 0.05$) variability was recorded in the A2.

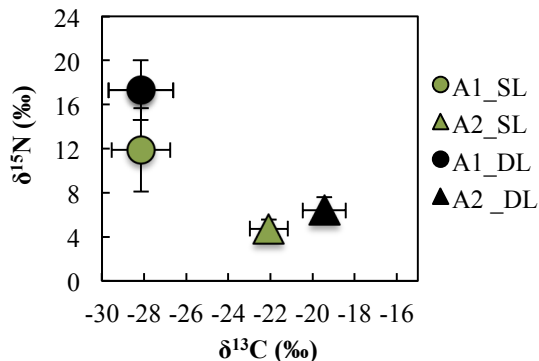


Figure. 2 The means of isotopic ratios of $\delta^{15}\text{N}$ and $\delta^{13}\text{C}$ observed in surface layer (SL) and in deep layer (DL) of area 1 (A1) and area 2 (A2).

In the A2, $\delta^{13}\text{C}$ showed $-22.07 \pm 0.90 \text{‰}$ and $-19.43 \pm 1.01 \text{‰}$, at the SL and the DL, respectively, while $\delta^{15}\text{N}$ showed $4.74 \pm 0.82 \text{‰}$ and $6.38 \pm 1.21 \text{‰}$ of $\delta^{15}\text{N}$, respectively.

Among areas, A2 showed significantly ($P < 0.01$) heavier $\delta^{13}\text{C}$ and lower $\delta^{15}\text{N}$ than A1 (Table. 1).

1.3.2. TRANSPARENT EXOPOLYMERIC PARTICLES

TEP concentrations values showed $88.87 \pm 65.50 \mu\text{g XG eq L}^{-1}$ and $23.96 \pm 8.63 \mu\text{g XG eq L}^{-1}$ on average of TEP at the SL and the DL of A1, respectively. TEP displayed $191.60 \mu\text{g XG eq L}^{-1}$ at the higher estuary and $149.95 \mu\text{g XG eq L}^{-1}$ at the fjord. While at the lower estuary TEP showed $63.51 \mu\text{g XG eq L}^{-1}$. At the head of the Laurentian trough (HLT) TEP increased gradually and exhibited $42.71 \pm 8.23 \mu\text{g XG eq L}^{-1}$ on average concentration (Fig. 3). At the DL, TEP concentrations had $23.96 \pm 8.63 \mu\text{g XG eq L}^{-1}$, on average value with the maximum concentration of $38.49 \pm 3.56 \mu\text{g XG eq L}^{-1}$ recorded at the DL of the lower estuary location (Fig. 3). At the SL of A2, higher values of TEP concentrations were displayed at F1- and F2- rather than F1+ and F2+ ($116.65 \mu\text{g XG eq L}^{-1}$ and $47.10 \mu\text{g XG eq L}^{-1}$, respectively at F1- and F1+; $90.33 \mu\text{g XG eq L}^{-1}$ and $74.52 \mu\text{g XG eq L}^{-1}$, respectively at F2- and F2+).

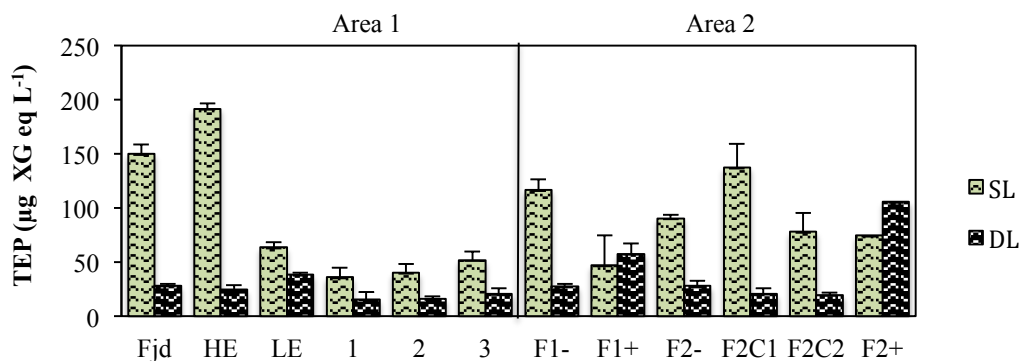


Figure. 3 Spatial distribution of transparent exopolymeric particles (TEP) in the areas 1 and the area 2. Green bars show data from the surface layer (SL) and black bars represent the deep layer (DL) measurements. Annotation: Fjd: fjord, HE: higher estuary and LE: lower estuary.

Relatively high concentration was recorded at F2C1 ($137.43 \mu\text{g XG eq L}^{-1}$), while F2C2 showed $78.06 \mu\text{g XG eq L}^{-1}$. At the DL of A2, TEP distribution showed, in contrast with the SL of A2, higher concentrations at F1+ and F2+ rather than F1- and F2- ($27.64 \mu\text{g XG eq L}^{-1}$ and $57.57 \mu\text{g XG eq L}^{-1}$, respectively at F1- and F1+; $27.84 \mu\text{g XG eq L}^{-1}$ and $105.77 \mu\text{g XG eq L}^{-1}$, respectively at F2- and F2+). Moreover, TEP in the DL of A2 showed maximum concentrations at the DL of F1+ and F2+. These values were higher than the corresponding SL concentrations of F1+ and F2+ (Fig. 3). Finally, in the center of F2, TEP was rather constant. It showed $20.82 \mu\text{g XG eq L}^{-1}$ and $19.70 \mu\text{g XG eq L}^{-1}$ at F1C1 and F1C2, respectively. Overall, transparent exopolymeric particles (TEP) spatial distribution exhibited no significant difference among areas, neither at the SL nor at the DL (Table. 2). Significant ($P \leq 0.01$) higher TEP concentrations were observed at the SL rather than the DL of the A1 and the A2.

1.3.3. PHYTOPLANKTON DENSITY

The spatial distribution of the phytoplankton density at the SL of the A1 showed maximum picophytoplankton ($<0.2 \mu\text{m}$) and nanophytoplankton ($2-20 \mu\text{m}$) at fjord, while maximum of microphytoplankton ($>20 \mu\text{m}$) was at the higher estuary Fig. 4). Phytoplankton cell density was higher at F1- and F2- than F1+ and F2+ (Fig. 4). At the SL of the A2, the phytoplankton sizes classes were significantly ($P < 0.01$) higher than the SL of A1 (Table. 2). It exhibited $4.47 \times 10^6 \text{ cell L}^{-1}$ at the SL of the A1 and $7.77 \times 10^6 \text{ cell L}^{-1}$ at the SL of the A2, on average cell density values. Results of the parametric analysis showed that among areas, microphytoplankton cells showed a significantly ($P < 0.01$) higher density in A2 rather than A1. Nanophytoplankton density was significantly ($P = 0.01$) higher at the DL of A2 rather than the DL of A1, whereas at the SL, no nanophytoplankton significant difference observed among areas. Finally, picophytoplankton did not show a significant difference among areas (Table. 2).

	Among areas				Among layers			
	Surface layer		Deep layer		Area 1		Area 2	
	T-value	P-value	T-value	P-value	T-value	P-value	T-value	P-value
TEP	0.97	0.35	-1.44	0.18	-4.07	<0.01	2.92	0.01
Micro	4.01	<0.01	-4.01	<0.01	2.34	0.04	-4.09	<0.01
Nano	0.63	0.54	-3.05	0.01	2.83	0.01	4.17	<0.01
Pico	-1.43	0.18	-0.44	0.66	-5.81	<0.01	5.41	<0.01
Bacteria	0.38	0.70	0.72	0.48	4.75	<0.01	3.97	<0.01
POC	-0.95	0.36	-0.58	0.57	2.75	0.02	-2.27	0.04

Table. 2 Results of the T-test analysis among areas and among layers carried out on transparent exopolymeric particle (TEP), microphytolankton ($>20 \mu\text{m}$) nanophytoplankton (2-20 μm) picophytoplankton ($<0.2 \mu\text{m}$), bacteria and particulate organic carbon (POC).

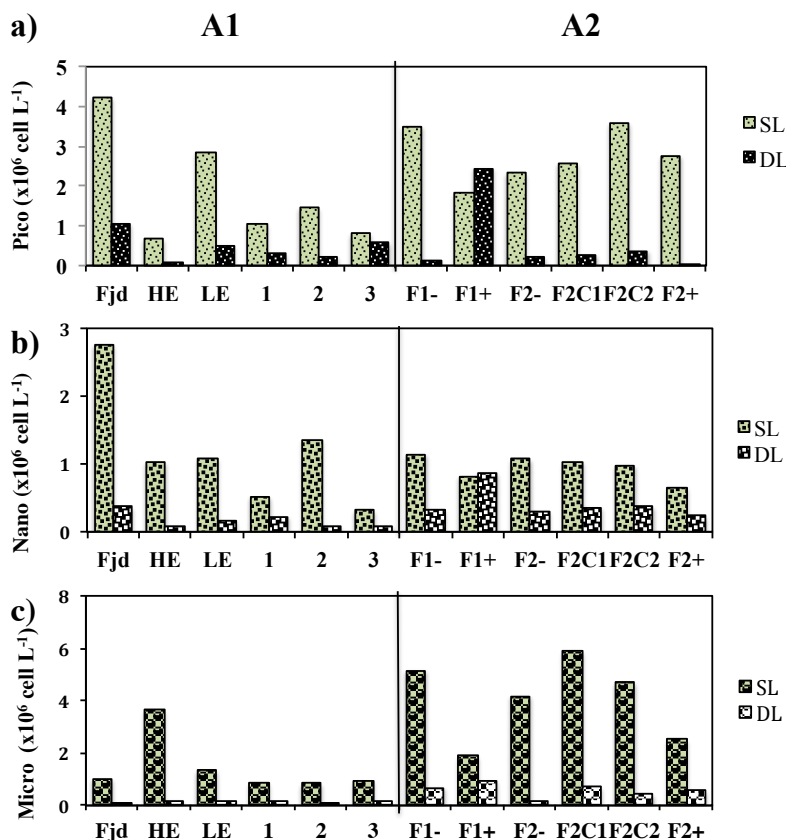


Figure. 4 Spatial distributions of phytoplankton cell density in both, areas 1 (A1) and area 2 (A2). Three size classes of phytoplankton were considered: a) picophytoplankton ($< 0.2 \mu\text{m}$) (a), nanophytoplankton (2-20 μm) (b) and microphytoplankton ($>20 \mu\text{m}$) (c). Green bars represent data from the surface layer (SL), while black and white bars correspond to deep layer (DL). Annotation: Fjd: fjord, HE: higher estuary and LE: lower estuary.

1.3.4. BACTERIAL DENSITY

Average bacterial density, recorded at the SL and the DL of A1, was $8.62 \pm 1.50 \times 10^8$ cell L⁻¹ and $5.02 \pm 1.10 \times 10^8$ cell L⁻¹, respectively. In the A2, it showed $8.24 \pm 1.90 \times 10^8$ cell L⁻¹ and $4.79 \pm 1.77 \times 10^8$ cell L⁻¹, respectively at the SL and the DL. The spatial distribution of bacteria showed no significant difference among different locations. Among areas, no significant difference was observed in the bacterial density. However among layers, bacterial density was significantly ($P < 0.01$) higher at the SL rather than the DL of both areas.

1.3.5. PARTICULATE ORGANIC CARBON

Concentrations of the total fraction of particulate organic carbon (POC) displayed varied between $89.23 \mu\text{g L}^{-1}$ and $245.70 \mu\text{g L}^{-1}$ at the SL and the DL of A1, respectively. POC concentration at fjord, higher estuary and lower estuary was relatively high ($189.85 \pm 26.39 \mu\text{g L}^{-1}$, on average value). Along the HLT transect, POC showed a gradually decreasing values, from $218.79 \mu\text{g L}^{-1}$ (at station 1) to $138.34 \mu\text{g L}^{-1}$ (at station 2) and $89.23 \mu\text{g L}^{-1}$ (at station 3). At the DL of A1, POC concentrations varied between $59.14 \mu\text{g L}^{-1}$ and $144.63 \mu\text{g L}^{-1}$ (Fig. 5). High values were exhibited by fjord, higher estuary and lower estuary locations ($126.76 \pm 15.50 \mu\text{g L}^{-1}$, on average value). Relatively low POC values were recorded at the HLT zone ($76.89 \pm 15.56 \mu\text{g L}^{-1}$, on average value). At the SL of A2, POC varied between $315.91 \mu\text{g L}^{-1}$ and $148.52 \mu\text{g L}^{-1}$. POC was higher at F1- rather F1+, while no significant difference recorded between the two water masses of F2 (Fig. 5). At the DL of the A2, POC ranged from $49.24 \mu\text{g L}^{-1}$ to $223.01 \mu\text{g L}^{-1}$. The DL of A2 exhibited similar distribution between F1 and F2. F1- and F2- displayed lower POC concentrations rather than F1+ and F2+ (Fig. 5). Highest DL concentration of POC were observed in the DL of A2, where in F1+ and F2+, POC exhibited respectively, $137.19 \mu\text{g L}^{-1}$ and $223.01 \mu\text{g L}^{-1}$. Results from T-test among layers showed that POC was significantly ($P < 0.05$) higher at the SL than the DL. Nevertheless, POC was rather constant among areas and showed no significant difference between A1 and A2.

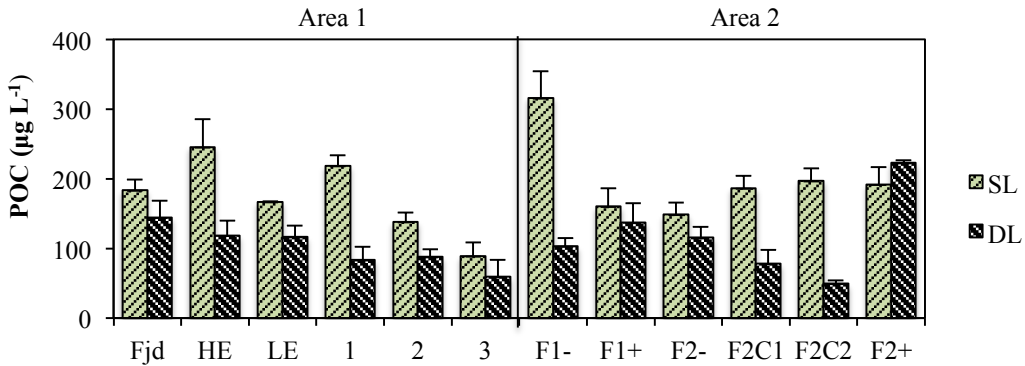


Figure. 5 Spatial distribution of particulate organic carbon (POC) concentrations ($\mu\text{g L}^{-1}$) in the area1 and the area 2. Green bars show data from the surface layer (SL) and black bars represent deep layer (DL). Annotation: Fjd: fjord, HE: higher estuary and LE: lower estuary.

1.3.6. CARBON CONTRIBUTION ESTIMATION

Linear regression analysis showed that POC concentrations were significantly correlated to the sum of the carbon estimations of TEP, bacteria and total phytoplankton. This sum will be defined as estimated POC (estim_POC) ($\text{POC} = 0.64 \times \text{Estim_POC} + 74.43$; $r = 0.81$; $p < 0.01$) (Fig. 6). Data collected from the SL and the DL showed, at a significant confidence interval, same correlation trend between POC and estim_POC. However, DL data presented several values away from the regression curve ($r = 0.81$) and were above the curve ($r = 1$). Separately, the DL POC data could form a significant positive regression with estim_POC ($\text{POC} = 0.76 \times \text{estim_POC} + 59.14$; $r = 0.80$) that would be entirely on the top of the curve $r = 1$, whereas the SL data varied more around the axis $r = 1$ ($\text{POC} = 0.54 \times \text{estim_POC} + 84.62$; $r = 0.85$). Spatial distribution of the relative carbon contribution (CC) of TEP (TEP_CC), phytoplankton (phyto_CC), bacteria (bact_CC), and detritus (det_CC) to POC concentrations is showed in Fig. 7. Det_CC was expressed as the residual part of POC and was obtained by subtracting estim_POC from POC. However, no data for det_CC was obtained for fjord, higher estuary, F2- and F2C1 stations, while at these stations estim_POC exceeded POC. During statistical analysis, it was considered as a missing data.

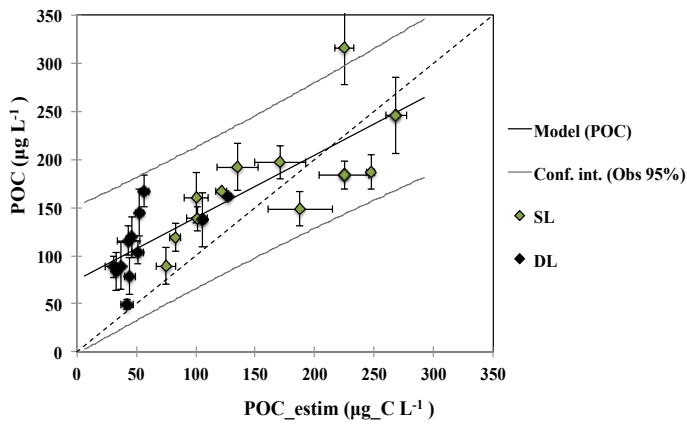


Figure. 6 Linear regression between particulate organic carbon (POC) and estimated POC (estim_POC) concentrations in the surface layer (SL) and the deep layer (DL) of both areas ($r= 0.81$; $P< 0.01$).

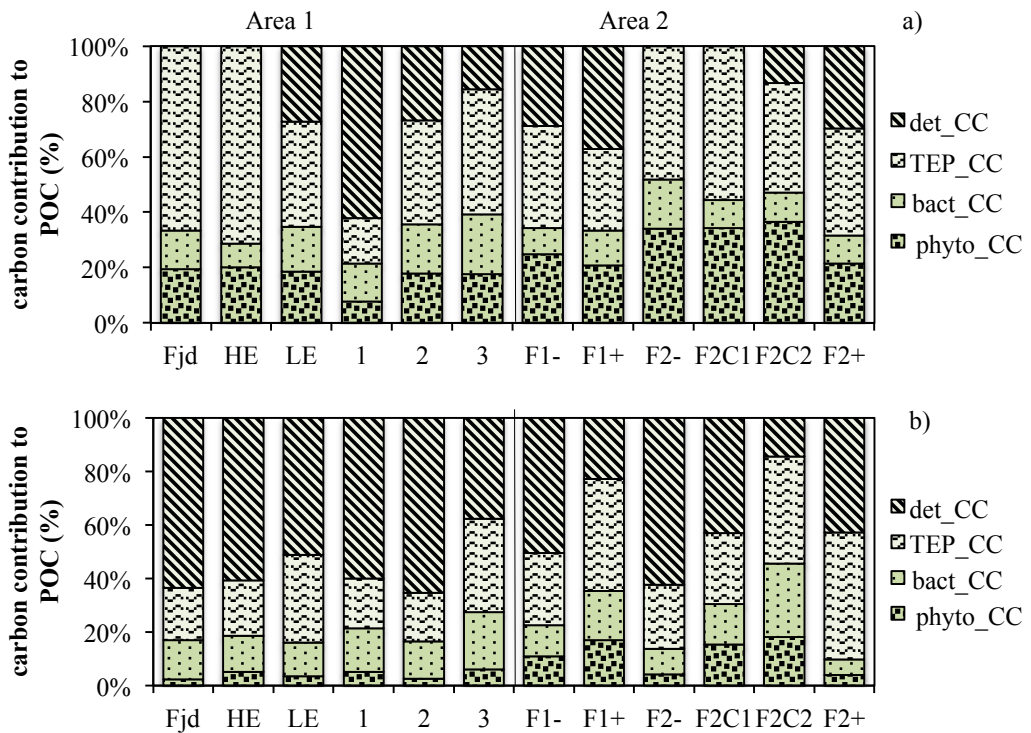


Figure. 7 Spatial distribution of the relative contribution of the estimated carbon concentrations from phytoplankton (phyto_CC), bacteria (bact_CC), transparent exopolymeric particles (TEP_CC) and other organic matter (detritus_CC) to total particulate organic carbon (POC) at the surface layer (a) and at the deep layer (b) of the area 1 and the area 2. Annotation: Fjd: fjord, HE: higher estuary and LE: lower estuary

At fjord and higher estuary TEP_CC and phyto_CC had rather constant contribution (81.62 % and 23.85 %, respectively at fjord; 77.98 % and 21.89 %, respectively at higher estuary). Relatively high contribution of the SL bact_CC was recorded at fjord station (16.92 %). At lower estuary phyto_CC and bact_CC exhibited similar contribution (18.47 % and 16.31 %, respectively), while TEP_CC and det_CC had relatively lower values (38.01 % and 27.21 %, respectively). Throughout the transect TEP_CC, phyto_CC and bact_CC gradually increased from station 1 to 3 (Fig. 7). On the other hand, det_CC exhibited a decreasing horizontal gradient with an opposite trend. At the SL of A2, result of the relative contributors to POC was not enough conclusive. Contribution seemed to be constant among locations. It showed 38.36 ± 12.42 % of TEP_CC, 33.98 ± 10.55 % of phyto_CC and 13.08 ± 4.85 % of bact_CC, on average values of the SL of the A2.

Carbon spatial distribution at the DL of A1 exhibited highest bact_CC and lowest phyto_CC at fjord (14.67 % and 2.30 %, respectively) (Fig. 7). Higher estuary had relatively high phyto_CC and lower bact_CC than fjord (5.08 % and 13.46 %, of respectively phyto_CC and bact_CC at fjord). The lower estuary station displayed relatively high TEP_CC and low det_CC (32.90 % and 51.16 %, respectively). At the DL of A2, F1+ showed higher TEP_CC, phyto_CC and bact_CC values and lower det_CC (41.97 %, 16.99 %, 18.27 % and 22.77 % respectively at F1+) rather than F1- (26.80 %, 10.94 %, 11.70 % and 50.57 %, respectively at F1-). At the DL of F2, TEP_CC and Bact_CC were higher at F2+ than F2- (24.08 % and 5.69 %, respectively at F2-; 47.43 % and 9.44 %, respectively at F2+). Phyto_CC was rather constant between F2- and F2+ (4.20 % and 4.05 %, respectively). Det_CC was higher at F2- rather than F2+ (62.28 % and 42.83 % respectively at F2- and F2+). No significant difference was recorded among areas and among layers within TEP_CC, bact_CC and det_CC, except phyto_CC which had a significantly higher contribution at the SL of A2 rather than A1 ($t_{0.05(2),6} = -2.97$, $P = 0.01$). The main contribution to POC seemed to be represented by TEP_CC at the SL of A1 and A2 (49.45 ± 25.42 % and 46.53 ± 16.92 %, on average of TEP_CC, respectively in the SL of A1 and the SL of A2). Yet, TEP_CC at the SL was not significantly higher than other contributors. At the SL of A1, TEP_CC was significantly higher than phyto_CC and than

bact_CC ($t_{0.05(2),6} = 2.97$, $P = 0.01$; $t_{0.05(2),6} = 3.18$, $P = 0.01$, respectively). Whereas, no significant difference recorded between TEP_CC and det_CC at the SL of A1 ($t_{0.05(2),6} = 1.08$, $P = 0.31$). Furthermore, at the SL of A2, TEP_CC was only significantly higher than bact_CC ($t_{0.05(2),6} = 4.65$, $P < 0.01$). No significant difference noted neither between TEP_CC and phyto_CC nor between TEP_CC and det_CC at the SL of A2 ($t_{0.05(2),6} = -1.76$, $P = 0.10$ and $t_{0.05(2),6} = 2.02$, $P = 0.07$, respectively). At the DL of A1 and A2, det_CC had relatively high contribution to POC, except at F1+ and F2+ stations. T-test results which showed that the DL det_CC was significantly higher than phyto_CC and bact_CC in the A1 ($t_{0.05(2),6} = 10.99$, $P < 0.01$ and $t_{0.05(2),6} = 9.22$, $P < 0.01$, respectively at the DL of A1) and in the A2 ($t_{0.05(2),6} = 3.60$, $P < 0.01$ and $t_{0.05(2),6} = -2.49$, $P = 0.03$, respectively in the DL of A2). However results of comparison between the DL Det_CC and the DL TEP_CC were dependent on area. At the DL of A1, Det_CC was significantly higher than TEP_CC ($t_{0.05(2),6} = -5.88$, $P < 0.01$). At the DL of A2, no significant difference recorded between the two parameters. Over all, the principal component was varying between TEP_CC, det_CC and phyto_CC, depending on the location.

1.4. DISCUSSION

1.4.1. TWO CONTRASTING AREAS OF THE LSLE

Area 1 and area 2 in this section will be named as the upwelling area and the front area, respectively. Characteristics of the surface layer (SL) and the deep layer (DL) of the lower St-Lawrence estuary (LSLE) were observed in our measurements. Temperature and salinity displayed a significant difference among layers. Upwelling and front areas displayed a warmer and low salinity SL in contrast with a colder and saltier DL. Furthermore, pH measurements in the upwelling area displayed more acidic values in the DL rather than the SL. This coincides with observations realized by Gilbert *et al.* (2005) and Mucci *et al.* (2011) who documented the development of persistent, severely hypoxic and acidic waters at the DL of the permanently stratified LSLE. In this study, determination

of pH was carried out only in the upwelling area, in order to examin the effect of the tidally-induced upwelling of the acidic and hypoxic DL on the SL biomass. Nevertheless, our observations of the pH spatial distribution did not detect the presence of acidic waters at the SL of A1. These results could be explained by the important role of the cold intermediate layer of the LSLE, which impedes the upwelling of the hypoxic and acidic DL to the SL (Mucci *et al.*, 2017). These explications was suggested by Mucci *et al.* (2017) which observed the variations of the pH of the water column over two tides cycles at the head of the Laurentian Trough (HLT) zone.. However, only the SL and the DL were considred in this work. The SL that, yearly becomes progressively warmer and less dense, as air temperature and tributary flow increases, until it seperates from the cold intermediate layer. The DL is a mixture of the Labrador Current and the North Atlantic Central waters whose proportions vary on a decadal or secular timescale (Gilbert *et al.*, 2005).

The examination of the natural density of stable carbon ($\delta^{13}\text{C}$) and nitrogen ($\delta^{15}\text{N}$) isotopes, suggested that particulate organic carbon (POC) in our study, had a different origin among areas. Our results are in accordance with estimates from earlier studies on the St-Lawrence estuary system (Pocklington and Tan, 1987). According to a three-year study performed in the St-Lawrence estuary, the limit between terrestrial and marine matter was considered to be -27.0 and +6.5 as the terrestrial end number of, respectively $\delta^{13}\text{C}$ and $\delta^{15}\text{N}$ (Pocklington and Tan, 1987). Moreover, in our observations $\delta^{13}\text{C}$ was heavier in the front area rather than the upwelling area, whereas $\delta^{15}\text{N}$ was heavier in the upwelling area than front area (Fig. 2). Then, upwelling area was dominated by terrestrial carbon, being in the proximity of the two important freshwater sources of the estuary (St-Lawrence and Saguenay rivers). The heavier limit of -25.55 ‰ for $\delta^{13}\text{C}$ observed at the upwelling area was probably related to the influence of the more oceanic DL water of the area. $\delta^{13}\text{C}$ recorded in the front area indicated the dominance of marine carbon, where the proportion of oceanic waters is more important than the upwelling area. In contrast, $\delta^{15}\text{N}$ in the upwelling area was heavier than that recorded in the front area and was probably originated from the oceanic waters upwelled from the DL. Moreover, upwelling area displayed no significant difference, of neither $\delta^{13}\text{C}$ nor $\delta^{15}\text{N}$ among layers. While in the front area, a

significant heavier $\delta^{13}\text{C}$ and $\delta^{15}\text{N}$ ratios were displayed in the DL rather than the SL. This reflected the differences in physical processes of each of these areas. Upwelling area is characterized by higher vertical mixing, which could explain the non-significant difference in the isotopic signature between the SL and the DL.

In this study, oceanic nutrients distribution was only observed in the upwelling area for nitrates and silicates, which exhibited significantly higher concentrations in the DL rather than the SL (Table. 1). However, in the area of front, they showed no significant difference between the SL and the DL. Moreover, phosphates concentrations were significantly higher at the SL rather than the DL of both areas. In the LSLE, nutrients distributions are determined by, the estuarine circulation pattern and the biological cycling (El-Sabh, 1990; Levasseur and Therriault, 1987). Nutrients are supplied to the SL by rivers discharge, and mostly by vertical mixing and upwelling (Greisman and Ingram, 1977). A high rivers discharge could explain the higher SL phosphates concentrations observed in our measurements. Relatively low silicates and nitrates at the SL suggested that these nutrients are limited and are quickly assimilated by the biomass. Moreover, the efficiency of the upwelling dynamics in the resuspension and the vertical oscillations of nutrients induce permanent higher silicates and nitrates concentrations at the DL of the upwelling area (Greisman and Ingram, 1977; Levasseur and Therriault, 1987). Moreover, the relatively constant nutrients concentrations observed at the SL and the DL of the front area could be related to the important role of front in vertical transport and the supply of nutrients to the euphotic zone (Mahadevan and Archer, 2000). Chlorophyll *a* (chl *a*) concentrations were significantly higher in the front area rather than the upwelling area. This can be related to the fact that sampling was in May and June, which correspond to the maximum of phytoplankton production activity related to the late spring bloom. Elevated chl *a* concentration observed in the A2 may be then related to a spring phytoplankton bloom (Therriault *et al.*, 1990; Annane *et al.*, 2015) or to a higher nutrients originated from physical pumping of the frontal zone that generates high phytoplankton productivity (Fernández *et al.*, 1993; Franks and Chen, 1996; Kahru *et al.*, 1984). The low dense water mass (F-) and the denser water mass (F+), which we will name in this section the light

water mass (LWM) and the heavy water mass (HWM), respectively. In the SL of both frontal zones, the LWM was relatively fresher, warmer, weaker in nutrients and richer in chl *a*. However, the HWM was relatively saltier, colder, richer in nutrients and weaker in chl *a*. These results suggested that fronts detected in our study were probably, formed by the warmer low salinity estuarine waters encountering the more saline and denser marine waters. Frontal zones observed in this study are probably related to a previously described fronts area of the region named the Pointe-des-Monts cold fronts (Lavoie *et al.*, 1985).

1.4.2. TEP SPATIAL DISTRIBUTION IN THE UPWELLING AND THE FRONT AREAS

Transparent exopolymeric particles (TEP) in this study were significantly higher at the SL than the DL (Fig. 3). Associated with phytoplankton bloom, TEP higher concentrations have been found in the euphotic zone than below it (Passow, 2002b; Passow *et al.*, 2001; Engel and Passow, 2001). Previous observations of the seasonal distribution of TEP in the LSLE showed that higher TEP concentrations coincided with the phytoplankton biomass peaks (Annane *et al.*, 2015). However average of TEP spring concentrations recorded in our study ($89.77 \pm 48.84 \mu\text{g XG eq L}^{-1}$, on average of TEP at the SL) were below concentrations of TEP recorded at late spring from Annane *et al.* (2015) observations ($306 \mu\text{g XG eq L}^{-1}$). In fact, their TEP spring results showed a phytoplankton pulse at late May, accompanied with high TEP values in the whole water column (up to $501 \mu\text{g XG eq L}^{-1}$). Considering these observations, we can suggest that our sampling period was before the spring bloom. In comparison with other estuarine environments, TEP in the SL of the LSLE are among the lowest estuarine concentrations displayed and among the highest marine concentrations (Table. 3). TEP values showed that, compared to marine environments, concentrations are higher in the SL of the LSLE rather than the northeast Atlantic Ocean and the Bay of Biscay, which displayed relatively comparable POC values. However, TEP/POC ratio estimated for the LSLE, were among the highest. Additionally, TEP at the LSLE was comparable to TEP recorded at Gulf of Aqaba and Cananéia estuary, which showed similar or even lower concentrations (Dona Paula bay) chl *a* concentrations

as that recorded at the LSLE. Moreover, TEP/chl α ratio for the LSLE estimated is among the highest estuarine ratios and within the average in comparaison with marine environements. TEP/chl α , of the LSLE are comparable to that calculated for Johor strait and Neuse river estuary which exhibited highest TEP concentrations.

TEP spatial distribution within the SL of the upwelling area exhibited highest concentrations at higher estuary and fjord. Lower values were recorded at the HLT and the lower estuary. This TEP distribution was possibly associated to the maximum microphytoplankton biomass observed at higher estuary and the maximum picophytoplankton and nanophytoplankton at fjord, in comparaison to the HLT. Despite the fact that, previous observations from the Saguenay fjord showed a low level of productivity (Côté and Lacroix, 1979; Pelletier *et al.*, 1999), high biomass of the smaller phytoplankton cells and bacteria cells were observed at fjord location of this study. Higher estuary was characterized by highest biomass of relatively larger phytoplankton cells (microphytoplankton) (Fig. 4). It is influenced by freshwater algae species (Lafleur *et al.*, 1979). Furthermore, the HLT zone displayed a relatively low phytoplankton and bacteria biomass. However, there are many other parameters that could explain the TEP spatial distribution obtained. At the HLT, the low TEP concentration observed could be related to phytoplankton low productivity. The vertical mixing that characterizes the zone could influence TEP concentration. Phytoplankton photosynthesis is often inhibited by high irradiance near the SL and is limited by low irradiance below the SL. So there is a narrow depth where light favors phytoplankton growth. In a location with a high vertical mixing, as the HLT, the downward light flux cannot be vertically mixed, while phytoplankton cells can be vertically redistributed relative to the vertical mixing of the region. Generally, vertical mixing affects the photoadaptation of the phytoplankton cells (Marra, 1978), by mixing the cells through a light gradient. This may affect certain species of phytoplankton that cannot respond to high-frequency light fluctuations (Harris, 1980).

Locations	TEP ($\mu\text{g XG eq L}^{-1}$)		POC ($\mu\text{g L}^{-1}$)		Chl <i>a</i> ($\mu\text{g L}^{-1}$)		TEP/POC	TEP/Chl(a)	Reference
Estuaries	mean	range	mean	range	mean	range			
Lower St-Lawrence estuary, Canada	90 306	36 - 192 140 - 501	187 197	89 - 316 48 - 409	2.5 4.4	0.2 - 6.8 3.2 - 6.2	0.4 1.5	36 69.5	This study Annane <i>et al.</i> , 2015
Chesapeake bay, USA	649	370 - 1326	943	712 - 1738	nd	5.7	3.5 - 7.6	0.6 nd	Malpezzi <i>et al.</i> , 2013
Cananéia estuary, Brazil	98	28 - 552	nd	nd	nd	nd	nd	17.2	Barrera-Alba <i>et al.</i> , 2012
Neuse river estuary, USA	1521	1512 - 1529	nd	nd	19	16 - 22	nd	80.5	Wetzel <i>et al.</i> , 2009
Johor strait, Singapore	2263	280 - 8026	nd	nd	74	5 - 183	nd	30.5	Worl and Holmes, 2008
Dona Paula bay, India	62	26 - 149	nd	nd	4.2	2.7 - 6.4	nd	14.7	Bhaska and Bholse, 2006
Marine environments									
Bay of Biscay	28	9 - 64	144	120 - 181	1.4	0.8 - 2	0.2	20	Harley <i>et al.</i> , 2009
Mediterranean sea	29	19 - 53	nd	0.02	0.01 - 0.06	nd	1450	Ortega-Petrueta <i>et al.</i> , 2010	
Gulf of Aqaba	114	23 - 228	nd	2.3	1.8 - 3.8	nd	49	Bar-Zeev <i>et al.</i> , 2009	
Northeast Atlantic Ocean	46	20 - 67	240	144 - 421	0.6	0.2 - 9.95	0.2 77	Engel, 2004	

Table 3 Average and range surface layer spring (May – Juin) values of transparent exopolymeric particles (TEP $\mu\text{g XG eq L}^{-1}$), particulate organic carbon (POC $\mu\text{g L}^{-1}$) and chlorophyll (a) (chl *a*; $\mu\text{g L}^{-1}$) for estuarine and marine environments. Ratios of the mean values were estimated and are showed for TEP/POC and TEP/chl *a*. Annotation: nd: not determined.

Furthermore, TEP low concentrations recorded at the HLT could be directly related to the vertical mixing. The internal tides and the vertical mixing of the zone could distribute TEP over the entire water column. In addition, the upwelling of waters from the DL with a significantly lower TEP concentration could impact TEP distribution.

In turn, the gradually seaward increased TEP concentration observed at the SL of the HLT was also observed in a gradually seaward increasing values of salinity and $\delta^{15}\text{N}$ and a decreasing values of temperature, chl *a*, and $\delta^{13}\text{C}$. At the DL of the HLT, a gradually seaward increasing values of temperature and $\delta^{13}\text{C}$ and a decreasing values of chl *a*, and $\delta^{15}\text{N}$ were recorded. This suggests an influence of internal tides generated at the HLT zone, which propagate seaward in a horizontal gradient that results in a large spatial horizontal gradient of density and influence the distribution of the biological parameters. Moreover, this gradient, especially at the SL, could be related to the intrusion of water masses from a mix between the higher estuary and fjord waters to the LSLE.

During the study of TEP distribution within the front area, two frontal zones were identified (F1 and F2). In the SL of the F1, the LWM displayed higher TEP concentrations in comparaison with the HWM (Fig. 3). This distribution was in accordance with chl *a* concentrations and the biomass of phytoplankton and bacteria. These results reflected the differences in organic carbon concentrations and origin between water masses of F1. Highest TEP concentrations were recorded in the center of F2. This distribution was in concordance with chl *a* concentration and microphytoplankton density. A prominent maximum of biomass has been usually found within fronts (Traganza *et al.*, 1987). This biomass accumulation decreases rapidly toward the nearshore of the front (Franks, 1992). Thus, the importance of the circulation pattern characterizing fronts that influenced biomass distribution. This frontal circulation, usually associated with a density difference between the two water masses, is convergent at the surface boundary and maintains the front as a sharp transition (Lacroix, 1998).

Observations at the DL of the front area showed that TEP concentrations in the DL of front area are lower or similar to the coresponding SL. In the HWM of both fronts of the

front area, higher TEP concentrations were recorded at the DL rather than the SL. The particularity of the DL of the front area was the relatively high temperature and chl *a* values. This was probably due to a downwelling flow identified with the pattern of the temperature of a phytoplankton thin layers study from the same mission (Accot, 2015). This downward vertical advection dynamics was confirmed by the dominance of a non-motile species, e.g. *Thalassiosira sp.* in the DL samples (Accot, 2015) and the vertical velocity of 10 m day^{-1} , estimated using data from the same cruise and a mixed layer quasi-geostrophic model (Robitaille, 2015). Moreover, Accot (2015) recorded an association between the fluorescence layer and the advection mechanisms and explained the exceptional phytoplankton biomass reported in the DL as an intrusion mechanism during frontal processes. Advection dynamics was caused by the frontal dynamics, which probably rapidly caused the downwelling of the SL phytoplankton cells. In a front typical physical processes characterized by an important vertical flux TEP may be easily downwelled to the DL of the LSLE, especially during spring. During spring, estuarine environments in cold temperate latitudes are strongly influenced by the peak of freshwater runoff. An important load of organic particles is transferred from rivers basins to the estuary. TEP formation and sedimentation during such a period is probably accelerated by the high detritus concentration and also front vertical downward advection. Relatively high concentrations of TEP recorded in the DL of the HWM of both fronts were considered as additional evidence that the cross-frontal density difference probably acted vertically on the water column and formed vertical flux (Garvine, 1974; 1977).

1.4.3. TEP AND POC CORRELATION

The hypothesis, that the presence of TEP was modulated by environmental parameters, was verified using a principal component analysis (data not shown). The results indicate that during our study TEP concentrations were mainly correlated to POC in the SL and the DL (Fig. 8). Gradients of salinity and temperature of our observations were not large enough to test a large variability. TEP showed a trend of correlation to phytoplankton

biomass but not a significant correlation. TEP concentrations were significantly and positively correlated to POC concentrations ($r= 0.77$; $P < 0.01$).

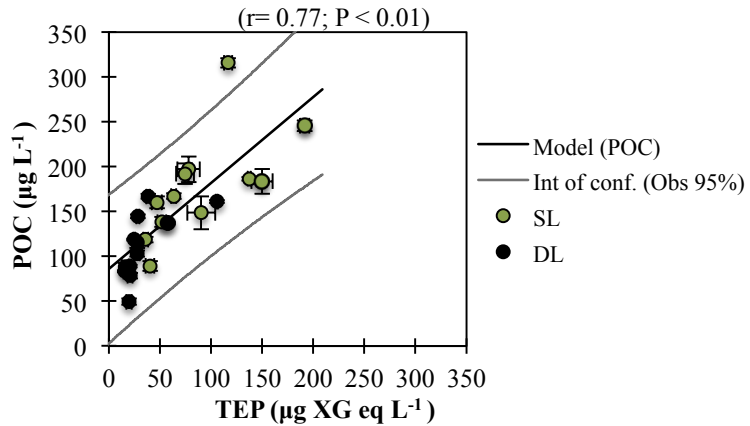


Figure. 8 linear regressions between data of transparent exopolymeric particles (TEP) and particulate organic carbon (POC) obtained at the surface layer (SL) and the deep layer (DL) of the upwelling area and the front area of the LSLE. Annotation: Int of conf: interval of confidence.

This direct relationship is in agreement with previous studies that highlighted the correlation between both variables in other aquatic environments (e.g. Mari, 1999; Engel and Passow, 2001) and in the LSLE (Annane *et al.*, 2015). TEP have been described to contribute to POC as conventional particles do (Passow, 2001).

1.4.4. SPATIAL DISTRIBUTION OF THE CARBON CONTRIBUTION OF TEP TO POC

Despite the particular physical hydrodynamics and the low phytoplankton biomass, POC on the upwelling area had relatively high values, which decreased seaward. At the SL of the upwelling area the main contributor to POC was varying between TEP carbon contribution (TEP_CC) and detritus carbon content (det_CC). Station 1 showed the lowest TEP_CC and the highest det_CC contributions to POC. Most of the POC pool of the station

1 was dominated by det_CC. Values of TEP_CC, bacteria carbon content (bact_CC) and total phytoplankton carbon content (phyto_CC) increased seaward at the HLT zone. Whereas det_CC decreased seaward. This distribution could be explained by the horizontal decreasing gradient of internal tides amplitude. Station 1 was the nearest to the topographic HLT and had the highest det_CC related to a possible highest internal tides.

Within the SL of the upwelling area, fjord and higher estuary showed the highest TEP_CC (82% and 78 %, respectively). Nevertheless, at fjord and higher estuary the estimated_POC exceeded the corresponding POC concentration. This may be related to an over-estimation of TEP concentrations. The colorimetric method, recommend the use of 0.2 μm polycarbonate filters, while for POC measurements we used 0.7 μm GF/F filters. There was a gap between both analytic methods adopted for both parameters. However, many studies suggested that 0.2 μm filters are the most efficient for TEP concentration measurements (Passow and Alldredge, 1995; Passow 2002; Wetz *et al.*, 2009). Passow and Alldredge (1995) observed that more than 50% and 42% of TEP concentrations are lost when using 0.6 μm or a 0.4 μm instead of 0.2 μm filters. Although the importance of the colloidal fraction (0.2 – 0.7 μm). It involves an active level of aggregation especially in highly hydrodynamic environments (Wells, 1998). In addition, other authors such as Beauvais *et al.* (2003) and Annane *et al.* (2015) recorded relatively excessive TEP_CC to POC. They related it to methodological constraints or to the fact that TEP_CC and POC relationship is specific species dependent. In our results, TEP and POC were significantly correlated and the estimated POC presented the best mean for the estimation of the relative contribution of TEP_CC, phyto_CC, bact_CC and det_CC to POC at the SL. However, this relationship was related to the location. As mentioned above, fjord and higher estuary showed relatively higher TEP_CC than other stations. This could be explained by a high concentration of the colloidal fraction of TEP at these locations, especially during spring. Retained on a filter of 0.2 μm , this fraction may explain the over-estimation of TEP. In fact, this result highlights the importance of the colloidal fraction of TEP within the higher estuary and the fjord.

At the SL of the front area, phyto_CC was significantly and relatively higher in comparaison with the SL of the upwelling area, while bact_CC was rather similar (Fig. 7). Significant high chl *a* and phytoplankton biomass recorded in the front area rather than the upwelling area (Fig. 4), could be related to a phytoplankton accumulation due to passive convergent transport toward the front and/or it may be due to in situ production in the front zone (Pingree *et al.*, 1975). Moreover, phytoplankton displayed in the front area only a significant higher microphytoplankton biomass in comparison with the upwelling area (Fig. 4), while no significant differences were observed in both picophytoplankton and nanophytoplankton biomass. Considering the short time scale (3 days) of the F1 and F2 survey, there were few phytoplankton species or groups, which can respond rapidly enough to the fluctuating physicochemical conditions to bring about a significant increase in their productivity in estuarine fronts (Tyler and Seliger, 1978; De Mendiola, 1981; Blasco *et al.*, 1981). In addition, Denman and Powell (1984) have shown through theoretical calculations, how short-period internal hydrodynamics can be important to the production of phytoplankton cells through a coupling of physical and biological times scales. This suggested that in situ production might be relevant for selected phytoplankton species that could explain the exclusive higher microphytoplankton biomass observed in our study. The main carbon contributor to POC, at the SL of the front area, varied among TEP_CC, det_CC and phyto_CC, depending on location. Phyto_CC in the front area had an important contribution to the POC pool, reaching a maximum of 45 %. Finally, det_CC contributions recorded at the SL of the front area were lower than that observed at the upwelling area. This reflected the dynamic of each area: upwelling or downward advection flux. At the DL of the upwelling area, TEP_CC was the second contributor to POC. Det_CC was the main contributor. This highlighted the importance of the det_CC in the DL of the upwelling area and suggested to be correlated to the resuspension of POC resulting from vertical mixing and internal tidal currents. At the DL of the front area, det_CC was not the main contributor to POC. No significant difference recorded between det_CC and TEP_CC at the DL of front area. This was related to a possible downward flux generated by the hydrodynamism of the front. These results are in accordance with the hypothesis that a cross-frontal downward vertical transfert of POC was the origin of the relatively high values of the DL

of the front area. Although, considering the fast sinking rates of POC previously recorded in the LSLE of about 10 to 100 m d⁻¹ (Larouche and Boyer-Villemaire, 2010), we hypothesize that under front dynamics, sinking rates could be accelerated and generated the DL high POC concentrations.

Overall, det_CC was either the main contributor or a part of the main contributor associated with TEP_CC and/or phyto_CC. Hence the importance of detritus and TEP biomass in the LSLE. Considering, that data of this study was collected during spring the St-Lawrence estuary receive the discharge of a critical amount of POC. A large part of this matter is transported to the LSLE. The organic carbon cycle of the LSLE is not only influenced by this discharge but also by the physical processes and the local productivity that characterizes the estuary. Our findings showed that, in an area with such dynamic, TEP represented an important part of the POC pool of the LSLE. However, limitation of our research is related to the fact that we only sampled the SL and the DL of the LSLE and we did not sample the colloidal fraction of TEP. Moreover, data concerning physical processes and amplitude of internal currents could give more certainty regarding TEP dynamics. Our study and Annane *et al.* (2015) research showed that TEP represents an important fraction of POC pool in the LSLE.

CHAPITRE 2

EFFECTS OF GLOBAL CHANGE ON TRANSPARENT EXOPOLYMERIC PARTICLES DURING A MESOCOSM SUB-ARCTIC DIATOM BLOOM

RESUME

Une expérience en mésocosmes a été réalisée dans l'optique d'évaluer les effets de l'augmentation de l'acidification et de la température sur les particules exopolymériques transparentes (TEP) de l'estuaire maritime du Saint-Laurent (LSLE, en anglais). Cinq valeurs de pH allant de 8,0 à 7,2 ont été testées dans deux niveaux de température (10 °C et 15 °C) durant un bloom de diatomés dominé par *Skeletonema costatum*. Nos résultats ont suggéré qu'une augmentation de l'acidité engendrée par l'augmentation de la concentration dissoute en CO₂ résulte en un plus faible taux de croissance du phytoplancton et une augmentation du taux d'assimilation du CO₂ qui se manifeste en un ratio TEP/carbone organique particulaire (POC) plus élevé. Une diminution de 0,2 unités du pH a entraîné une diminution moyenne de $0,03 \pm 0,07 \text{ d}^{-1}$ dans le taux de croissance spécifique du phytoplancton et une diminution moyenne de $86,28 \pm 19,61 \mu\text{g C L}^{-1}$ et de $119 \pm 6,03 \mu\text{g C L}^{-1}$ dans les concentrations des TEP et du POC enregistrés au maximum de la chlorophyll a, respectivement. La quantification des monosaccharides a montré une réponse significativement positive du glucose et du galactose et une réponse significativement négative de l'arabinose et du mannose au gradient décroissant du pH. Une diminution de 0,2 unité du pH a engendré une augmentation moyenne de $0,20 \mu\text{g L}^{-1}$ dans la concentration totale en carbohydrates normalisée à la biomasse du phytoplancton. L'augmentation de la température a eu un effet positif sur la biomasse phytoplanctonique, la concentration en carbohydrates et un effet négatif sur les ratios TEP/phytoplancton et TEP/POC. La hausse de la température a suggéré une accélération du taux de croissance du phytoplancton ce qui a induit une biomasse dominée par de petites cellules phytoplanctoniques résultant en une concentration plus importante en monosaccharides. Ceci a résulté en une concentration plus importante en monosaccharides qui ont probablement demeuré dans la fraction dissoute en raison d'une température plus élevée qui a probablement bloqué la formation des TEP. L'effet de l'augmentation de la température et de l'acidification demeure incertain suggérant une adaptation du phytoplancton des régions côtières face à ces changements.

Mots clefs : LSLE, TEP, POC, phytoplancton, pH, température et mésocosme.

ABSTRACT

A mesocosm experiment was carried out to evaluate the effects of increased acidification and temperature on transparent exopolymeric particles (TEP) in the lower St-Lawrence estuary (LSLE). Five pH values ranging from 8.0 to 7.2 were tested in two temperature levels (10°C and 15°C) during a *Skeletonema costatum* dominated diatom bloom. Our results have suggested that an increase in the acidity caused by the increase in the dissolved CO_2 concentration results in a lower phytoplankton growth rate and an increase in the CO_2 assimilation rate which manifests in a higher TEP/particulate organic carbon (POC) ratio. A decrease of 0.2 pH units resulted in an average decrease of $0.03 \pm 0.07 \text{ d}^{-1}$ in the phytoplankton specific growth rate and an average decrease of $86.28 \pm 19.61 \mu\text{gC L}^{-1}$ and of $119 \pm 6.03 \mu\text{gC L}^{-1}$ in the concentrations of TEP and POC recorded at maximum of chlorophyll *a*, respectively. Monosaccharides quantification showed a significantly positive glucose and galactose response and a significantly negative response of arabinose and mannose to the decreasing pH gradient. A decrease of 0.2 pH units resulted in an average increase of $0.20 \mu\text{g L}^{-1}$ in the total carbohydrate concentration normalized to phytoplankton biomass. The increase of the temperature had a positive effect on phytoplankton biomass, carbohydrate concentration and a negative effect on TEP/phytoplankton and TEP/POC ratios. The rise in temperature suggested an acceleration of the growth rate of phytoplankton which probably induced a higher biomass resulting in a higher concentration of monosaccharides. Mostly of these monosaccharides probably remained in the dissolved fraction due to a higher temperature that may have decelerate the formation of TEP. The effect of increasing temperature and acidification remains uncertain suggesting an adaptation of coastal regions phytoplankton to these global changes.

Key words : LSLE, TEP, POC, phytoplankton, pH, temperature and mesocosm.

1. 1. INTRODUCTION

The ongoing climate change is induced anthropogenically and is causing alterations of the world's oceans. The rise of the atmospheric carbon dioxide (CO₂) concentration increases radiative forcing, thereby warming the atmosphere and the ocean. Additionally, oceans act as a CO₂ sink (Doney, 2010). Approximately 25% of the emitted atmospheric CO₂ is absorbed into the oceans (Riebesell *et al.*, 2010), and thereby lowering ocean pH through chemical reactions between CO₂ and seawater. Temperature of the ocean's surface is expected to increase by 1.8 – 4.0 °C at the end of the 21st century (Solomon *et al.*, 2007). In turn, the average pH of ocean surface waters is expected to fall another 0.3 - 0.4 units by the year 2100 if the burning of fossil fuels continues at current rates (Caldeira and Wickett, 2003).

Rising oceans temperature and acidification are impacting biological community composition and physiological responses, as well as the vertical export of particulate organic carbon (POC) from the euphotic zone to the deep ocean (Passow and Carlson 2012). Additionally, changes in nutrient inputs and oxygen concentrations are affecting the oceans biological productivity and their role as a climate regulator (Doney, 2010). Future elevated temperature and CO₂ conditions will change key phytoplankton processes, such as growth rate (Feng *et al.*, 2008; Berge *et al.*, 2010), primary production (Rost *et al.*, 2008; Egge *et al.*, 2009), calcification (Langdon and Atkinson, 2005; Delille *et al.*, 2005; Rost *et al.*, 2008), nitrogen fixation (Rost *et al.*, 2008) and production of extracellular molecules (Engel, 2002; Engel *et al.*, 2004b; Engel *et al.*, 2011). During the last two decades, responses of dissolved organic carbon (DOC) and POC to increased CO₂ concentrations and rising temperature have been studied under controlled experiments. It has been hypothesized that under elevated CO₂ conditions, its uptake by phytoplankton will increase (Arrigo, 2007; Riebesell *et al.*, 2007), as well as exudation of DOC, leading to a higher production of gel particles like the transparent exopolymeric particles (TEP). This suggests an increased formation and sinking of TEP aggregates (Engel, 2005) that could change the sinking velocity of marine aggregates (Armstrong *et al.*, 2002; Klaas and Archer, 2002).

Experimental experiments revealed ambiguous evidence regarding the increase of TEP production under elevated CO₂ conditions. For instance, Engel *et al.* (2014) found higher concentration of TEP at higher CO₂. Engel (2005) have shown, through a mesocosm experiment, that TEP normalized to phytoplankton cell density increases under elevated CO₂ concentrations (i.e., 750 to 1000 ppm of CO₂). Other studies did not show a direct relationship between elevated CO₂ and increased TEP concentration (Egge *et al.*, 2009). Seebah *et al.* (2014) showed that higher TEP concentration at high CO₂ concentrations may not always related to an enhancement in aggregation and particle sinking. Mari (2008) found that TEP formed under low pH conditions (7.36) had a larger size and were more positively buoyant than those formed at higher pH (8.16). The author hypothesized that the excess of organic matter produced under high CO₂ conditions could accumulate in the surface microlayer instead of sinking. However Passow (2012) found that, elevated CO₂ conditions do not affect the abiotic formation of TEP and suggested that results from Mari (2008) show changes in TEP size and concentration due to changes in total alkalinity, rather than ocean acidification, since the acidification method used involved the addition of strong acid, which alters pH and total alkalinity (Passow, 2012). So the results of experiments carried to test the effect of increased CO₂ on TEP dynamic still remains inconclusive.

Ocean acidification is only one of the expected alterations in the future ocean. Higher seawater temperature has been reported to be responsible of a sea level rise rate of about 2.5 mm/year in the 1993-2003 decade based on satellite altimetry (Cazenave *et al.*, 2008), increased stratification, decreased sea-ice cover in the Arctic (Polyakov *et al.*, 2010) and the Antarctic (Stammerjohn *et al.*, 2008) and changes in precipitation, fresh water inputs and circulation patterns. This will also cause a reduction in nutrient injection in surface waters, thus decreasing phytoplankton new production (Doney, 2010). With increasing temperature, phytoplankton growth rate will rise and many phytoplankton physiological processes will be altered (Claquin *et al.*, 2008; Taucher *et al.*, 2015). Recent studies revealed that phytoplankton responses (photosynthesis, TEP production, and acclimation ability) to elevated temperature are species dependent. Claquin *et al.* (2008) showed that

temperature affects TEP production in three species of diatoms, but not in *Emiliania huxleyi* and *Lepidodinium chlorophorum*.

Nevertheless, few studies focused on the effects of multiple stressors on phytoplankton (Borchard *et al.*, 2011; Cai *et al.*, 2011). Experiments with both elevated CO₂ and temperature showed a reduction in the growth rate, DOC exudation and the formation of TEP aggregates and an increase of POC (Borchard *et al.*, 2011). The combined effect of elevated CO₂ and temperature on the origin and fate of marine gel particles is essential for the prediction of the intensity and efficiency of the biological pump in future ocean scenarios. The aim of this study was to test, through an indoor mesocosm experiment, the hypothesis that the combined effects of CO₂ and temperature increases will modify actual phytoplankton biomass, concentrations of TEP, POC and total carbohydrate.

1.2. MATERIAL AND METHODS

1.2.1. Experimental design

Mesocosm experiments were conducted during fall 2014, from September 28th to October 15th, at the Aquaculture Laboratory of the UQAR-ISMER at Pointe-au-Père (University of Quebec à Rimouski-Institut des sciences de la mer de Rimouski). Geographic position of the experimental site is shown at Fig. 1. Seawater was pumped from the lower St-Lawrence estuary (LSLE) at Rimouski dock 3-5 m depth and transported to the Aquaculture Laboratory in stainless steel tanks previously cleaned with an organic detergent and rinsed four times with fresh seawater. A Transportable Automated Mesocosms system was used for the experiment. This system is equipped with twelve 2.5 m³ mesocosms installed in two 12 m standard containers. All mesocosms were filled simultaneously with seawater using a single container that distributed the water homogenously by gravity, as described in Moreau *et al.* (2014). The water poured into this distributor was filtered through a 300 µm Nitex mesh to eliminate larger organisms (i.e. mesozooplankton). Mesocosms were filled on day -2 and initial measurements were made

on day -1. Regarding the treatments, mesocosms were divided into two groups of six mesocosms, corresponding to two levels in the temperature treatment: 10 °C and 15 °C, respectively. On day 0, each mesocosm had reached its target temperature. For the acidification treatment, a pH gradient was considered, which was the same within each level of the temperature treatment. To allow the application of a linear regression model, as suggested by Riebesell *et al.* (2010), a significant decreasing pH gradient was established in five mesocosms (8.0; 7.8; 7.6; 7.4 and 7.2), with a 0.2 unit increase between treatments (Fig. 2). To maintain these experimental conditions, the system was included with automated probes for the continuous monitoring of pH and temperature.



Figure. 1 Map showing the location of the mesocosm experiment in relation to the Lower St-Lawrence estuary.

A pH monitoring was made every 15 minutes using a sensor (Hach pHD online process pH sensor, accuracy ± 0.02) in each mesocosm. Moreover, the system was equipped with an automatic system of adjustment of the pH that pump CO₂-enriched artificial seawater. This artificial water was made by adding NaCl to reverse-osmosis water until 26 PSU (in situ salinity). CO₂ was regularly bubbled to ensure CO₂ saturation of the artificial water. The pH manipulation was made during the night between days 2 and 3. Day 3 was the first

sampling point for which appropriate treatment levels were attained in all mesocosms. The pH was regularly measured by spectrophotometry according to Dickson (1993) and Wedborg *et al.* (2007). The temperature was measured every 15 minutes with a temperature sensor (12-BitTemperature smart sensor, accuracy ± 0.2 °C) and was adjusted with a resistance immersion heater (Process Technology TTA1.8215) and a glycol refrigeration system. Chlorophyll α concentrations were monitored using a submersible Cyclops-7 sensor. Each mesocosm was equipped with a pH, temperature a chl α sensors. Two mesocosms where pH was unaltered and allowed to drift during the experiment. However they were subjected to the temperature treatment. To assure the homogeneous distribution of the plankton inside each mesocosm, an automatic propeller (10 cm s^{-1}) was continuously assuring mixing of the water. Each mesocosm was exposed to natural light through a transparent plexiglass cover. No nutrients were added. The initial concentrations were sufficient to support a phytoplankton bloom. Sampling was carried out using a sampling port located at the third of the way between the bottom and the top of each mesocosm.

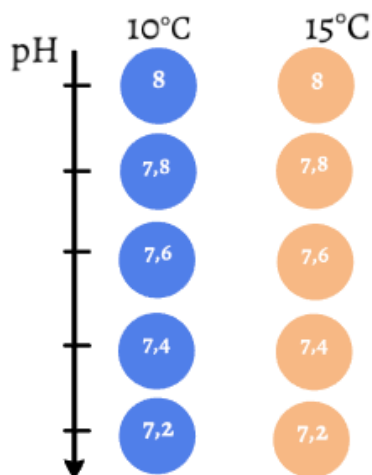


Figure. 2 Experimental mesocosm design. Two temperature treatments with two levels (10 °C and 15 °C, respectively) and the acidification treatment with five pH levels. pH levels were decreased by 0.2 units. The first series of 10 °C is composed by blue circles, while 15 °C is displayed by orange circles. Each pH treatment is shown in one circle. One control mesocosm was added to each series.

Mesocosms was sampled randomly every morning. Daily, a volume of 10 L was collected from each mosocosm to allow sampling for all the collaborators of the experiment. For this study, a volume of 1 L from each mosocosm was collected at day 0 ($t + 0$), day 3 ($t + 3$), day 6 ($t + 6$), day 9 ($t + 9$), day 12 ($t + 12$) and day 16 ($t + 16$).

1.2.2. TEP CONCENTRATION DETERMINATION

TEP concentrations were measured using the colorimetric method described in Passow and Alldredge, (1995). Triplicate seawater samples of volume between 70 and 100 mL were filtered onto 0.2 µm polycarbonate membrane filters (Whatman Nucleopore) at low pressure (<10 mbar) using a vacuum pump. Once the volume of seawater was fully filtered, 500 µL of Alcian Blue solution was passed through the filters in order to stain the retained TEP. Excess of Alcian Blue was eliminated with 1 mL of deionized water. Filters were stored at -80 °C until analysis. In the laboratory, filters were immersed in 6 mL of 80% sulfuric acid solution continuously stirred with an orbital agitator (BUNSEN AO-400) during 2 h. The absorbance of the solution was determined spectrophotometrically at 787 nm. A virgin filter stained with Alcian Blue was used as a blank and values were subtracted from the absorptions of the samples. The absorbance of the Xanthan gum at the same wavelengths was used for the calibration (5 dilutions) of the Alcian Blue absorption. TEP concentrations were calculated using the equation from Passow and Alldredge, (1995). TEP carbon concentration was estimated using the conversion factor given by Engel (2004).

1.2.3. TOTAL CARBOHYDRATE CHEMICAL COMPOSITION

The chemical composition of TEP was determined using a trimethylsilylation protocol. Samples of 25 mL were firstly desalted by ultrafiltration, centrifuged for 20 min (3000 x g) using Amicon ultracentrifugal filter (15 mL with a cutoff of 3 kDa) and then washed three times with 10 mL of deionised water. The supernatants were transferred to other tubes for derivatization. The volumes recovered were then hydrolyzed with 2 mL of trifluoroacetic acid at 65 °C for 12 h according to a modified procedure based on Yang *et al.* (2009). In a third step, the trimethylsilylation was achieved according to Shexia *et al.* (2009) and Girard *et al.* (2013). After hydrolysis, the volume was evaporated to dryness using a nitrogen flow. The solid was suspended in freshly distillated anhydrous pyridine (2.2 mL) and was then treated with 0.2 mL of *N,O*-bis(trimethylsilyl)trifluoroacetamide during 12 h at room temperature. Finally, the solution was dried with a nitrogen flow to

dryness, dissolved in hexane (2 mL) and filtrated through glass wool. The solution was analyzed by gas chromatography-mass spectrometry using an Agilent Technologies chromatograph, GC model 6850 series II and MS model 5975B equipped with a HP-5MS capillary column (30 m × 250 µm × 0.25 µm film thickness) with 5% phenyl methyl siloxane. Initial oven temperature was 80 °C for 5 min and was increased at a rate of 4 °C min⁻¹ until it reached 290 °C followed by a post-run at 300 °C. Injector temperature was 250 °C and a constant helium flow of 1.2 mL min⁻¹ was used. A volume of 1 µL of sample was injected. Lyxose was used as internal standard: 1 mL of lyxose standard solution (7.5 10⁻³ g L⁻¹) was added to each sample as internal standard just before TFA hydrolysis. Commercial sugars were used for calibration.

1.2.4. PARTICULATE ORGANIC CARBON QUANTIFICATION

Triuplicate water samples varying between 250 mL to 500 mL were filtered onto Whatman GF/F (25 mm) filters, pre-combusted at 450 °C during 4 h. Filters were preserved at -80 °C. In the laboratory, filters were freeze-dried and then encapsulated in tin foil capsules. Particulate organic carbon (POC) concentrations were measured using an elemental analyser COSTECH system 4010 equipped with an auto-sampler zero blank, connected to the mass spectrometer DeltaPlus XP ThermoScientific. Standards were analyzed on every sequence of 36 samples or less and were weighed with a *Mettler Toledo (Mx5 model, Dispersion Laboratory)* microbalance.

1.2.5. PHYTOPLANKTON DENSITY

Phytoplankton analyses were performed considering three phytoplankton size classes: picophytoplankton (<0.2 µm), nanophytoplankton (2-20 µm) and microphytoplankton (>20 µm). Two replicate samples of 5 mL and 12 mL were collected and immediately preserved with, respectively, 20 µL and 96 µL of glutaraldehyde 25% (final concentration of 0.1 %), and stored at -80 ° C until analysis. In the laboratory, cell counts were carried out depending on cell size ranges: the 5 mL samples were used for

enumeration of picophytoplankton and nanophytoplankton cells, while the 12 mL samples were for microphytoplankton enumeration. Moreover, nanophytoplankton and picophytoplankton total cell numbers were determined following Belzile *et al.* (2008). Each sample was thawed and immediately mixed with a vortex. 1 μ L of a beads solution (10 μ m) was added. 1000 μ L of each sample was pipetted in tubes and analyzed by flow cytometry with a *Beckman Coulter Epics Altra* cytometer. Microphytoplankton cell numbers were determined using a portable benchtop flow cytometer (CytoSense analyser CS-2009-27) equipped with a solid-state laser beam (Coherent Saphyre, 488 nm, 15 mW) and a peristaltic pump. 1 mL of 1:10 Tris-EDTA 10x (pH 8) solution was used as a buffer and 200 μ L of standard beads (10 μ m) suspension were added for calibration. Sample intake speed was 5 μ L min⁻¹. Nanophytoplankton was estimated using both methods described above, in order to verify variability that could be related to the application of the methods. Phytoplankton carbon biomass was expressed following a conversion factor based on carbon to biovolume equations estimated by Menden-Deuer and Lessard (2000). Phytoplankton specific growth rate was estimated unsing $\mu = \ln(X_6/X_0)/(t + 6) - (t + 0)$ (Levasseur *et al.*, 1993), where X0 and X6 are the phytoplankton biomass values at day 0 and day 6 of the experiment, respectively.

1.2.6. BACTERIAL DENSITY

Duplicate of 5 mL subsamples were filtered on 200 μ m, were fixed with 50 μ L of glutaraldehyde (0.5 % final concentration), kept in the dark for fixation at 4 °C for 15 minutes (min) and then stored at -80 °C until analysis. Bacterial density was determined by flow cytometry following the protocol of Belzile *et al.* (2008), adapted from Marie *et al.* (1997) and Lebaron *et al.* (1998) and using the nucleic acid stain SYBER Green I. In the laboratory, 200 μ L of each sample were pipetted and stained with 0.3 μ L of SYBR-Green I (0.1% final concentration; Molecular Probes Inc. # S-7585) for 15 min in the dark to optimize the staining. 800 μ L of Tris-EDTA10x buffer pH were added to each sample to insure a stable pH and avoid coincidence of several particles in the laser beam. As an internal standard, 1 μ L of a solution of 1 μ m Polysciences Fluoresbrite beads was added.

Samples were analyzed with an Epics Altra flow cytometer (Beckman Coulter) fitted with a 488 nm laser operated at 15 mW. Each sample was run twice following a flow rate of 60 $\mu\text{L min}^{-1}$ for bacterial counts and discrimination according to their size and nucleic acid content. The bacterial cell carbon was calculated using a conversion factor of bacterial cell to biomass of 30 fg carbon cell $^{-1}$ was used (Fukuda *et al.*, 1998).

1.2.7. STATISTICAL ANALYSIS

To test the significance of the differences observed between treatments a parametric student's T-test was carried out. Data of TEP, phytoplankton, bacteria and POC used in this study, were all expressed into carbon concentrations and were used for the statical analysis. Carbon concentrations data will be used and expressed in $\mu\text{gC L}^{-1}$. Homoscedasticity was verified using Levenne and Bartlett test. To test for treatment effects over the course of the experiment, a multiple linear regression with the factors time, temperature and pH was carried out. The 7.2 treatment of 15 °C was excluded from these analyses, however the control mesocosmos were added using real pH and temperature values. Normality of variables was tested using Shapiro-Wilk test. When normality and/or homoscedasticity were not respected, data were transformed. The software used was XLstat.

1.3. RESULTS

The measured initial pH ranged from 7.95 to 7.97 (NBS) and the initial temperature ranged from 9.92 °C to 11.09 °C. The targeted pH values was reached on day 3 and remained constant and slightly decreased over time (Fig. 3). The control mesocosmos were allowed to drift during the experiment. It reached 8.4 at 10 °C (Fig. 3a) and 8.8 at 15 °C (Fig. 3b). The temperature remained constant during the experiment (Fig. 4). The 7.2 treatment at 15 °C, displayed a significant unexpected difference. Determination of Cook distance showed that data of 7.2 at 15 °C treatment is aberrant to the regression test. Then, data of 7.2 at 15 °C were excluded from the regression analysis. The onset of the bloom

was indicated by the exponential rise of chlorophyll *a* (chl *a*) concentrations (Fig. 5), which reached maximum values at (*t* + 9) and displayed $36.74 \pm 4.85 \mu\text{g L}^{-1}$ on average of chl *a* at (*t* + 9) at 10 °C (Fig. 5a). At 15°C, the bloom developed faster and peaked earlier than at 10°C (Fig. 5b). Maximum of chl *a* at 15 °C was recorded at (*t* + 6) and showed $39.17 \pm 2.32 \mu\text{g L}^{-1}$, on average value of chl *a*.

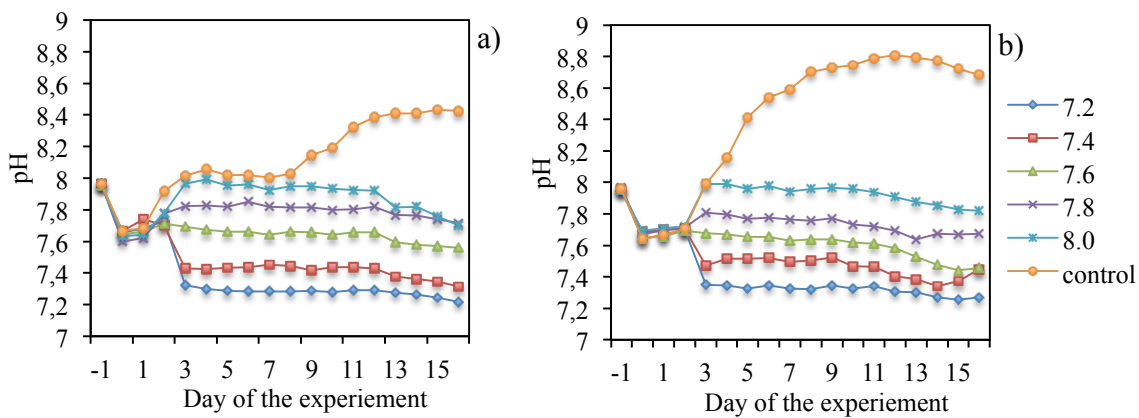


Figure. 3 Temporal pH monitoring within the mesocosms at 10°C (a) and 15°C (b) during all the days of the experiment. The targeted pH values are showed in the legend (pH was allowed to drift in the control mesocosms).

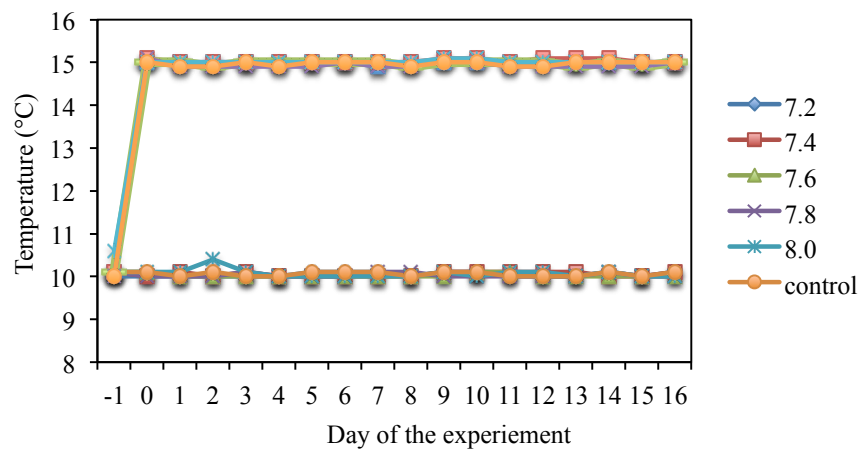


Figure. 4 Temperature (°C) in each mesocosm during all the days of the experiment.

Chl *a* concentrations highlighted a possibly slower bloom progression at three anomalous mesocosms: 7.2 and 7.6 at 10°C and 7.4 at 15°C.

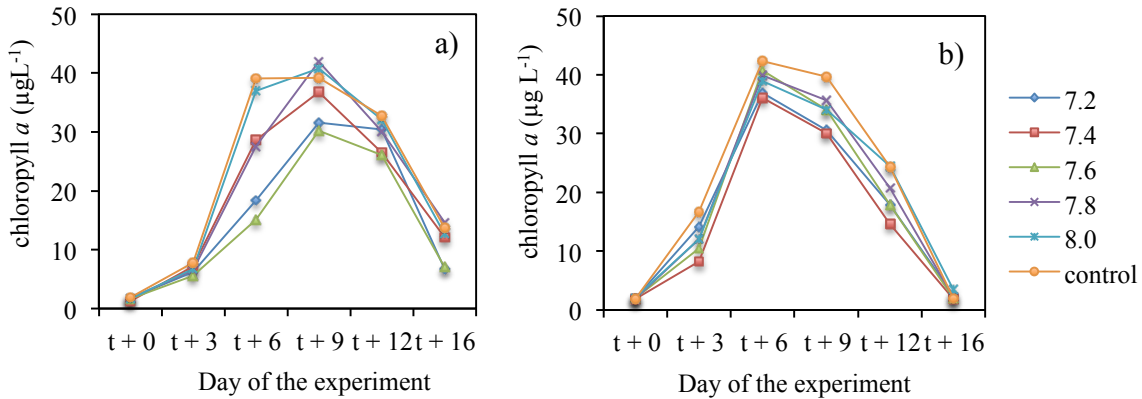


Figure 5 Temporal development of chlorophyll *a* concentration within the mesocosms at 10°C (a) and 15°C (b) during the experiment.

1.3.1. TRANSPARENT EXOPOLYMERIC PARTICLES

1.3.3.1. Monitoring of TEP carbon concentration

The time variation of transparent exopolymeric particles (TEP) at 10 °C are shown in Fig. 6a. TEP, at the beginning of the experiment were relatively high ($335.18 \pm 15.20 \mu\text{g C L}^{-1}$, on average of TEP at t + 0, at 10 °C). High starting TEP concentrations decreased, during the beginning of the experiment (t + 0 to t + 6), increased from (t + 6) to (t + 12) and stabilized until (t + 16). Highest TEP were recorded at (t + 12) ($487.60 \pm 21.25 \mu\text{g C L}^{-1}$, on average of TEP at t + 12 at 10 °C), while at (t + 16) concentrations were relatively high but slightly lower than (t + 12) ($416.93 \pm 106.64 \mu\text{g C L}^{-1}$, on average of TEP at t + 16, at 10 °C).

1.3.3.2. Effect of pH decrease

At 10 °C pH decreasing gradient showed a positive significant correlation with TEP during stationary phase ($t + 9$ and $t + 12$) ($r = 0.87$, $P = 0.023$; $r = 0.83$, $P = 0.037$, respectively) (Table. 1). Moreover, there was a temporal deviation in the increase of TEP depending on pH value. TEP at 7.6, 7.8, 8.0 and control increased at ($t + 9$), while at 7.2 and 7.4 TEP started increasing at ($t + 12$) (Fig. 6a). A decrease of 0.2 units of pH caused a decrease in TEP concentration of average $86.28 \pm 19.61 \mu\text{gC L}^{-1}$ at ($t + 9$) and a decrease of average $43.42 \pm 32.67 \mu\text{gC L}^{-1}$ at ($t + 12$).

1.3.1.3. Effect of temperature increase

At 15 °C, high TEP concentrations at the beginning of the experiment decreased during the following three days and began to increase again at ($t + 3$). TEP started increasing 3 days in advance at 15 °C rather than 10 °C. TEP maximum values were recorded at ($t + 16$) (Fig. 6a'). It displayed $517 \pm 96.35 \mu\text{gC L}^{-1}$, on average of TEP at ($t + 16$), at 15 °C. TEP exhibited a similar range of values at both temperatures studied. Values varied between $119.6 \pm \mu\text{g L}^{-1}$ (7.2) and $610.3 \pm \mu\text{gC L}^{-1}$ at 10 °C and between $135 \mu\text{gC L}^{-1}$ (7.4) to $631 \mu\text{gC L}^{-1}$ at 15 °C. Temperature increasing seemend to not influence TEP maximum concentrations.

1.3.1.3. Combined effect of pH decrease and temperature increase

At 15 °C, a positive response to combined effect of pH decrease and temperature increase was observed on TEP. Significant correlations between pH decrease and TEP were recorded at ($t + 6$), ($t + 9$) and ($t + 16$) at 15 °C ($r = 0.89$, $P = 0.04$, $r = 0.87$, $P = 0.04$ and $r = 0.96$, $P < 0.01$, respectively) (Table. 1). Theses correlations were in accordance with the temporal increasing of TEP inside the mesocosms (Fig. 6b'). At 15 °C, a decrease of 0.2 pH unit caused a drop of average $70.42 \pm 52.28 \mu\text{gC L}^{-1}$ at ($t + 9$) and $27.85 \pm 94.04 \mu\text{gC L}^{-1}$ at ($t + 16$). However, the combined effect of pH decrease and temperature increase exhibited same relationship between TEP and pH at 10 °C and 15 °C (Fig. 7). A

significantly higher phyto biomass at 15 °C yielded to TEP values as almost as that obtained at 10 °C.

1.3.2. PHYTOPLANKTON BIOMASS

1.3.2.1. Bloom development

A diatom-dominated bloom (mainly *Skeletonema costatum* - based on Flow-Cam daily observations made during the experiemnt, data not shown) was developed in all mesocosms. An exponential phase [(t + 0) – (t + 6)], a stationary phase [(t + 6) - (t + 12)] and a post-bloom phase [(t + 12) - (t +16)] were observed at 10 °C (Fig. 6b). Total phytoplankton bimass raised from $3.80 \pm 1.64 \mu\text{gC L}^{-1}$ to $338.48 \pm 67.12 \mu\text{gC L}^{-1}$. The total phytoplankton growth rate (data not shown) estimated was equal to $0.32 \pm 0.08 \text{ d}^{-1}$, on average of 10 °C mesocosms. Contribution of each phytoplankton size class (data not shown) showed that at the beginning of the experiment, picophytoplankton was significantly higher than nanophytoplankton biomass ($t_{0.05(2),6} = -6.04$, $P < 0.01$) and microphytoplankton ($t_{0.05(2),6} = -7.17$, $P < 0.01$). Picophytoplankton decreased during the experiment from $51.30 \pm 5.89 \%$ at (t + 0) to $2.83 \pm 0.89 \%$ at (t + 6), on average of picophytoplankton contribution at 10 °C. Nanophytoplankton contribution increased during the experiment and reached their highest contribution at (t + 6) (up to $77.21 \pm 7.27 \%$, on average of nanophytoplankton contribution at t + 6 at 10 °C), while microphytoplankton exhibited its highest contribution at (t + 12) ($30.76 \pm 10.45 \%$, on aversage of microphytoplankton contribution at t + 12, at 10 °C). Overall, nanophytoplankton had the highest contribution to total phytoplankton of our 10 °C experiment.

1.3.2.2. Effect of pH decrease

Phytoplankton specific growth rate and biomass dropped as a function of pH decrease. At 10 °C, specific growth rate displayed a significant ($r = 0.86$; $P = 0.02$) correlation with pH (Fig. 8).

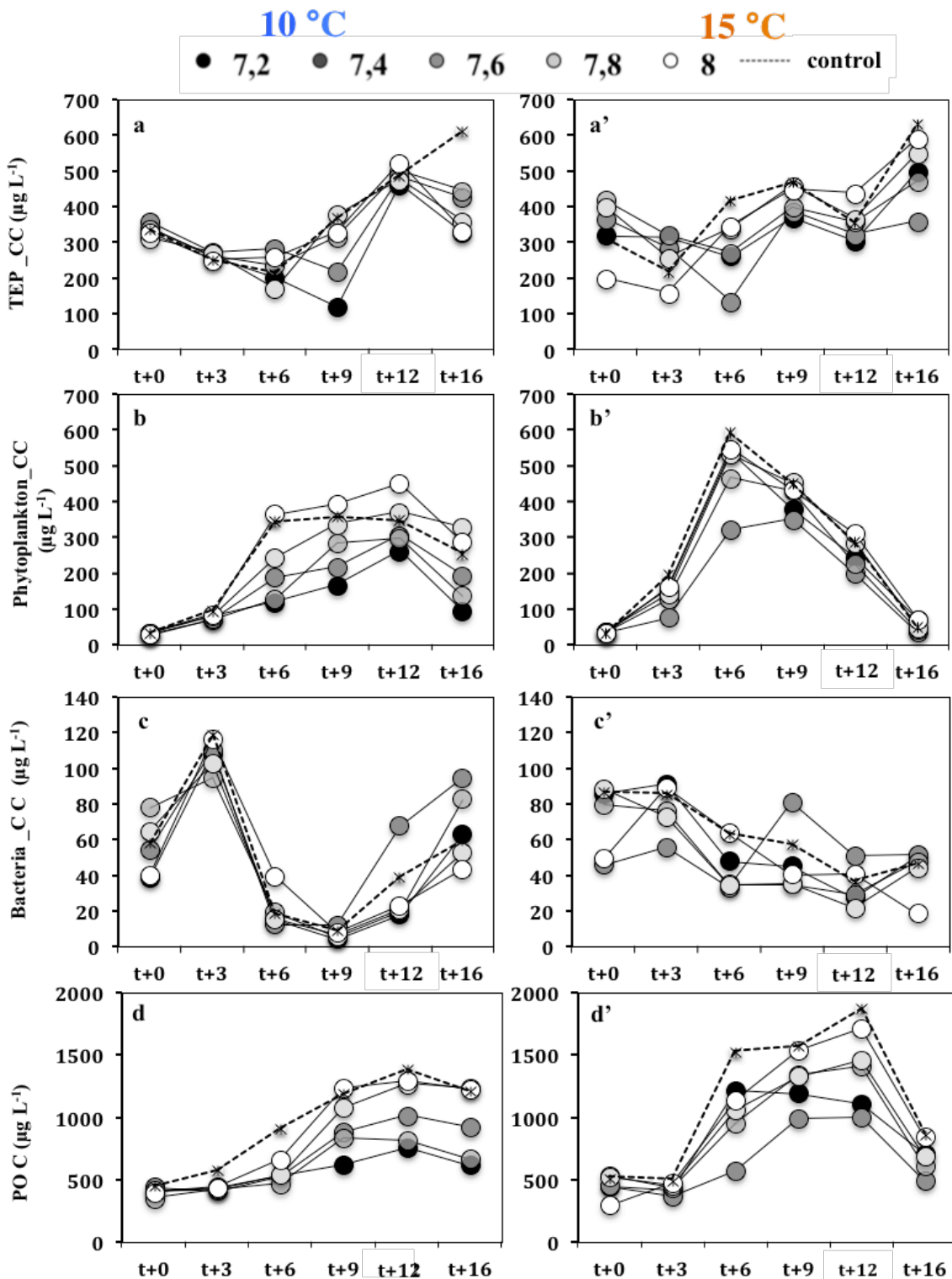


Figure 6 Temporal variation of carbon concentration (CC) corresponding to transparent exopolymeric particles (TEP) (a), phytoplankton (b), bacteria (c) and particulate organic carbon (POC) (d) at different levels of the pH treatment and control at $10\text{ }^{\circ}\text{C}$ and $15\text{ }^{\circ}\text{C}$ levels for the temperature treatment (a', b', c' and d').

		10 °C		15 °C	
		<i>r</i> ²	<i>P</i>	<i>r</i> ²	<i>P</i>
(t+0)	Phyto	0.00	0.85	0.00	0.79
	TEP	0.30	0.25	0.57	0.78
	POC	0.00	0.87	0.09	0.61
(t+3)	Phyto	0.53	0.09	0.72	0.05
	TEP	0.27	0.28	0.66	0.09
	POC	0.27	0.29	0.91	0.01
(t+6)	Phyto	0.81	0.01	0.80	0.04
	TEP	0.01	0.84	0.90	0.01
	POC	0.55	0.08	0.94	<0.01
(t+9)	Phyto	0.89	<0.01	0.44	0.22
	TEP	0.76	0.02	0.77	0.04
	POC	0.88	<0.01	0.71	0.07
(t+12)	Phyto	0.88	0.01	0.50	0.17
	TEP	0.70	0.03	0.29	0.34
	POC	0.78	0.01	0.84	0.02
(t+16)	Phyto	0.70	0.07	0.21	0.43
	TEP	0.33	0.22	0.94	<0.01
	POC	0.65	0.05	0.81	0.03
Maximum	Phyto	0.88	0.01	0.83	0.02
	TEP	0.74	0.02	0.96	<0.01
	POC	0.80	0.01	0.84	0.02

Table. 1 Results of linear regressions (*r*² and *P* values) obtained between pH decrease and carbon concentrations of phytoplankton (phyto), transparent exopolymeric particles (TEP), particulate organic carbon (POC) and for maximum values recorded at 10 °C and 15 °C.

A decrease of 0.2 units in seawater pH caused the decrease of average $0.03 \pm 0.02 \text{ d}^{-1}$ in the specific growth rate of phytoplankton at 10 °C. The pH decrease caused also a significant ($p < 0.01$) decrease in the phytoplankton. This effect was observed during the phytoplankton exponential and stationary phases at 10 °C. Phytoplankton displayed a significant ($p < 0.01$) correlation with pH decrease from (t + 3) to (t + 12) (Table. 1; Fig. 9a). Moreover, nanophytoplankton, which had the significant higher contribution to phytoplankton, also displayed a significant correlation ($p < 0.01$) with pH decrease (Fig. 9b). Highest correlation obtained between microphytoplankton and pH decrease was recorded at (t + 9) and it had a

correlation coefficient equal to 0.75. Finally, picophytoplankton exhibited no significant correlation with pH decrease (data not shown).

1.3.2.3. Effect of temperature increase

Phytoplankton blooms recorded at 15 °C had an exponential growth phase [($t + 0$) – ($t + 6$)], while the stationary phase was absent in comparison with 10 °C (Fig. 6b'). Specific growth rates were significantly higher at 15 °C than 10 °C ($t_{0.05(2),6} = -3.03$, $P = 0.01$). Moreover, at 15 °C phytoplankton development had no stationary phase but displayed a longer post-bloom phase [$(t + 6) – (t + 16)$]. The effect of increasing temperature could also be observed through comparison between 10 °C and 15 °C controls. Specific growth rate was higher at 15 °C than 10 °C (0.39 d^{-1} and 0.47 d^{-1} , at 10 °C and 15 °C, respectively). Maximum of phytoplankton displayed lower concentration at 10 °C control than 15 °C control ($358.25 \mu\text{gC L}^{-1}$ and $564.07 \mu\text{gC L}^{-1}$ at 10 °C and 15 °C, respectively). Temperature increase had no effect on the contribution of each phytoplankton size classes (data not shown). Nanophytoplankton had significantly the highest contribution to phytoplankton ($P < 0.01$). It ranged between 24.78 % and 73.58 % at 10 °C and between 25.49 % and 75.02 % at 15 °C.

1.3.2.4. Combined effect of pH decrease and temperature increase

At 15 °C, specific growth rate and maximum of phytoplankton did not display a significant correlation with pH decrease ($r = 0.84$, $P = 0.07$ and $r = 0.78$, $P = 0.11$, respectively) (Fig. 8; Fig. 9a; Table. 1). Highest phytoplankton and specific growth rate at 15 °C displayed respectively $486 \pm 99.49 \mu\text{gC L}^{-1}$ and $0.44 \pm 0.04 \text{ d}^{-1}$, on average values. Nevertheless, nanophytoplankton exhibited a significant correlation with pH decrease ($t + 6$) at 15 °C (Fig. 9b) ($r = 0.97$, $P < 0.01$) and also at ($t + 3$) ($r = 0.95$, $P < 0.01$).

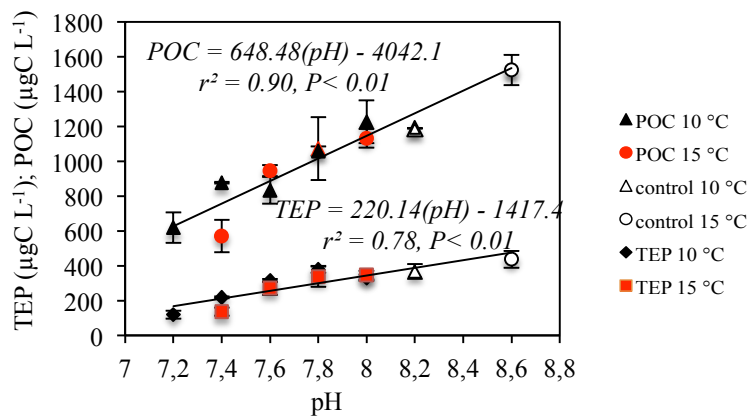


Figure. 7 The variations of particulate organic carbon (POC) and transparent exopolymeric particles (TEP) as a function of pH decrease at maximum of chl *a*, at 10 °C and 15 °C.

1.3.3. BACTERIAL BIOMASS

1.3.3.1. Monitoring of bacteria biomass

At 10 °C, biomass of bacteria evolved in a different way than phytoplankton. It showed two growth phases and one declining phase (Fig. 6c). At 10 °C, bacteria increased during the first three days from $55.51 \pm 14.89 \mu\text{g L}^{-1}$, on average of bacteria at (*t* + 0), to highest values at (*t* + 3) and exhibited $108.3 \pm 8.85 \mu\text{gC L}^{-1}$, on average at (*t* + 3). Then, bacteria decreased until (*t* + 9) and displayed its lowest concentration ($7.56 \pm 2.82 \mu\text{gC L}^{-1}$, on average of bacteria at *t* + 9, at 10 °C). Thereafter, bacteria increased again during the phytoplankton post-bloom phase. We recorded $65.85 \pm 19.11 \mu\text{gC L}^{-1}$, on average of bacteria at (*t* + 16) at 10 °C.

1.3.3.2. Effect of pH decrease

Bacteria showed no significant correlation with pH decrease (data not shown). The decrease of pH does not appear to clearly affect the development of bacteria. The biomass changes showed a rather similar response to pH during growth and decline phases (Fig. 6c).

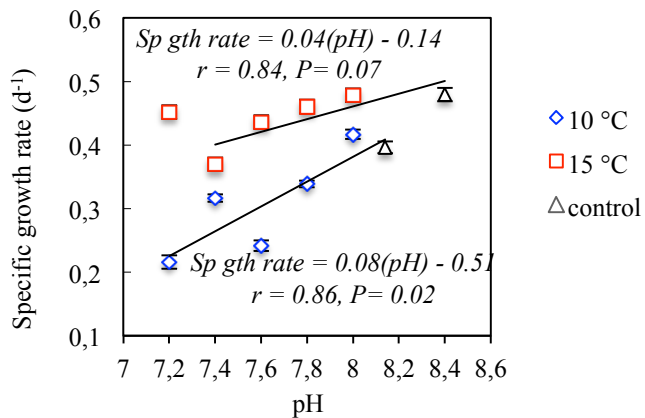


Figure. 8 The variation in the phytoplankton specific growth rate estimated at different pH at 10 °C and 15 °C. At (t + 6) pH in the 10 °C control was equal to 8.1, while in the 15 °C, control pH displayed 8.4. Annotation: Sp gth rate: sepcific growth rate.

1.3.3.3. Effect of temperature increase

Temporal monitoring of bacteria at 15 °C showed a long decline phase during the whole experiment. Starting concenrations ($72.43 \pm 19.63 \mu\text{gC L}^{-1}$, on average of bacteria at (t + 0) at 15 °C) were the highest values recorded. Values decreased until (t + 12) and exhibited $34.35 \pm 10.72 \mu\text{gC L}^{-1}$, on average of bacteria at (t + 12) at 15 °C (Fig. 6c').

1.3.3.4. Combined effect of pH decrease and temperature increase

At 15 °C, bacteria displayed a significant answer to the combined effect of pH decrease and temperature increase at (t + 3), (t + 6) and (t + 9). Significant correlations between bacteria and pH decrease were observed at (t + 3) ($r= 0.93, P= 0.04$), at (t + 6) ($r= 0.94, P= 0.01$) and at (t + 9) ($r= 0.87, P= 0.05$).

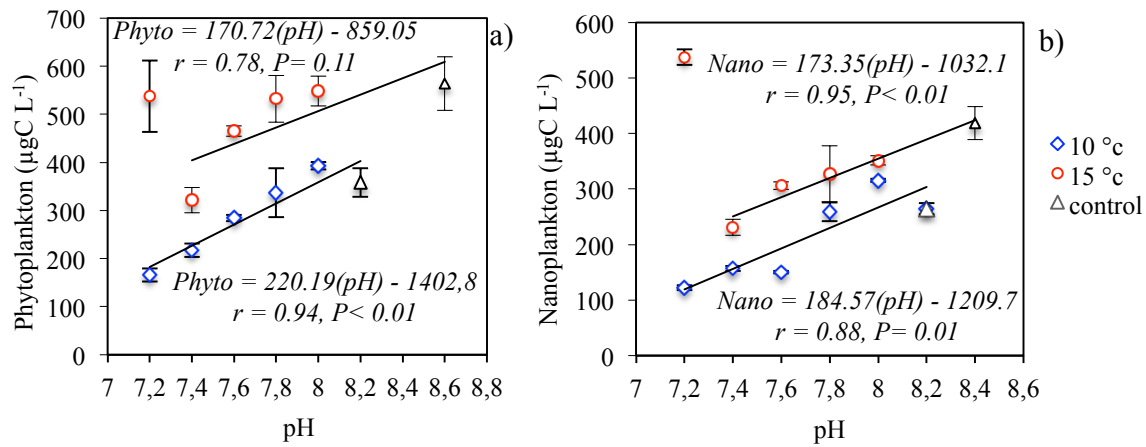


Figure. 9 Variation in maximum of phytoplankton (a) and maximum of nanoplankton biomass (b) observed at different pH and controls at 10 °C and 15 °C.

1.3.4. PARTICULATE ORGANIC CARBON

1.3.4.1. Temporal monitoring of POC

At 10 °C concentrations of particulate organic carbon (POC) increased from the beginning of the experiment until ($t + 12$) ($408.85 \pm 33.46 \mu\text{gC L}^{-1}$ and $1085.71 \pm 245.57 \mu\text{gC L}^{-1}$, on average of POC at respectively, $t + 0$ and $t + 12$ at 10 °C) (Fig. 6d). Maximum values of POC at 10 °C coincided with the maximum of phytoplankton. At the last day of the experiment, POC displayed relatively high values ($977 \pm 293.20 \mu\text{gC L}^{-1}$, on average of POC at $t + 16$, at 10 °C). Furthermore, estimated POC, based on sum of the total amount of TEP, phytoplankton and bacteria exhibited a significant positive correlation with measured POC ($r = 0.80$; $P < 0.01$) (Fig. 10). This correlation was obtained using all data collected. Below $\approx 700 \mu\text{gC L}^{-1}$, values of estimated and measured POC were well correlated and close to the theoretical linear regression ($r^2 = 1$). For higher than $\approx 700 \mu\text{gC L}^{-1}$, there was a greater divergence between concentrations of estimated and measured POC.

1.3.4.2. Effect of pH decrease

During the growth-stationary and decline phases of 10 °C, POC was positively correlated to pH decrease. Significant positive correlations ($p \leq 0.05$) were recorded from $(t + 9)$ (maximum of chl *a*) to $(t + 16)$ (Table. 1). A decrease of 0.2 units of pH caused a decrease of average, $119 \pm 6.03 \mu\text{gC L}^{-1}$ of POC at the time of maximum of chl *a* at 10 °C. At $(t + 16)$ the same pH decrease caused a decrease of average, $118.4 \pm 318.74 \mu\text{gC L}^{-1}$ at 10 °C.

1.3.4.3. Effect of temperature increase

As for 10 °C, POC concentrations at 15 °C increased from the begining of the experiment to $(t + 12)$. Values of POC exhibited $458.45 \pm 95.89 \mu\text{gC L}^{-1}$ and $1420.98 \pm 285.57 \mu\text{gC L}^{-1}$, on average of POC at, respectively $(t + 0)$ and $(t + 12)$ at 15 °C (Fig. 6d'). POC concentrations during the post-bloom phase decreased at 10 °C, whereas at 15 °C, it continued to increase until $(t+12)$ and stabilizes at the end of the experiment.

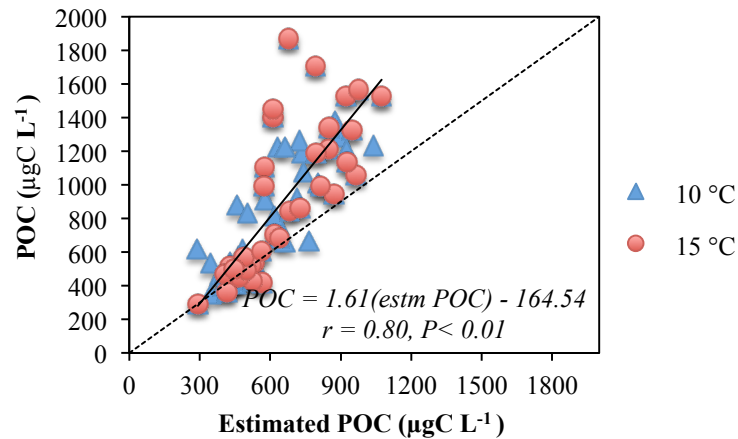


Figure. 10 Linear regressions between estimated particulate organic carbon (POC), defined as the converted biological carbon biovolume and POC at 10 °C and 15 °C. The dotted line corresponds to ($r= 1$).

POC concentrations displayed $699.11 \pm 128.67 \mu\text{gC L}^{-1}$, on average value at ($t + 16$) at 15 °C. At maximum of chl *a* POC concentration displayed $969.29 \pm 233.29 \mu\text{gC L}^{-1}$ and $1073.62 \pm 250.44 \mu\text{gC L}^{-1}$, on average of POC at maximum of chl *a* at respectively, 10 °C and 15 °C. At maximum of chl *a*, no significant differences were recorded between POC concentrations at 10 °C and that at 15 °C (Fig. 7). Maximum of POC concentrations exhibited $1438.7 \pm 267.82 \mu\text{gC L}^{-1}$ and $1088.34 \pm 242.27 \mu\text{gC L}^{-1}$, on average values, at respectively, 10 °C and 15 °C. Maximum of POC did not show a significant differences among 10 °C and 15 °C data.

1.3.4.4. Combined effect of pH decrease and temperature increase

At 15 °C POC concentrations increased exponentially inside the mesocosms from ($t + 3$) to ($t + 6$) following a trend similar to phytoplankton. POC was significantly ($P = 0.03$) correlated to phytoplankton during the growth phase. The decrease of pH exhibited significant positive correlations ($p < 0.05$) with POC concentrations at ($t + 3$), ($t + 6$), ($t + 12$) and ($t + 16$) (Table. 1). At 15 °C, a decrease of 0.2 units of pH caused an average decrease of $238 \pm 168.79 \mu\text{gC L}^{-1}$ at maximum of chl *a* and an average decrease of $151.72 \pm 63.80 \mu\text{gC L}^{-1}$ at ($t + 12$). The increase of 5 °C in seawater temperature induced rather similar POC concentrations in comparaison with 10 °C (Fig. 7). Overall, the effect of pH decrease was shown to have a positive response of phytoplankton, TEP and POC. Nevertheless, these observations were not significant only at maximum concentrations of TEP and POC and maximum of phytoplankton biomass. The effect of pH decrease was noted at 15 °C with a positive correlation with phytoplankton growth rate and phytoplankton biomass. The effect of temperature increase was observed on phytoplankton, by generating a higher biomass and a faster growth rate. At 15 °C, TEP and POC concentrations varied in the same range of those recorded at the 10 °C. However, TEP and POC normalized to phytoplankton show that temperature increase engender a lower TEP / phytoplankton ratio (Fig. 11), since significant higher phytoplankton was observed at 15 °C than 10 °C, while TEP and POC ranged in the same level at 10 °C and 15 °C.

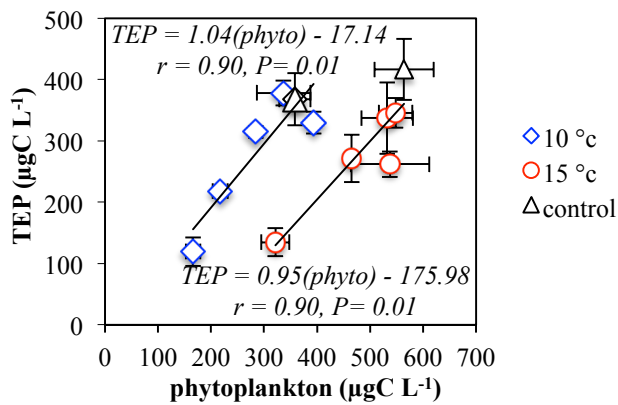


Figure. 11 Variations in the concentrations of transparent exopolymeric particles carbon concentration (TEP) versus the phytoplankton carbon concentration at maximum of chl *a*, at 10 °C and 15 °C. Annotation: phyto: phytoplankton.

1.3.5. CARBOHYDRATE CHEMICAL COMPOSITION

1.3.5.1. Total carbohydrate concentration

Total carbohydrate concentration displayed rather constant values from the beginning of the experiment, until ($t + 6$) at 10 °C and, until ($t + 3$) at 15 °C (Fig. 12). At 10 °C, maximum values were recorded at ($t + 9$) ($24.97 \pm 5.88 \mu\text{g L}^{-1}$). Higher total carbohydrate concentrations dropped markedly in all mesocosms during the following sampling days and ended with a relatively low value ($17.46 \pm 4.84 \mu\text{g L}^{-1}$ and $19.53 \pm 8.37 \mu\text{g L}^{-1}$ on average of total carbohydrate concentration at ($t + 16$), at 10 °C). The effect of pH decrease on total carbohydrate concentration displayed no significant response at 10 °C (Table. 2). However, at 15 °C total concentration showed at ($t + 6$) and ($t + 12$) significant positive correlations with pH decrease ($r^2 = 0.79$, $P = 0.04$ and $r^2 = 0.87$, $P = 0.01$, respectively). The temperature increase influenced the temporal development of total carbohydrate concentrations, leading to an earlier exponential increase and maximum values (Fig. 12). At 15 °C, highest total carbohydrate concentrations were recorded at ($t + 6$) ($42.1 \pm 6.5 \mu\text{g L}^{-1}$, on average of total carbohydrate concentrations at ($t + 6$), at 15 °C). A shift of 3 days, as for the other parameters studied, was observed between maximum carbohydrate

concentrations recorded at 10 °C and that observed at 15 °C. T-test results showed that during the sampling days, no significant differences were evident between total carbohydrate concentration recorded at 10 °C and at 15 °C, except at maximum of chl *a*, and at (t + 16). A significantly higher concentration was observed at 15 °C, at maximum of Chl (a) and, at (t + 16) ($t_{0.05(2),6} = -5.08$, $P < 0.01$ and $t_{0.05(2),6} = -5.31$, $P < 0.01$, respectively).

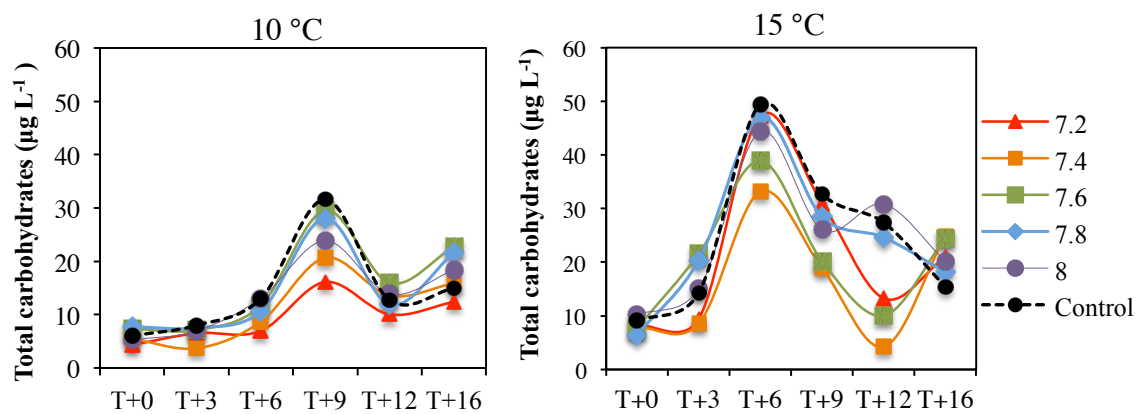


Figure. 12 Variations of total carbohydrate concentrations measured at different pH and controls at 10 °C and 15 °C during sampling days.

1.3.5.2. Monosaccharide concentrations and contributions to the total carbohydrate

Each monosaccharide contribution to the total measured carbohydrate concentration varied depending on the nature of the monosaccharide, day of the experiment, pH and temperature. Monosaccharide analysis revealed that the different fractions within the total organic matter carbohydrate pool are essentially constituted by arabinose, mannose, glucose, galactose, fructose, ribose and xylose. Samples at the beginning of the experiment showed all these compounds, at the exception of xylose (Fig. 13). Despite the lack of a significant effect of pH on total carbohydrate concentration at 10 °C, a clear effect on individual monosaccharide concentration and contribution to the total fraction has been observed. Significant correlations of monosaccharides with pH decrease were mainly

observed during the period of highest total carbohydrates concentrations at ($t + 9$) at 10 °C and ($t + 6$) at 15 °C (Table. 2).

1.3.5.2.1. Glucose

Overall, the main component to total carbohydrate concentration was glucose (glu) ($54.85 \pm 8.47\%$ and $58 \pm 13.07\%$, on average of glucose contribution, respectively at 10 °C and 15 °C) (Fig. 13). Glucose had different dynamics depending on pH value and temperature. At 7.8, 8.0 and control glucose contribution was relatively high during sampling days at 10 °C and 15 °C. It displayed maximum concentrations at ($t + 9$) at 10 °C and at ($t + 6$) at 15 °C ($82.1 \pm 4.9\%$ and $76.2 \pm 1.8\%$, on average of glu contribution at 7.8, 8.0 and control respectively). At pH 7.6 and 10 °C, glucose was rather constant among sampling days and displayed its highest contribution at ($t + 9$) (76.4 %, on average of glu contribution at $t + 9$, at 10 °C), whereas, at 7.6 and 15 °C glucose contribution decreased and showed the lowest value at ($t + 6$) (8.21 %). Nevertheless, glucose contribution ended with relatively high values at the end of the experiment at both temperatures (Fig. 13). This glucose response was also observed at pH 7.2 and 10 °C. The relatively high contribution of glucose observed at ($t + 0$) (60.3 %, on average of glucose contribution at ($t + 0$) at 10 °C) decreased and exhibited its lowest contribution at ($t + 12$) (10.6 %). At pH 7.4 glucose contribution decreased during the first three days and remained relatively low until the end of the experiment at 10 °C and 15 °C ($51.3 \pm 9.6\%$ and $44.5 \pm 16.9\%$, on average of glucose contribution between ($t + 3$) and ($t + 6$) at, respectively 10 °C and 15 °C). Consequently, at 10 °C at ($t + 9$) and ($t + 12$) glucose concentration showed a significant positive correlation with seawater pH decrease ($P = 0.02$). Similarly, at 15 °C glucose concentration displayed a significant positive correlation with pH at ($t + 6$) and ($t + 12$) ($P \leq 0.02$) (Table. 2).

1.3.5.2.2. Arabinose and mannose

Arabinose and mannose were the second most important contributors to the total carbohydrate poll ($15.19 \pm 6.62\%$; $15.79 \pm 5.61\%$, on average of respectively arabinose and

mannose at 10 °C and $12.29 \pm 6.49\%$; $15.03 \pm 5.80\%$, %, on average of respectively arabinose and mannose at 15 °C). Contribution of arabinose and mannose displayed high values at (t + 0) ($15.3 \pm 2.5\%$ and $11.5 \pm 2.1\%$, on average of respectively arabinose and mannose at t + 0). At 7.8, 8.0 and control starting contributions of arabinose and mannose decreased and exhibited lowest values at (t + 9) at 10 °C ($3.9 \pm 3.2\%$ and $1.2 \pm 0.7\%$, on average of respectively, arabinose and mannose contribution to total carbohydrate at 7.8, 8.0 and control at t + 9, at 10 °C), while at 15 °C weakest values were observed at (t + 6) ($3.5 \pm 1.7\%$ and $5.6 \pm 1.3\%$, on average of respectively, arabinose and mannose at 7.8, 8.0 and control at t + 9, at 15 °C) (Fig. 13). However, at 7.2, 7.4 and 7.6 arabinose and mannose starting contribution has either remained constant or has increased during the sampling days and reached maximum values at (t + 9) at 10 °C ($31.8 \pm 18.4\%$ and $29.6 \pm 20.0\%$, on average of respectively arabinose and mannose contributions at 7.2, 7.4 and 7.6 at t + 9, at 10 °C). At 15 °C, maximum values were observed at (t + 9) for arabinose ($36.8 \pm 22.6\%$, on average of arabinose contribution at 7.2, 7.4 and 7.6 at t + 9, at 15 °C) and at (t + 12) for mannose ($30.4 \pm 16.3\%$, on average of mann contribution at 7.2, 7.4 and 7.6 at t + 12, at 15 °C). Yet, arabinose and mannose concentrations, in contrast to glucose, displayed significant negative correlations with pH decrease. Arabinose significant correlations with pH decrease ($P= 0.01$) were observed at (t + 9) at 10 °C and at (t + 6) at 15 °C. Mannose was significantly negatively correlated to pH decrease ($P \leq 0.05$) at (t + 9) and (t + 12) at 10 °C. However, at 15 °C no significant correlation was recorded for mannose (Table. 2).

1.3.5.2.2 Galactose

At 10 °C, galactose contribution to total carbohydrate concentration was low and constant along the experiment ($5.1 \pm 2.1\%$, on average of gal contribution at 10 °C). At 10 °C, higher values were observed at (t + 0) at 7.2, 7.4 and 7.6.

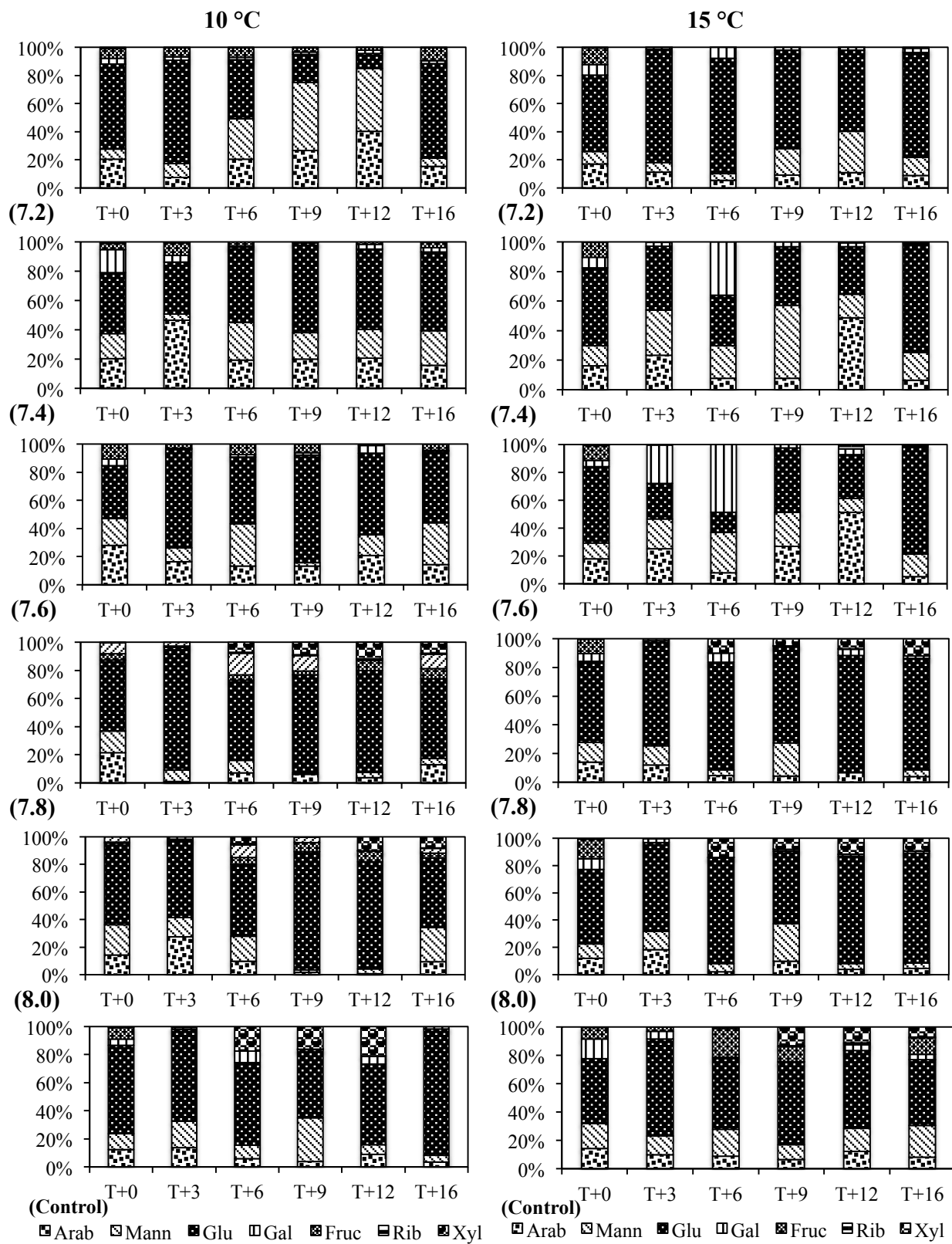


Figure 13. Monosaccharide contribution (%) to the total carbohydrates pool present at different pH and controls at 10 °C and 15 °C. Notation: Ara: Arabinose; Man: Mannose; Glc: Glucose; Fru: Fructose; Rib: Ribose; Xyl: Xylose

Galactose starting contribution decreased during sampling days in all mesocosms except at 7.4 and 7.6 at 15 °C. At 15 °C, higher gal contribution was recorded at (t + 6). Gal exhibited relatively low values at 7.8, 8.0 and control ($5.2 \pm 2.3\%$, on average of galactose at 7.8, 8.0 and control at t + 6, at 15 °C), whereas it displayed highest contribution at 7.2, 7.4 and 7.6 ($37.4 \pm 17.7\%$, on average of galactose at 7.2, 7.4 and control at (t + 6), at 15 °C). Thereby, galactose exhibited at 10 °C and at 15 °C significant correlations with pH decrease at (t + 6) and (t + 9) ($P= 0.04$; $P= 0.03$, respectively at 10 °C and $P= 0.01$; $P= 0.04$, respectively at 15 °C) (Table. 2). However, galactose correlation with pH decrease was positive at 10 °C and negative at 15 °C.

1.3.5.2.3. Fructose

Fructose was mainly detected at 10 °C ($5.0 \pm 3.7\%$, on average of fructose contribution at 10 °C). Higher values of fruc contribution to total carbohydrate were recorded at 8.0 and control (10 °C). Fructose contribution showed a significant negative correlation with pH decrease at (t + 12). Despite these observations, no clear effect of pH decrease observed on fructose concentrations (Table. 2). Temperature increase seemed to inhibit fructose production, while it was mainly observed at (t + 0) at 15 °C.

1.3.5.2.4. Ribose

Ribose had the lowest contribution ($0.3 \pm 0.2\%$, on average of ribose contribution at 10 °C and 15 °C). At 10 °C, starting ribose contribution seemed to decrease during sampling days at 7.2, 7.4 and 7.6. Yet, 7.8 and 8.0 and control showed increasing ribose contributions (0.6 %, 1.0 % and 1.1 %, on maximum of ribose contribution respectively at 7.8, 8.0 and control). A significant positive correlation ($P= 0.04$) was recorded at (t + 6) at 10 °C. At 15 °C, ribose showed a significant negative correlation ($P= 0.04$) at (t + 9) (Table. 2).

1.3.5.2.5. Xylose

At both temperature, xylose were firstly detected at ($t + 6$) and remained constant until the end of the experiments ($19.3 \pm 4.7\%$, on average of xylose contributon at $10\text{ }^{\circ}\text{C}$ and $15\text{ }^{\circ}\text{C}$). Moreover, xylose was noted only at 7.8, 8.0 and control at $10\text{ }^{\circ}\text{C}$ and at $15\text{ }^{\circ}\text{C}$. This was the only pH effect observed on xylose.

1.4. DISCUSSION

During this section pH decrease will be expresssed as CO_2 increase. The aim of this study was to test, through an indoor mesocosm experiment, the hypothesis that CO_2 concentration and/or temperature can affect phytoplankton, transparent exopolymeric particules (TEP), particulate organic carbon (POC) and total carbohydrate concentrations, during the course of a phytoplankton fall bloom in the lower Saint Lawrence estuary (LSLE). Our results revealed that a significant CO_2 increase had a significant positive correlation with phytoplankton, TEP, POC and carbohydrate concentrations, mostly at maximum of chlorophyll *a* (chl *a*), and/or at maximum of pthyoplankton. Temperature increase resulted in a significantly ($p < 0.05$) higher phytoplankton, similar POC and a significantly lower TEP normalized to phytoplankton. TEP and POC concentrations recorded at $10\text{ }^{\circ}\text{C}$ were rather similar at $15\text{ }^{\circ}\text{C}$.

1.4.1. PHYTOPLANKTON RESPONSE

During this mesocosm experiment, a diatom bloom (mainly *Skeletonema costatum*) was developed. The effect of a significant increasing CO_2 gradient showed positive interaction with phytoplankton and phytoplankton specific growth rate. At $10\text{ }^{\circ}\text{C}$, specific growth rate displayed a significant ($P < 0.05$) negative response to CO_2 increase (Fig. 8).

10 °C	Arabinose		Mannose		Glucose		Galactose		Fructose		Ribose		Total								
	<i>r</i>²	P	slope	<i>r</i>²	P	slope															
<i>(t+0)</i>	0.03	0.76	-0.18	0.18	0.46	0.32	0.23	0.40	0.49	0.42	0.23	-0.10	0.05	0.70	-0.07	0.79	0.04	-0.02	0.13	0.53	0.42
<i>(t+3)</i>	0.01	0.86	0.104	0.00	0.99	8.75	0.09	0.62	0.56	0.28	0.35	-0.03	0.54	0.15	-0.08	0.31	0.32	-0.00	0.20	0.44	0.54
<i>(t+6)</i>	0.56	0.14	-0.75	0.15	0.51	-0.77	0.57	0.13	2.75	0.77	0.04	0.36	0.32	0.31	0.71	0.77	0.04	0.07	0.23	0.41	2.39
<i>(t+9)</i>	0.91	0.01	-9.57	0.77	0.05	-1.66	0.84	0.02	4.12	0.82	0.03	0.23	0.34	0.29	0.31	0.67	0.08	0.02	0.72	0.06	2.16
<i>(t+12)</i>	0.75	0.05	-0.86	0.89	0.01	-0.85	0.85	0.02	2.77	0.69	0.08	0.32	0.68	0.07	-0.03	0.14	0.52	0.00	0.43	0.22	1.25
<i>(t+16)</i>	0.15	0.52	-0.38	0.06	0.67	1.10	0.71	0.07	1.12	0.29	0.34	0.37	0.00	0.89	-0.06	0.06	0.69	0.00	0.18	0.47	2.16
Maximum	0.66	0.09	-0.81	0.56	0.14	-0.72	0.87	0.02	2.81	0.82	0.03	0.29	0.00	0.93	0.00	0.41	0.24	0.01	0.43	0.22	1.58
15 °C	Arabinose		Mannose		Glucose		Galactose		Ribose		Total										
	<i>r</i>²	P	slope	<i>r</i>²	P	slope															
<i>(t+0)</i>	0.01	0.82	0.136	0.20	0.44	0.45	0.09	0.61	0.30	0.05	0.70	-0.238	0.11	0.57	0.34	0.06	0.68	0.24			
<i>(t+3)</i>	0.73	0.06	-0.85	0.72	0.06	-0.85	0.01	0.86	0.10	0.33	0.30	-0.577	0.30	0.33	-	0.00	0.88	-0.09			
<i>(t+6)</i>	0.90	0.01	-0.94	0.67	0.08	-0.81	0.97	0.00	0.98	0.88	0.01	-0.942	0.00	0.88	0.08	0.79	0.04	0.89			
<i>(t+9)</i>	0.37	0.27	0.61	0.65	0.09	-0.80	0.04	0.73	0.20	0.80	0.04	-0.894	0.79	0.04	-	0.18	0.46	-0.43			
<i>(t+12)</i>	0.16	0.50	-0.40	0.03	0.77	0.17	0.84	0.02	0.91	0.36	0.28	0.599	0.01	0.85	0.11	0.87	0.01	0.93			
<i>(t+16)</i>	0.11	0.57	-0.34	0.69	0.07	-0.83	0.07	0.65	0.27	0.02	0.82	0.142	0.56	0.14	-	0.20	0.43	-0.45			
Maximum	0.98	0.00	-0.99	0.65	0.09	-0.80	0.96	0.00	0.98	0.88	0.01	-0.938	0.00	0.88	0.09	0.79	0.04	0.89			

Table. 2 Linear regression coefficients, signification levels (P value) and slopes of the regression between each monosaccharide concentration and gradient of pH decrease during the sampling days at 10 °C and 15 °C experiments.

Previous studies highlighted the correlation between CO₂ and chl *a*, and/or phytoplankton (Engel *et al.*, 2014; Taucher *et al.*, 2015). Density of *E. huxleyi* was significantly reduced in a high CO₂ environment (Rost *et al.*, 2003). However, other studies have explored the effect of acidification on phytoplankton, using a narrow pH range (from 8.2 to 7.8) (e.g. Wang *et al.*, 2010; Yang and Gao, 2012). It is problematic to use such a narrow range of pH to study the tolerance of coastal phytoplankton to acidification, given that pH in coastal waters fluctuates within a large range of values. Effect of the CO₂ increase on growth rate observed in this study, is consistent with results from a mesocosm experiment, performed in Disko Bay on Arctic diatoms (Thoissen *et al.*, 2015). They suggested that a decrease of 0.3 units in pH caused a decrease of average 0.09 d⁻¹ in the phytoplankton growth rate. However, in our study the influence of CO₂ increase was lower than that observed by Thoissen *et al.* (2015). Other studies have documented small effects of CO₂ increase on marine phytoplankton growth rates and/or community structure (Hare *et al.*, 2007; Riebesell *et al.*, 2007; Ramos *et al.*, 2010; Coello-Camba *et al.*, 2014) and primary production (Tortell *et al.*, 2002; Engel *et al.*, 2013). It has previously been shown that not all phytoplankton species respond similarly to high CO₂ (Tortell *et al.*, 2002; Kim and Lee, 2006; Berge *et al.*, 2010 and Thoisen *et al.*, 2015). Diatoms seem to be less sensitive to different CO₂ levels than other phytoplankton groups (Engel *et al.*, 2008). Recent investigations on CO₂ uptake by marine phytoplankton species demonstrated that many phytoplankton groups, including diatom species, use carbon assimilation mechanism (CAM) (Rost *et al.*, 2003). CAM can be understood as a physiological regulation of CO₂ acquisition to maintain high photosynthetic rates even at reduced CO₂. During a mesocosm study, in the coastal North Sea an increase in the uptake of CO₂ by phytoplankton at elevated CO₂ concentration was recorded by Riebesell *et al.* (2007). They observed that the excess of inorganic carbon consumption was not used to increase biomass. Moreover, CAM is known to have variable specie-specific efficiencies (Reinfelder, 2010 and 2012; Rost *et al.*, 2008). Studies showing a positive response of phytoplankton to elevated CO₂ explained these results as a consequence of a lower energetic cost of CAM (Tortell *et al.*, 2008a and b). Our results from our mesocosm experiment with constant CO₂

concentrations suggested that phytoplankton CAM rates were probably related to the gradient of CO₂ concentration tested. This could explain the negative effect observed on phytoplankton growth rate. Phytoplankton in our study, showed a positive response to temperature increase. At 15 °C, phytoplankton bloom had a significant ($p < 0.05$) higher growth rate (Fig. 8). Yet, it resulted in a more rapid nutrients depletion at 15 °C than 10 °C (3 days earlier). Higher seawater temperature enhanced growth rate and biomass content. This is consistent with experimental results showing that phytoplankton responded positively to temperature (Claquin *et al.*, 2008; Borchard *et al.*, 2011). In addition, our results are similar to those from an indoor mesocosm experiment performed with a natural phytoplankton community from the Baltic Sea (Taucher *et al.*, 2012). Furthermore, a three-dimensional coupled hydrodynamic ecosystem model had showed the same trend in terms of temperature increase effect on phytoplankton for the Baltic sea, Bay of Biscay and the Black ea (Chust *et al.*, 2014). A similar response was observed in a mesocosm research performed in the Espeland field station (Norway), with temperature increased of 5 °C above the *in situ* temperature (Lassen *et al.*, 2010). Temperature in these cases does not act as a phytoplankton inhibitor but plays a fundamental role in the regulation of metabolic processes (Iribarri *et al.*, 1985; White *et al.*, 1991), resulting in an increasing net cell growth rate (Eppley, 1972; Goldman and Carpenter, 1974; Montagnes and Franklin, 2001). Few experiments have addressed responses to a synergistic effect of warming and elevated CO₂. Our results provide evidence of a Sub-Arctic diatom bloom to a combined effect of a 5 °C increase in temperature and a gradient of CO₂ concentration. However, interactive effects of temperature increase and gradient of CO₂ concentration were generally weak. The negative response to the gradient of CO₂ increase showed at 10 °C, was also observed at 15 °C with a significant higher phytoplankton.

1.4.2. BACTERIA RESPONSE

Bacteria biomass decreased during the phytoplankton the exponential and stationary phases. This may be explained by zooplankton predation on bacterial cells, as proposed by Motwani and Gorokhova (2013). Observations from Lemlih Mohamed Khales

(personal communication) on zooplankton monitoring during the same experiment showed the presence of an important biomass of zooplankton with *Rimostrombidium*. sp as the dominant group.

1.4.3. TRANSPARENT EXOPOLYMERIC PARTICLES RESPONSE

The relatively higher transparent exopolymeric particles (TEP) concentration at the start of the experiment is consistent with Annane *et al.* (2015) who showed a peak of TEP in the SL of the lower St-Lawrence estuary (LSLE) in early Fall (September). TEP biomass measured by Annane *et al.* (2015) exhibited up to $975 \mu\text{gC L}^{-1}$ in early September and remained between $150 \mu\text{gC L}^{-1}$ and $315 \mu\text{gC L}^{-1}$ until early October. During the mesocosm experiment, the highest concentrations of TEP were observed at the phytoplankton stationary and post-bloom phases. Since bacteria decreased during the course of the experiment (Fig. 6c), the increase of TEP could not be attributed to bacteria. Additionally, a significant positive correlation was recorded between TEP and phytoplankton at the maximum of chl *a* (Fig. 11). Moreover, daily microscopic observations showed a dominance of *Skeletonema costatum* diatom specie (data not shown). Up to 70 % of TEP related to *Skeletonema costatum* polysaccharide production has been shown to increase during both the stationary and post-bloom phases (Fukao *et al.*, 2010). These phases are characterized by low nutrient concentrations. It is well known that carbon overconsumption after nutrient depletion is mainly released as dissolved organic carbon (DOC). This carbon mechanism helps to preserve the metabolic system of the cell when there is an imbalance between light and nutrients (Fogg, 1983). Globally, TEP exudation in our experiment is suggested to be related to nutrient limited condition. So, the relatively higher concentration of TEP during the stationary and post-bloom phases suggests a flocculation of phytoplankton polysaccharide exudates to form TEP. Dissolved to particulate transfer of polysaccharides is enhanced by TEP, which is known to favor the sink of organic matter due to its high stickiness (Dam and Drapeau, 1995; Passow *et al.*, 1994). Previous studies have shown that abiotic formation can transform a substantial fraction of DOC exudates into TEP at very short timescales (Passow, 2000; Engel *et al.*,

2004c). This suggests that an important part of DOC freshly released comprised TEP precursors, which were quickly transformed into TEP. However, it is important to mention that the colorimetric method used to determine TEP concentration (Passow and Alldredge, 1995) is semi-quantitative because the amount of adsorbed Alcian Blue is directly related to the standardization with the acidic polysaccharide Xanthan Gum (Van Oostende *et al.*, 2013).

Previous mesocosm experiments showed that under elevated CO₂ concentrations (e.g. 750 to 1000 ppm), the consumption of CO₂ by phytoplankton increases and may be transformed into TEP (Riebesell *et al.*, 2007). Generally, some phytoplankton species utilize both HCO₃⁻ and CO₂ for photosynthesis, while others use either HCO₃⁻ or CO₂ (e.g. Giordano *et al.*, 2005). Increased CO₂ concentration could potentially increase primary production, resulting in a positive response especially for species relying on diffuse CO₂ uptake. This increase of the primary production has been related to significantly increase TEP concentrations in a nutrient-limited experiment with *Emiliania huxleyi* (Borchard and Engel, 2012). This increase in TEP concentration may be caused by an increase in DOC exudates that act as TEP precursors. Engel *et al.* (2014) found higher concentrations of TEP at higher CO₂, and suggested that considering TEP as a photosynthetic product, enhancing CO₂ uptake would enhance carbohydrates exudation and TEP formation (Engel, 2002). However, evidence related to the hypothesis that high CO₂ results in a high phytoplankton CO₂ uptake, which explain TEP increase, is contradictory. Other studies did not show a direct relationship between elevated CO₂ concentration and increased TEP concentration (Egge *et al.*, 2009). Mari (2008) found that TEP formed under low pH conditions (pH 7.3) are larger in size, but more positively buoyant than those formed at higher pH (pH 8.1). Additionally, increasing DOC exudates does not necessarily translated into increased TEP particle formation (Egge *et al.*, 2009). Our results showed that TEP had not a clear response but showed a significant negative response at maximum of chlorophyll *a* (chl *a*), and maximum of phytoplankton. Most phytoplankton species have active uptake systems for inorganic carbon that renders phyotosynthetic CAM essentially saturated under

high CO₂ levels. It is possible that constant elevated CO₂ could not result in an increase of their assimilation rates (Giordano *et al.*, 2005). Then, our results could also be associated to previous work, which suggests that further increases in CO₂ may not lead to a higher CO₂ conversion of inorganic carbon to TEP, as the rate of TEP production possibly is at its maximum under lower CO₂ concentrations (Engel, 2002), and that abiotic formation of TEP is not altered by high CO₂ concentrations and low pH (Passow, 2012). However, our observations of TEP significant negative response at maximum of phytoplankton could be associated to a negative response.

The 15 °C treatment had a relatively higher phytoplankton (Fig. 6b, b') than the 10 °C treatment. A larger bloom and a higher chl *a* concentration should lead to more TEP. However, in our experiment rather similar TEP values were observed for both treatments. Moreover, TEP/phytoplankton ratio was significantly higher at 10 °C than 15 °C at maximum of chl *a*. Consequently, our results suggest that the increase of temperature does not lead to a higher TEP production and/or formation. These observations are not consistent with Claquin *et al.* (2008) and Seebah *et al.* (2014) results that showed a potential increase in TEP as temperature increases. However, the response of TEP to the increasing temperature is species-specific and presents an optimal type of response curve (Claquin *et al.*, 2008). Furthermore, the lack of an apparent increase in TEP with elevated temperature might be explained by an inhibition of the aggregation process caused by higher temperature. Previous observations are in agreement with our results (Chen *et al.*, 2015; Seebah *et al.*, 2014). Increasing temperature by 2 °C slows and could hinder the ability of DOC precursors to self-assemble (Chen *et al.*, 2015; Engel *et al.*, 2008). Additionally, Seebah *et al.* (2014) found smaller TEP aggregates at higher temperatures. Moreover, the effect of temperature increase on TEP observed at 15 °C, during our study, could be related to a decrease in the rate of CAM which may resulted in a decrease in the TEP production. Phytoplankton carbon uptake has been shown to be dependent on species and also temperature (Taucher *et al.*, 2015). Warming from 15 °C to 20 °C resulted in an increase of 31 % in carbon uptake by *T. weissflogii*, and a 33 % decrease of carbon uptake

by *D. fragilissimus* (Taucher *et al.*, 2015). The negative response of TEP to CO₂ gradient was also observed at 15 °C. Then, either the temperature increase affected the aggregation rate of the DOC fraction or it influenced the response of the phytoplankton by reducing carbon uptake and therefore TEP formation.

1.4.4. PARTICULATE ORGANIC CARBON RESPONSE

Our results showed that the effect of the increasing CO₂ concentration on POC concentration was not significant during the phytoplankton exponential phase. However, during the stationary and post-bloom phases the increasing CO₂ gradient tested showed a significant negative response of POC concentration. Our findings suggest a reduction of the concentration of the POC under elevated CO₂ conditions. It showed a significant decreasing trend with CO₂ increase at max of chl *a*, and maximum of phytoplankton biomass and maximum of TEP (Table. 1). This coincides with the significant negative response of phytoplankton and TEP. POC dynamics is mainly, driven by biological processes and net phytoplankton and TEP concentrations, which are related to the balance between the processes of carbon production and consumption. Given that the main source of organic matter in the ecosystem is phytoplankton photosynthesis, changes in POC may be related indirectly to the effect of CO₂ increase on phytoplankton. CO₂ increase caused the decrease of the phytoplankton growth rate and resulted in a lower phytoplankton TEP and POC. Yet this hypothesis is more valid if we consider that the loss of energy in cell growth was probably attributed to a higher CAM. Nevertheless, the TEP contribution to POC pool could be considered as a possible evidence for an increased CAM with increasing CO₂ concentration. At maximum of chl *a*, TEP contribution to POC had a significant ($P= 0.04$) positive correlation with CO₂ increase (Fig. 14). This relation was observed in a trend of the decreasing of TEP contribution to POC noted from the beginning of the experiment until the end at 10 °C. High CO₂ concentration treatments (pH 7.2, 7.4 and 7.6) showed a significant ($P= 0.05$) higher carbon contribution of TEP than lower CO₂ concentration (pH 7.8, 8.0 and control). At maximum of the chl *a*, this increase in TEP contribution to POC has been estimated to 16 % as a function of the CO₂ increase that

causes 0.2 decrease of the pH. Thus, under a CO₂ increase that causes a 0.2 reduction of the pH, phytoplankton could increase the efficiency of it CAM by increasing CO₂ uptake that results in a 16 % higher TEP contribution to POC at maximum of chl *a*. However, these results should be taken with caution given that we started our experiments with high TEP contribution to POC. Nevertheless, TEP high starting values decreased during the exponential phase (Fig. 6a). Bacterial respiration could explain this decrease of TEP, since bacteria displayed a marked augmentation in the early period of the experiment in coincidence with TEP drop. Also carbon losses as sediment in the bottom of the mesocosms are probably weak due to the homogeneous mixing within the system.

POC in our experiment increased from the beginnig of the experiment until and the end of it. It followed the phytoplankton bloom development and beyond. POC was significantly ($P= 0.03$) correlated to phytoplankton during the exponential phase, while during stationary and post-bloom phase POC was significantly ($P= 0.01$) positively correlated to TEP. During the exponential phase, POC was dominated by phytoplankton (up to 75.2 %), while, at the stationary and the post-bloom phases TEP was the main contributor to POC (up to 66.8 %). This was similar to our field observations and results reported by Annane *et al.* (2015), who observed TEP contribution to POC reached up to 60 % in the LSLE. These results agree with estimates under low nutrient concentrations (Bar Zeev *et al.*, 2011), but are the double of values estimated under eutrophic conditions (Engel, 2004a). In contrast, TEP contribution to POC could be more variable. The TEP colorimetric method is semi-quantitative and it would have been more appropriate to follow the adaptation of the colorimetric method according to Villacorte *et al.* (2009). They suggested to include measurments of the smaller fractions of TEP (< 0.4 μm) by filtering 250 mL on a 0.4 μm pore size filters (47 mm) and then to filter 100 mL of these filtrate onto 0.05 μm pore size filters. This modification enable to detect the colloidal fraction of TEP and hence a better estimation of TEP contribution to POC. TEP colloidal fraction has been suggested to be three times more abundant than the particulate form (Villacorte *et al.*, 2009). Although, estimated POC, based on the sum of carbon

concentration in TEP, phytoplankton and bacteria, exhibited a significant positive correlation with measured POC ($r= 0.80$; $P< 0.01$) (Fig. 10). This highlighted the correlation between POC and other carbon variables that clearly influence it. However, this correlation was not valid during the whole sampling days. Beyond $\approx 700 \text{ } \mu\text{gC L}^{-1}$, estimated POC became underestimated. This was explained by the contribution of detritus that increased during stationary and post-bloom phases but was not considered in our estimation of POC.

The effect of temperature increase on POC concentration displayed no significant differences at 10°C , contrasting with that recorded at 15°C . Despite the significant higher phytoplankton measured at 15°C , these results were not observed in the POC. This may be explained by a probable phytoplankton cell size reduction at 15°C , as previously suggested by Peter and Sommer (2013) study on the Baltic Sea phytoplankton community. These authors observed that under high nutrient stress, rising temperature caused a reduction of 46 % in the mean cell size of the phytoplankton per $^\circ\text{C}$ and 4.7 % under low nutrient stress. Previous studies have also shown that temperature increase is associated with a decline in phytoplankton cell size (Agawin *et al.*, 2000; Hare *et al.*, 2007; Li *et al.*, 2009). Furthermore, some other studies highlighted an effect of temperature increase on phytoplankton community structure. A dominance of, phytoplankton species with smaller cell sizes at increased temperature treatments from experiment carried out on an Arctic phytoplankton community (Coello-Camba *et al.*, 2014). However, the lack of a significant POC increase with the increasing temperature could be related to phytoplankton cell size reduction during the exponential phase. During, the post-bloom phase, POC is mainly dominated by TEP. Similar POC concentrations could be attributed to a slower ability of the DOC to self-assemble to form TEP aggregates. These results have been observed by, Chen *et al.* (2015) through a study of ocean warming and acidification synergic effect on DOC assembly. Moreover, studies of aggregation and sedimentation processes under an increased temperature and CO_2 showed that aggregation that was measured as total aggregated volume, was higher at 15°C treatments than 20°C treatments (Seebah *et al.*,

2014). Also, the formation of aggregates by the diatom *Skeletonema* sp. were significantly reduced at 10 °C compared to 20 °C (Thornton and Thake, 1998). It was suggested that the average stickiness of particles was lower at 20 °C than at the lower temperatures tested. This was not consistent with Piontek *et al.* (2009) and Taucher *et al.* (2012) who recorded an increasing aggregation process at higher temperature using a range varying between 2.5 °C and 8.5 °C.

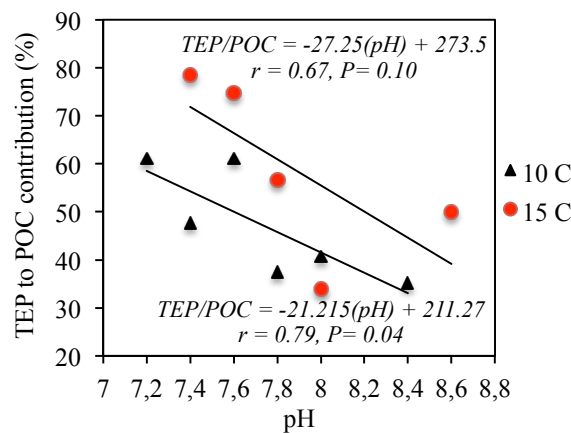


Figure. 14 Variations in the contribution (%) of transparent exopolymeric particles (TEP) normalized to particulate organic carbon (POC) versus CO₂ increase (pH decreasing gradient values) at maximum of chl *a*, at 10 °C and 15 °C.

Therefore, observations about temperature effect on aggregation are contradictory. Aggregation rate is a function of collision rate and stickiness. Collision rate depends on the density and size of the particles, density and size of the cells, turbulence and shear. Yet, it is important to consider all parameters related to aggregation dynamics in future research and consider that DOC assembly is a reversible process (Verdugo, 2012). The combined effects of temperature and CO₂ increase at 15 °C showed a rather similar response to that observed at 10 °C. At 15 °C a significant correlation was found for POC as a function of CO₂ increase at the maximum of the chl *a* (Table. 1). Moreover, TEP contribution to POC concentration showed a significant ($P < 0.05$) positive response to increasing CO₂ at the

maximum of chl *a* (Fig. 14), and at (t + 16) (data not shown). This suggested that the increasing of CAM with increasing CO₂ probably occurred at 15 °C too. However, while we recorded a significant ($P < 0.05$) higher TEP/Phytoplankton ratio at 10 °C rather than 15 °C, it was possible that temperature increase limited the aggregation process of carbohydrates. This could explain the fact that temperature increase (15 °C) resulted in a higher carbohydrates and not higher TEP than 10 °C.

1.4.5. CARBOHYDRATE CHEMICAL COMPOSITION

Sugar determination methodologies have been greatly improved during last decade (Kerhervé *et al.*, 1995; Hernes *et al.*, 1996; Panagiotopoulos *et al.*, 2001). Difficulties have begun quantitatively extracting and concentrating sugars from seawater with high salt content. This concern was one of the problems we tried to solve during sugar analysis of this study. Furthermore, carbohydrates have different charge states at seawater pH including neutral carbohydrates (Mopper *et al.*, 1992; Borch and Kirchman, 1997; Skoog and Benner, 1997), positively charged amino carbohydrates (Kaiser and Benner, 2000), and negatively charged uronic acids (Mopper *et al.*, 1995; Hung *et al.*, 2001). However, new analytical methods for carbohydrates determination have emerged and others have evolved. Detection limitation has been overcome due to the advent of sensitive chromatographic instruments such as gas chromatography-mass spectrometry. To remove salt from seawater, in this study we used ultra-filtration by centrifugation using amicon tubes (10 KDa), but the use of anion exchange resins or dialysis techniques are also efficient methods (Mopper *et al.*, 1992; Rich *et al.*, 1996; Borch and Kirchman, 1997; Skoog and Benner, 1997; Amon and Benner, 2003). Our determination of the chemical composition of the total carbohydrate fraction was aimed to studying the specific behavior of the monosaccharide compounds in the samples, which provides basic information about the dynamics of TEP precursors. The difference in concentration ranges observed between the colorimetric and the methylsilylation methods can be explained by the analytical differences between them. The two methods do not analyze the same thing (oxidized

sugars for colorimetric and neutral sugars for the methylsilylation). In the colorimetric method, the carboxylate groups of the oxidized sugars (glucuronate) undergo and exchange with Alcian blue, in order to color them. This staining is then analyzed by absorption spectroscopy and compared with Xanthan Gum. The total quantity of carbohydrate is then extrapolated from the quantity of oxidized sugars, hence the Xanthan Gum equivalents. On the other hand, in the methylsilylation method, the neutral sugars (non-oxidized) are derivatized and analyzed. Moreover, the total amount of carbohydrates is independent of the number of carboxylate groups.

Total carbohydrates concentrations increased along our experiment and peaked during the phytoplankton stationary phase at maximum of chl *a*. High carbohydrates exudations during the stationary phase have been noted previously in batch cultures of other diatom species (Granum *et al.*, 2002; Underwood *et al.*, 2004). Total carbohydrate chemical composition showed the presence of the following monosaccharides: glucose, arabinose, mannose, galactose, fructose, ribose and xylose. This carbohydrate composition differs from other studies that examined TEP chemical composition, which detected the predominance of fucose, rhamnose and arabinose (Mopper *et al.*, 1995; Zhou *et al.*, 1998). Carbohydrates composition in our study is more consistent with the carbohydrates composition of extracellular polysaccharides (Fogg, 1983; Myklestad, 1995; Urbani *et al.*, 2005). Nevertheless, chemical composition of phytoplankton exudates is known to vary between species and is dependent on the physiological status of these organisms (Arnoldi, 1993; Myklestad, 1995; Aluwihare and Repeta, 1999). Furthermore, our results are in accordance with a laboratory experiment performed on the extracellular production of carbohydrates by marine diatoms, which suggested that monosaccharide composition during the growth of *Skeletonema costatum* was glucose, galactose, mannose, xylose, arabinose, rhamnose and fucose (Urbani *et al.*, 2005). Additionally, the dominance of glucose detected in our study (up to 72 % of total carbohydrate) agrees with Urbani *et al.* (2005) observations (up to 60 % of total carbohydrate).

Our results of the increasing gradient of CO₂ concentration showed no significant response of the total carbohydrate concentration at 10 °C (Table. 2). Only a decreasing trend was observed at maximum of chl *a*, at 10 °C. However, the dynamics of each specific carbohydrate displayed at 10 °C a significant negative response of glucose and galactose and a significant positive response of arabinose and mannose to CO₂ increasing. Moreover, no clear effects were observed for fructose and ribose. In addition, total carbohydrate concentration was standardized to the sum of phytoplankton and bacteria. Here we added bacteria to insure maximum of precision, while bacteria was low but not abscente. Values varied between 0.06 µg and 0.1 µg of normalized carbohydrates. It showed a significant ($r= 0.81, P= 0.04$) negative correlation with pH decrease and a positive reponse to increasing CO₂ at maximum of chl *a*, at 10 °C (Fig. 15).

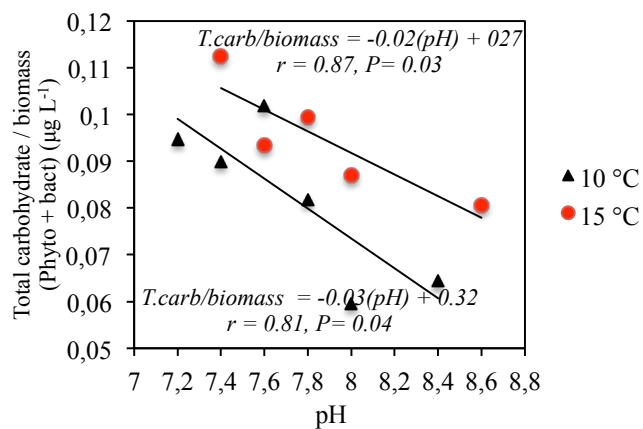


Figure. 15 Variation in total carbohydrate concentration normalized to total biomass of phytoplankton at maximum of chl *a*, at 10 °C and 15 °C. Annotation: phyto: phytoplankton; bact: bacteria; T.carb/biomass: Total carbohydrate / biomass

A CO₂ increase that causes a decrease of 0.2 units in pH caused the increase of average 0.20 µg L⁻¹ in the carbohydrate concentration normalized to phyto and bact biomass. This was in accordanc with the positive response of TEP contribution to POC. However, total carbohydrate normalization to chl *a* concentrations 0.62 ± 0.11, on average of total

carbohydrate to chl *a* ratio at maximum of chl *a*, at 10 °C. These data did not exhibit a significant response to CO₂ increase. It is important to note that these results needs more evidence to be validated. But they suggested that phytoplankton and bacteria carbohydrate concentration were influenced by CO₂ increasing gradient tested. The effect of temperature increase showed significantly ($P < 0.01$) higher total carbohydrate concentrations at 15 °C than 10 °C. The coefficient of increase of the carbohydrates concentration induced by temperature increase was calculated from the ratio between biomass recorded at 15 °C to those recorded at 10 °C. At maximum of chl *a*, temperature increase induced, on average $1.8 \pm 0.5 \mu\text{g L}^{-1}$ more carbohydrate at 15 °C than at 10 °C. On the other hand, temperature generated, on average $1.8 \pm 0.7 \mu\text{g L}^{-1}$ more phytoplankton at 15 °C than 10 °C. In contrast, no significant differences were observed in chl *a* concentration ($37.5 \pm 3.8 \mu\text{g L}^{-1}$ and $39.1 \pm 2.3 \mu\text{g L}^{-1}$). The simultaneous temperature and CO₂ increase showed a significant negative response of total carbohydrates concentrations at max of chl *a*, and (T + 16) (Table. 2). In addition, specific monosaccharide contribution to total carbohydrate concentrations displayed at 15 °C a positive response of arabinose, mannose and galactose and a negative response of glucose and ribose to CO₂ increasing gradient tested (Table. 2). This heterogeneity in the response of each monosaccharide to CO₂ increase is possible to be related to an adaptation of phytoplankton by a selective carbohydrate chemical composition. Glucose contribution to total carbohydrate decreased with increasing CO₂ concentration, while arabinose, mannose at 10 °C and arabinose, mannose and galactose at 15 °C displayed a decreasing contribution with increasing CO₂.

Overall, our observations suggest that a significant increasing gradient of CO₂ concentrations had a significant response of organic carbon parameters at maximum of chl *a*, and phytoplankton. The effect of CO₂ increase induced a decrease in the phytoplankton growth rate and biomass that resulted in a decrease of total concentrations of TEP and POC. Additionally, acidification of the water induced an increase in total carbohydrate / phytoplankton and bacteria ratio. This could also be observed in the higher TEP contribution to POC observed at elevated CO₂ treatments. These observations may be

attributed to an increasing CAM response to increasing CO₂. However, some studies found carbon overconsumption to be channelled mainly into an increase in the DOC fraction (Sambrotto *et al.*, 1993; Koeve, 2004), whereas others could trace this additional carbon almost entirely to POC and TEP (Engel *et al.*, 2002; Wetz and Wheeler, 2007). In this sense, it is difficult to compare our results to other observations. Our results did not exhibit a clear response to increasing CO₂, but it showed significant responses at maximum of chl *a*. Moreover, analytical differences between studies also limit comparisons. For example, it is important to note that comparisons of carbohydrate results reported from marine samples is difficult given the wide range of hydrolysis protocols used and the lack of intercomparison studies between the various analytical procedures (Mopper, 1995; Burney and Sieburth, 1977; Borch and Kirchmann, 1997; Kerhervé *et al.*, 2002).

Finally, observations in this study showed the important range of tolerance of phytoplankton coastal species to acidification. Even under high CO₂ concentration phytoplankton growth and production rates (personal communication from Robin Bénard) were maintained relatively high. A bloom was developed in all treatments and we hypothesize that a regulation system was adapted to the concentrations of CO₂ set during our experiment. It is important to mention that the responses of phytoplankton species to ocean acidification are shown to be very different depending on the organism and its ability to assimilate carbon (Rost *et al.*, 2008). Coastal species experience a large variability across a broad range of spatial and temporal scales, which allows an important degree of adaptation to these environmental conditions. The diversity of phytoplankton and TEP sensitivities to elevated CO₂ experiments is a result of complex interactions between environmental and biological variables, acting together on phytoplankton, TEP production and aggregation and TEP consumption and disaggregation processes.

CONCLUSION GENERALE

Cette étude présente le travail de recherche effectué sur les particules exopolymériques transparentes (TEP, en anglais) de l'estuaire maritime du Saint-Laurent (LSLE, en anglais). Le LSLE est un lieu de rencontre de masses d'eaux d'origines variées. En conséquent, la colonne d'eau du LSLE est stratifiée, ayant une fine couche de surface plus fluviale et plus chaude qu'une couche profonde plus océanique, plus salée, plus acide et plus froide. L'étude de distribution spatiale des TEP a été réalisée au sein de deux régions clefs du LSLE. Premièrement une zone de remontée des eaux profonde. Cette zone a été montrée caractéristique d'une matière organique d'origine terrestre et d'une concentration élevée de nutriment surtout en couche profonde. De plus, parmi les spécificités de cette zone, le fort mélange vertical qui a été observée à travers l'absence de différence significative entre certains paramètres environnementaux mesurées dans la couche de surface et la couche profonde de la même zone. Deuxièmement, les TEP ont été collectées dans une zone de front du LSLE. Deux fronts ont été échantillonnés durant cette étude. Ces fronts étaient probablement formés par la rencontre entre une masse d'eau estuarienne plus chaude, moins salée et moins dense avec une masse d'eau plus salée, plus dense et plus océanique. Cette zone de front a montré la dominance d'une matière organique d'origine plus océanique. En plus, de fortes concentrations de chlorophylle *a* (chl *a*) ont été observées dans la zone de front et un fort flux vertical de la couche de surface vers la couche profonde. Les TEP ont montré des concentrations moyennes des deux zones égale à $89,77 \pm 48,84 \mu\text{g XG eq L}^{-1}$ et $33,59 \pm 21,12 \mu\text{g XG eq L}^{-1}$ en couche de surface et en couche profonde, respectivement. Les TEP n'avaient aucune corrélation significative avec les paramètres environnementaux mesurés dans cette étude. Cependant, des observations caractéristiques de chaque zone étaient observées dans les TEP. Dans la zone de remontée des eaux profonde la concentration des TEP a montré un gradient au niveau de

la tête du chenal Laurentien. Ce gradient a aussi, été observé en couche de surface et en couche profonde sur les mesures de salinité, température, rapports isotopiques, concentration de chl *a* et estimation de concentration en détritus. Ce gradient était probablement relié à l'intrusion graduelle de masses d'eaux de différentes origines, au niveau de la tête du chenal Laurentien. Les concentrations de TEP les plus élevées ont été observé au niveau de l'estuaire supérieur et du fjord de Saguenay et ont été expliqués par une forte concentration de la fraction coloïdale au niveau de ces deux milieux. Au niveau de la zone de front, les TEP ont montré de concentrations plus élevées au niveau de la masse d'eau de caractère estuarien que la masse d'eau de caractère océanique. En outre, des concentrations élevées en TEP ont été observés au niveau de la couche profonde de la zone de front. Cela a été attribué au probable flux vertical enregistré. Durant cette étude les concentrations en TEP étaient significativement ($p < 0.01$) et positivement corrélées aux concentrations en carbone organique particulaire (POC, en anglais). Les TEP ont montré une contribution allant jusqu'à 82 % du POC du LSLE. Comparées à d'autres environnements aquatiques, les TEP standardisées à la concentration en chl *a* présentait de valeurs élevées au niveau du LSLE. D'où l'importance de ces particules dans la dynamique du carbone organique de l'estuaire. Les TEP étant en équilibre entre la fraction particulaire et dissoute jouent un rôle primordial dans le devenir de la production primaire et dans l'export du carbone (Passow, 2002; Thornton, 2002). Cependant, les TEP n'étaient pas le principal contributeur au pool de POC du LSLE. Dépendamment de la distribution spatiale, le POC dans la couche de surface était dominé par les TEP ou le phytoplancton ou les détritus. Dans la couche profonde les détritus étaient significativeent le contributeur principal au POC. Mais les détritus étaient exprimés par la différence entre les concentrations en POC mesurées et ceux estimées par la somme de la concentration en carbone organique des TEP, le phytoplancton et les batéries. Dans ces mesures seule les TEP qui peuvent avoir une surestimation de concentration reliée au protocole expérimental. D'où l'importance de la détermination de la fraction colloïdale des TEP.

L'étude des changements globaux et de leurs effets sur les TEP est nécessaire afin de bien comprendre les répercussions qui leur sont associées. Dans le cadre de

l'augmentation de la température globale et de l'acidification des océans, une expérience en mésocosme a été réalisée afin d'étudier l'effet de l'augmentation du pH et de la température sur les TEP. La pertinence des informations obtenues par ces expériences est plus importante lors de l'intégration de plus d'un élément perturbateur. L'acidification et le réchauffement des eaux sont des changements qui s'accentuent dans les années à venir. Nos résultats d'un bloom de *Skeletonema costatum* du LSLE suggèrent que l'augmentation de l'acidification engendre une diminution significative de la biomass de phytoplankton. De plus, l'effet de l'augmentation de l'acidification a aussi été observé sur les TEP et le POC principalement durant le maximum de chl *a* et le maximum des concentrations en TEP et en POC. L'augmentation de l'acidification entraînera une possible diminution significative de la concentration en TEP mais une augmentation significative de la contribution des TEP au POC. Cela a été expliqué par le fait que durant de plus faible valeur de pH, donc de plus forte concentration en CO₂, le phytoplankton augmente son assimilation du carbone. Celà résulte en des TEP plus concentrées en POC. L'effet de l'augmentation de l'acidification a aussi été enregistré sur les précurseurs des TEP. La concentration totale en carbohydrates a aussi été influencée par le gradient décroissant du pH testé dans cette étude. Les carbohydrates étaient composés de glucose, galactose, ribose, mannose arabinose et fructose. Le glucose avait la plus forte contribution à la concentration totale. De plus, le glucose et le galactose ont montré une réponse significativement positive à la diminution du pH. Par contre, l'arabinose et le mannose ont montré une réponse significativement négative. Cela a été supposé d'être expliqué par une production sélective de carbohydrate en fonction des concentrations en CO₂. En augmentant la concentration en CO₂, il est possible que le phytoplankton diminue son taux de croissance pour en parallèle augmenter son assimilation du carbone inorganique et le concentré dans les TEP. Cependant la plus faible biomasse phytoplanktonique engendré à de plus forte concentration en CO₂ résulte en de plus faible concentration en TEP. L'effet de l'augmentation de l'acidification a aussi été observé à de température de l'eau 5 °C plus élevées. L'augmentation de la température a eu un effet positif sur la biomasse phytoplanktonique et la concentration en carbohydrates mais pas sur la concentration en absolue en TEP et en POC. Cependant, les TEP et le POC normalisées à

la biomasse phytoplanctonique était plus élevée à 10 °C qu'à 15 °C. Étant donnée que la concentration en carbohydrates a aussi été significativement augmenté à 15 °C, l'absence de concentration plus élevée en TEP a été expliquée par l'effet de l'augmentation de la température qui a possiblement inhiber l'assemblage des carbohydrates en TEP, ainsi la diminution de la concentration des TEP. Alors, suivant notre évaluation à travers une expérience en mésocosme, l'effet de l'augmentation de l'acidification et de la température semble être présent et avoir une explication. Cependant, cet effet reste significatif principalement au maximum de biomasse phytoplanctonique et n'est pas clairement défini. Celà suggère que lorsqu'il s'agit d'un milieu estuaire, l'influence d'une multitude de processus atmosphériques, terrestres et océaniques donne comme résultat un milieu côtier où les organismes qu'y habitent sont adaptés à de forte fluctuations ayant alors le potentiel d'être résilient face à certains changements environnementaux. L'impact de ces changements diffère alors d'un milieu à un autre. De plus le fait qu'en réalité ces changements se produiront graduellement sur plusieurs décennies pourrait permettre l'adaptation des organismes côtiers.

PERSPECTIVES

- Durant cette étude des données de la distribution temporelle des particules exopolymériques transparentes (TEP, en anglais) ont été prélevées durant deux cycles de marées consécutifs au niveau de la tête du chenal Laurentien. Une analyse ultérieure de ces données pourrait fournir plus de détails quant à la dynamique temporelle des TEP dans un milieu de remontée des eaux profondes reliées aux courants des marées.
- Une plus vaste étude sur la distribution spatiale des TEP couvrant un plus grand espace géographique de l'estuaire maritime du Saint-Laurent (LSLE, en anglais) pourra nous fournir une visibilité plus claire quant à leur dynamique et leur rôle surtout dans un écosystème ayant une couche profonde hypoxique et plus acide comme le LSLE.
- Déterminer la teneur spécifique des TEP en carbone organique au sein du LSLE car les coefficients déterminés par d'autres auteurs sont probablement pas applicables à l'estimation de la teneur des TEP en carbone organique dans le LSLE qui présente de fortes contributions des TEP au pool de carbone organique particulaire.
- Étant tamponnées par l'hydrodynamique du milieu où elles se trouvent, une étude de distribution des TEP doit prendre en considération les données de la dynamique physique du milieu, tel que la vitesse du courant. Cela permettra une meilleure interprétation des concentrations des TEP et de leur lien avec les paramètres environnementaux.
- La méthode colorimétrique de mesure de la concentration des TEP est semi-quantitative et il sera plus intéressant d'adopter l'adaptation proposée par Villacorte *et al.* (2009) qui suggère d'utiliser des filtres de porosité de 0.4 µm en plus des filtres de porosité de 0.2 µm. Ceci permettra de quantifier la fraction colloïdale des TEP. Cette fraction

semble avoir une forte contribution à la concentration totale en TEP au niveau de l'estuaire supérieur et du fjord de Saguenay. De plus, la fraction coloïdale semble être importante dans une prochaine étude de l'effet de l'augmentation de la température sur les TEP. La température semble ralentir ou inhiber le processus d'aggrégation des TEP. D'où l'intérêt de la quantification de la fraction coloïdale des TEP.

- Une évaluation du taux d'assimilation du carbone inorganique par les diatomées tel que *Skeletonema costatum*. Une étude de ce type pourra fournir une idée si de telles espèces sont capables d'augmenter leur assimilation de carbone inorganique ou que ce mécanisme est constamment gardé à son maximum peu importe la concentration en carbone inorganique à l'extérieur de la cellule phytoplanctonique.
- Une évaluation spécifique de la concentration des TEP en carbone organique en fonction de différentes concentrations en CO₂ sera utile pour évaluer l'hypothèse que l'augmentation de la concentration en CO₂ engendre des TEP plus concentrées en carbone organique.
- Une détermination du possible lien qui pourra exister entre la concentration en CO₂ du milieu et la composition chimique des carbohydrates. Cette approche va évaluer si certaines concentrations en CO₂ peuvent déclencher un mécanisme adaptatif du phytoplancton permettant une production sélective de carbohydrates spécifiques.

RÉFÉRENCES BIBLIOGRAPHIQUES

- Accot, R. (2015). Caractérisation des couches minces phytoplanctoniques et comparaison des mécanismes les affectant dans l'estuaire maritime du Saint-Laurent et dans la baie de Monterey (Doctoral dissertation, Université du Québec à Rimouski).
- Aitsam, A., Hansen, H. P., Elken, J., Kahru, M., Laanemets, J., Pajuste, M., and Talpsepp, L. (1984). Physical and chemical variability of the Baltic Sea: a joint experiment in the Gotland Basin. *Continental Shelf Research*, 3(3), 291-310.
- Alldredge, A. L., and Silver, M. W. (1988). Characteristics, dynamics and significance of marine snow. *Progress in oceanography*, 20(1), 41-82.
- Aluwihare, L. I., and Repeta, D. J. (1999). A comparison of the chemical characteristics of oceanic DOM and extracellular DOM produced by marine algae. *Marine Ecology Progress Series*, 186, 105-117.
- Agawin, N. S., Duarte, C. M., and Agustí, S. (2000). Nutrient and temperature control of the contribution of picoplankton to phytoplankton biomass and production. *Limnology and Oceanography*, 45(3), 591-600.
- Amon, R. M., and Benner, R. (2003). Combined neutral sugars as indicators of the diagenetic state of dissolved organic matter in the Arctic Ocean. *Deep Sea Research Part I: Oceanographic Research Papers*, 50(1), 151-169.
- Annane, S., St-Amand, L., Starr, M., Pelletier, E., and Ferreyra, G. A. (2015). Contribution of transparent exopolymeric particles (TEP) to estuarine particulate organic carbon pool. *Marine Ecology Progress Series*, 529, 17-34.
- Arnosti, C. (1993). Structural characterization and bacterial degradation of marine carbohydrates (No. WHOI-93-26). Woods hole oceanographic intitutuion..
- Armstrong, R., Lee, C., Hedges, J., Honjo, S., and Wakeham, S., (2002). A new, mechanistic model for organic carbon fluxes in the ocean based on the quantitative association of POC with ballast minerals. *Deep-Sea Res, Part II*, 49: 219.
- Arrigo, K.R., (2007). Carbon cycle: Marine manipulations. *Nature*, 450(7169), 491-492.
- Azam F., Malfatti F. (2007). Microbial structuring of marine ecosystems. *Nat. Rev. Microbiol.* 5, 782–791. 10.1038/nrmicro1747.

- Bar-Zeev, E., Berman-Frank, I., Liberman, B., Rahav, E., Passow, U., and Berman, T. (2009). Transparent exopolymer particles: Potential agents for organic fouling and biofilm formation in desalination and water treatment plants. *Desalination and Water Treatment*, 3(1-3), 136-142.
- Bar-Zeev, I., Berman-Frank, O., and Girshevitz. (2012). Revised paradigm of aquatic biofilm formation facilitated by microgel transparent exopolymer particles. *Proc. Natl. Acad. Sci.*, 109, 9119–9124.
- Bar-Zeev, E., Berman, T., Raha,v E., Dishon, G., Herut, B., and Berman-Frank. (2011). Transparent exopolymer particle (TEP) dynamics in the eastern Mediterranean Sea. *Marine Ecology Progress Series*, 431, 107–118.
- Beauvais, S., Pedrotti, M.L., Egge, J., Iversen, K., and Marrasé, C., (2006). Effects of turbulence on

TEP dynamics under contrasting nutrient conditions: implications for aggregation and sedimentation processes. *Mar. Ecol. Progr. Ser.*, 323: 47-57.

- Beauvais, S., Pedrotti, M. L., Villa, E., and Lemée, R. (2003). Transparent exopolymer particle (TEP) dynamics in relation to trophic and hydrological conditions in the NW Mediterranean Sea. *Marine Ecology Progress Series*, 262, 97-109.
- Belzile, C., Brugel, S., Nozaïs, C., Gratton, Y., and Demers, S. (2008). Variations of the abundance and nucleic acid content of heterotrophic bacteria in Beaufort Shelf waters during winter and spring. *Journal of Marine Systems*, 74(3), 946-956.
- Benner, R., Pakulski, J.D., McCarthy, M., Hedges, J.I., and Hatcher, P., (1992). Bulk chemical characteristics of dissolved organic matter in the ocean. *Science*, 255, 1561–1564.
- Berge, T., Daugbjerg, N., Andersen, B. B., and Hansen, P. J. (2010). Effect of lowered pH on marine phytoplankton growth rates. *Marine Ecology Progress Series*, 416, 79-91.
- Blasco, D., Estrada, M., and Jones, B. H. (1981). Short Time Variability of Phytoplankton Populations in Upwelling Regions-The Example of Northwest Africa. *Coastal upwelling*, 339-347.
- Borch, N. H., and Kirchman, D. L. (1997). Concentration and composition of dissolved combined neutral sugars (polysaccharides) in seawater determined by HPLC-PAD. *Marine Chemistry*, 57(1-2), 85-95.
- Borchard, C., and Engel, A. (2012). Organic matter exudation by *Emiliania huxleyi* under simulated future ocean conditions. *Biogeosciences (BG)*, 9(8), 3405-3423.
- Borchard, C., Borges, A. V., Hänel, N., and Engel, A. (2011). Biogeochemical response of *Emiliania huxleyi* (PML B92/11) to elevated CO₂ and temperature under phosphorous limitation: a chemostat study. *Journal of Experimental Marine Biology and Ecology*, 410, 61-71.
- Borch, N. H., and Kirchman, D., L. (1997). Concentration and composition of dissolved combined neutral sugars (polysaccharides) in seawater determined by HPLC-PAD. *Marine Chemistry*, 57(1-2), 85-95.
- Burney, C. M., and Sieburth, J. M. (1977). Dissolved carbohydrates in seawater. II, A spectrophotometric procedure for total carbohydrate analysis and polysaccharide estimation. *Marine Chemistry*, 5(1), 15-28.
- Burd, A. B., and Jackson, G. A. (2009). Particle aggregation. *Annual Review of Marine Science*, 1, 65-90.
- Cai, W. J., Hu, X., Huang, W. J., Murrell, M. C., Lehrter, J. C., Lohrenz, S. E., and Zhao, P. (2011). Acidification of subsurface coastal waters enhanced by eutrophication. *Nature Geoscience*, 4(11), 766-770.
- Cai, W. J. (2011). Estuarine and coastal ocean carbon paradox: CO₂ sinks or sites of terrestrial carbon incineration?. *Annual Review of Marine Science*, 3, 123-145.
- Caldeira, K., and Wickett, M. E. (2003). Oceanography: anthropogenic carbon and ocean pH. *Nature*, 425(6956), 365-365.
- Cazenave, A., Dominh, K., Guinehut, S., Berthier, E., Llovel, W., Ramillien, G., and Larnicol, G. (2009). Sea level budget over 2003–2008: A reevaluation from GRACE space gravimetry, satellite altimetry and Argo. *Global and Planetary Change*, 65(1), 83-88.
- Chust, G., Allen, J., Bopp, L., Schrum, C., Holt, J., Tsiaras, K., and Daewel, U. (2014). Biomass changes and trophic amplification of plankton in a warmer ocean. *Global change biology*, 20(7), 2124-2139.
- Chen, C.-S., Anaya, J.M., Chen, E.Y.T., Farr, E. and Chin, W.-C. (2015). Ocean warming–acidification synergism undermines dissolved organic matter assembly. *Plos one*,10(2), e0118300.
- Chin, W., Orellana, M.V. P. (1998). Spontaneous assembly of marine dissolved organic matter into polymer gels. *Nature*, 391, 568–572.
- Chust, G., Allen, J., Bopp, L., Schrum, C., Holt, J., Tsiaras, K., and Daewel, U. (2014). Biomass changes and trophic amplification of plankton in a warmer ocean. *Global change biology*, 20(7),

2124-2139.

- Claquin, P., Probert, I., Lefebvre, S., and Veron, B. (2008). Effects of temperature on photosynthetic parameters and TEP production in eight species of marine microalgae. *Aquatic Microbial Ecology*, 51(1), 1-11.
- Clayton, T. D., and Byrne, R. H. (1993). Spectrophotometric seawater pH measurements: total hydrogen ion concentration scale calibration of m-cresol purple and at-sea results. *Deep Sea Research Part I: Oceanographic Research Papers*, 40(10), 2115-2129.
- Coello-Camba, A., Agustí, S., Holding, J., Arrieta, J. M., and Duarte, C. M. (2014). Interactive effect of temperature and CO₂ increase in Arctic phytoplankton. *Frontiers in Marine Science*, 1, 49.
- Corzo, A., Morillo, J. A., and Rodríguez, S. (2000). Production of transparent exopolymer particles (TEP) in cultures of *Chaetoceros calcitrans* under nitrogen limitation. *Aquatic Microbial Ecology*, 23(1), 63-72.
- Dam, H. G., and Drapeau, D. T. (1995). Coagulation efficiency, organic-matter glues and the dynamics of particles during a phytoplankton bloom in a mesocosm study. *Deep Sea Research Part II, Topical Studies in Oceanography*, 42(1), 111-123.
- De Mendiola, B., R. (1981). Seasonal phytoplankton distribution along the Peruvian coast. *Coastal upwelling*, 348-356.
- Delille, B., Harlay, J., Zondervan, I., Jacquet, S., Chou, L., Wollast, R., and Gattuso, J. P. (2005). Response of primary production and calcification to changes of pCO₂ during experimental blooms of the coccolithophorid *Emiliania huxleyi*. *Global Biogeochemical Cycles*, 19(2).
- Denman, K. L., and Powell, T. M. (1984). Effects of physical processes on planktonic ecosystems in the coastal ocean. *Oceanography and marine biology*, 22, 125-168.
- Dickson, A. G. (1993). The measurement of sea water pH. *Marine Chemistry*, 44(2), 131-142.
- Ding, Y. X., Hung, C. C., Santschi, P. H., Verdugo, P., and Chin, W. C. (2009). Spontaneous assembly of exopolymers from phytoplankton. *Terrestrial, Atmospheric and Oceanic Sciences*, 20(5), 741.
- Doney, S. C. (2010). The growing human footprint on coastal and open-ocean biogeochemistry science, 328(5985), 1512-1516.
- Dufour, R., Benoît, H., Castonguay, M., Chassé, J., Devine, L., Galbraith, P., and Savard, L. (2010). Ecosystem status and trends report: Estuary and Gulf of St. Lawrence ecozone. DFO Can. Sci. Advis. Sec. Res. Doc, 30, 2010.
- Egge, J.K., Thingstad, T.F., Larsen, A., Engel, A., Wohlers, J., Bellerby, R.G.J., and U. Riebesell., (2009). Primary production during nutrient-induced blooms at elevated CO₂ concentrations. *Biogeosciences*, 6(5): 877-885.
- El-Sabh, M. I., and Silverberg, N. (1990). The St. Lawrence Estuary.
- El-Sabh, M. I., and Silverberg, N. (Eds.). (2012). *Oceanography of a large-scale estuarine system: the St. Lawrence* (Vol. 39). Springer Science & Business Media.
- Engel, A., Piontek, J., Grossart, H. P., Riebesell, U., Schulz, K. G., and Sperling, M. (2014). Impact of CO₂ enrichment on organic matter dynamics during nutrient induced coastal phytoplankton blooms. *Journal of Plankton Research*, 36(3), 641-657.
- Engel, A., Borchard, C., Piontek, J., Schulz, K. G., Riebesell, U., and Bellerby, R. (2013). CO₂ increases 14C-primary production in an Arctic plankton community. *Biogeosciences (BG)*, 10(3), 1291-1308.
- Engel, A., Piontek, J., Grossart, H. P., Riebesell, U., Schulz, K. G., and Sperling, M. (2014). Impact of CO₂ enrichment on organic matter dynamics during nutrient induced coastal phytoplankton blooms. *Journal of Plankton Research*, 36(3), 641-657.
- Engel, A., Händel, N., Wohlers, J., Lunau, M., Grossart, H. P., Sommer, U., and Riebesell, U. (2011). Effects of sea surface warming on the production and composition of dissolved organic

matter during phytoplankton blooms: results from a mesocosm study. *Journal of Plankton Research*, 33(3), 357-372.

- Engel, A. (2009). Determination of marine gel particles. *Practical Guidelines for the Analysis of Seawater*, 125-142.
 - Engel, A., Schulz, K. G., Riebesell, U., Bellerby, R., Delille, B., and Schartau, M. (2008). Effects of CO₂ on particle size distribution and phytoplankton abundance during a mesocosm bloom experiment (PeECE II). *Biogeosciences*, 5, 509–521.
 - Engel, A. (2005). Testing the direct effect of CO₂ concentration on a bloom of the coccolithophorid *Emiliania huxleyi* in mesocosm experiments. *Limnol. Oceanogr.*, 50, 493-504.
 - Engel, A. (2004a). Distribution of transparent exopolymer particles (TEP) in the northeast Atlantic Ocean and their potential significance for aggregation processes. *Deep Sea Research Part I: Oceanographic Research Papers*, 51(1), 83-92.
 - Engel, A., Delille, B., Jacquet, S., Riebesell, U., Rochelle-Newall, E., Terbrüggen, A., and Zondervan, I. (2004b). Transparent exopolymer particles and dissolved organic carbon production by *Emiliania huxleyi* exposed to different CO₂ concentrations: a mesocosm experiment. *Aquatic Microbial Ecology*, 34(1), 93-104.
 - Engel, A., Thoms, S., Riebesell, U., Rochelle-Newall, E., Zondervan, I. (2004c). Polysaccharide aggregation as a potential sink of marine dissolved organic carbon. *Nature*, 428, 929-932.
 - Engel, A., Goldthwait, S., Passow, U., and Alldredge, A. (2002). Temporal decoupling of carbon and nitrogen dynamics in a mesocosm diatom bloom. *Limnology and Oceanography*, 47(3), 753-761.
 - Engel, A. (2002). Direct relationship between CO₂ uptake and transparent exopolymer particles production in natural phytoplankton. *J. Plankton Res.*, 24(1): 49-53.
 - Engel, A., and Passow, U. (2001). Carbon and nitrogen content of transparent exopolymer particles (TEP) in relation to their Alcian Blue adsorption. *Mar. Ecol. Progr. Ser.*, 219, 1-10.
 - Engel, A. (2000). The role of transparent exopolymer particles (TEP) in the increase in apparent particle stickiness a during the decline of a diatom bloom. *J. Plankton Res.*, 22(3): 485-497.
 - Eppley, Richard, W. (1972). Temperature and phytoplankton growth in the sea. *Fish. Bull.* vol. 70, no 4, 1063-1085.
-
- Falkowski, P. G., and Raven, J. A. (2013). *Aquatic photosynthesis*. Princeton University Press.
 - Franks, P. J., and Chen, C. (1996). Plankton production in tidal fronts: a model of Georges Bank in summer. *Journal of Marine Research*, 54(4), 631-651.
 - Fernández, E., Cabal, J., Acuña, J., Bode, A., Botas, A., and García-Soto, C. (1993). Plankton distribution across a slope current-induced front in the southern Bay of Biscay. *Journal of Plankton Research*, 15(6), 619-641.
 - Feng, Y., Warner, M. E., Zhang, Y., Sun, J., Fu, F.X., Rose, J. M., and D.A. Hutchins., 2008. Interactive effects of increased pCO₂, temperature and irradiance on the marine coccolithophore *Emiliania huxleyi* (Prymnesiophyceae). *Eur. J. Phycol.*, 43(1): 87-98.
 - Fogg, G. E. (1983). The ecological significance of extracellular products of phytoplankton photosynthesis. *Botanica marina*, 26(1), 3-14.
 - Franks, P. J. (1992). Sink or swim: Accumulation of biomass at fronts. *Marine ecology progress series*. Oldendorf, 82(1), 1-12.
 - Fry, B. (2006). *Stable isotope ecology* (Vol. 521). New York, Springer.
 - Fukao, T., Kimoto, K., and Kotani, Y. (2010). Production of transparent exopolymer particles by four diatom species. *Fisheries science*, 76(5), 755-760.
 - Fukuda, R., Ogawa, H., Nagata, T., and Koike, I. (1998). Direct determination of carbon and nitrogen contents of natural bacterial assemblages in marine environments. *Applied and environmental microbiology*, 64(9), 3352-3358.

- Garvine, R. W., and Monk, J. D. (1974). Frontal structure of a river plume. *Journal of Geophysical Research*, 79(15), 2251-2259.

- Garvine, R. W. (1977). Observations of the motion field of the Connecticut River plume. *Journal of Geophysical Research*, 82(3), 441-454.
- Girard, J. M., Deschênes, J. S., Tremblay, R., and Gagnon, J. (2013). FT-IR/ATR univariate and multivariate calibration models for in situ monitoring of sugars in complex microalgal culture media. *Bioresource technology*, 144, 664-668.
- Gilbert, D., Sundby, B., Gobeil, C., Mucci, A., and Tremblay, G. H. (2005). A seventy-two-year record of diminishing deep-water oxygen in the St. Lawrence estuary: The northwest Atlantic connection. *Limnology and Oceanography*, 50(5), 1654-1666.
- Gearing, J. N., and Pocklington, R. (1990). Organic geochemical studies in the St. Lawrence Estuary. In *Oceanography of a Large-Scale Estuarine System* (pp. 170-201). Springer New York., 180, 254-265.
- Giordano, M., Beardall, J., and Raven, J. A. (2005). CO₂ concentrating mechanisms in algae: mechanisms, environmental modulation, and evolution. *Annu. Rev. Plant Biol.*, 56, 99-131.
- Goldman, J. C., and Carpenter, E. J. (1974). A kinetic approach to the effect of temperature on algal growth. *Limnology and Oceanography*, 19(5), 756-766.
- Granum, E., Kirkvold, S., and Myklestad, S. M. (2002). Cellular and extracellular production of carbohydrates and amino acids by the marine diatom *Skeletonema costatum*: diel variations and effects of N depletion. *Marine Ecology Progress Series*, 242, 83-94.
- Grasshoff, K., Kremling, K., and Ehrhardt, M. (Eds.). (2009). *Methods of seawater analysis*. John Wiley and Sons.
- Greisman, P., and Ingram, G. (1977). Nutrient distribution in the St. Lawrence estuary. *Journal of the Fisheries Board of Canada*, 34(11), 2104-2116.

- Hare, C. E., Leblanc, K., DiTullio, G. R., Kudela, R. M., Zhang, Y., Lee, P. A., and Hutchins, D. A. (2007). Consequences of increased temperature and CO₂ for phytoplankton community structure in the Bering Sea. *Marine Ecology Progress Series*, 352, 9-16.
- Harris, G. P. (1980). Temporal and spatial scales in phytoplankton ecology. Mechanisms, methods, models, and management. *Canadian Journal of Fisheries and Aquatic Sciences*, 37(5), 877-900.
- Hernes, P. J., Hedges, J. I., Peterson, M. L., Wakeham, S. G., and Lee, C. (1996). Neutral carbohydrate geochemistry of particulate material in the central equatorial Pacific. *Deep Sea Research Part II: Topical Studies in Oceanography*, 43(4), 1181-1204.
- Holm-Hansen, O., Lorenzen, C. J., Holmes, R. W., and Strickland, J. D. (1965). Fluorometric determination of chlorophyll. *Journal du Conseil*, 30(1), 3-15.
- Hoskins, B. J., and Bretherton, F. P. (1972). Atmospheric frontogenesis models: Mathematical formulation and solution. *Journal of the Atmospheric Sciences*, 29(1), 11-37.
- Hung, C. C., Tang, D., Warnken, K. W., and Santschi, P. H. (2001). Distributions of carbohydrates, including uronic acids, in estuarine waters of Galveston Bay. *Marine Chemistry*, 73(3), 305-318.
- Hung, C. C., Tang, D., Warnken, K. W., and Santschi, P. H. (2001). Distributions of carbohydrates, including uronic acids, in estuarine waters of Galveston Bay. *Marine Chemistry*, 73(3), 305-318.
- Ingram, R. G. (1975). Influence of tidal-induced vertical mixing on primary productivity in the St. Lawrence estuary. *Memoires de la Societe Royale des Sciences de Liege. Coastal and Shelf Science*, 16(3), 333-338. In *Oceanography of a large-scale estuarine system*. Springer New York.
- Ingram, C. L., and Hessler, R. R. (1983). Distribution and behavior of scavenging amphipods from the central North Pacific. *Deep Sea Research Part A. Oceanographic Research Papers*, 30(7), 683-706.

- Ingram, R. G. (1983). Vertical mixing at the head of the Laurentian Channel. *Estuarine*,
- Iribarri, J., Undurraga, A., Muela, A., and Egea, L. (1985). Heterotrophic bacterial activity in coastal waters: functional relationship of temperature and phytoplankton population. *Ecological Modelling*, 28(1), 113-120.
- Iribarri, J., Undurraga, A., Muela, A., and Egea, L. (1985). Heterotrophic bacterial activity in coastal waters: functional relationship of temperature and phytoplankton population. *Ecological Modelling*, 28(1-2), 113-120.
- Jackson, G. A. (1995). TEP and coagulation during a mesocosm experiment. *Deep Sea Research Part II: Topical Studies in Oceanography*, 42(1), 215-222.
- Jones, B. H., and Halpern, D. (1981). Biological and physical aspects of a coastal upwelling event observed during March-April 1974 off northwest Africa. *Deep Sea Research Part A: Oceanographic Research Papers*, 28(1), 71-81.
- Kahl, L. A., Vardi, A., and Schofield, O. (2008). Effects of phytoplankton physiology on export flux. *Marine Ecology Progress Series*, 354, 3-19.
- Kaiser, K., and Benner, R. (2000). Determination of amino sugars in environmental samples with high salt content by high-performance anion-exchange chromatography and pulsed amperometric detection. *Analytical Chemistry*, 72(11), 2566-2572.
- Kepkay, P., 1994. Particle aggregation and the biological reactivity of colloids. *Mar. Ecol., Prog. Ser.* 109, 293–304.
- Kerhervé, P., Buscail, R., Gadel, F., and Serve, L. (2002). Neutral monosaccharides in surface sediments of the northwestern Mediterranean Sea. *Organic geochemistry*, 33(4), 421-435
- Kerhervé, P., Charrière, B., and Gadel, F. (1995). Determination of marine monosaccharides by high-pH anion-exchange chromatography with pulsed amperometric detection. *Journal of Chromatography A*, 718(2), 283-289.
- Kim, J. M., Lee, K., Shin, K., Kang, J. H., Lee, H. W., Kim, M., and Jang, M. C. (2006). The effect of seawater CO₂ concentration on growth of a natural phytoplankton assemblage in a controlled mesocosm experiment. *Limnology and oceanography*, 51(4), 1629-1636.
- Kiørboe, T., and Hansen, J. L. (1993). Phytoplankton aggregate formation: observations of patterns and mechanisms of cell sticking and the significance of exopolymeric material. *Journal of Plankton Research*, 15(9), 993-1018.
- Klaas, C., and Archer, D. E. (2002). Association of sinking organic matter with various types of mineral ballast in the deep sea: Implications for the rain ratio. *Global Biogeochemical Cycles*, 16(4).
- Koeve, W. (2004). Spring bloom carbon to nitrogen ratio of net community production in the temperate N. Atlantic. *Deep Sea Research Part I: Oceanographic Research Papers*, 51(11), 1579-1600.
- Lacroix, J. C., Fraoua, K., and Lacaze, P. C. (1998). Moving front phenomena in the switching of conductive polymers. *Journal of Electroanalytical Chemistry*, 444(1), 83-93.
- Lafleur, P. E., Legendre, L., and Cardinal, A. (1979). Dynamique d'une population estuarienne de Diatomées planctoniques: effet de l'alternance des marées de morte-eau et de vive-eau. *Oceanologica Acta*, 2(3), 307-315.
- Langdon, C., and Atkinson, M. J. (2005). Effect of elevated pCO₂ on photosynthesis and calcification of corals and interactions with seasonal change in temperature/irradiance and nutrient enrichment. *Journal of Geophysical Research: Oceans*, 110(C9).
- Larouche, P., and Boyer-Villemaire, U. (2010). Suspended particulate matter in the St. Lawrence estuary and Gulf surface layer and development of a remote sensing algorithm. *Estuarine, Coastal and Shelf Science*, 90(4), 241-249.

- Lassen, M. K., Nielsen, K. D., Richardson, K., Garde, K., and Schlüter, L. (2010). The effects of temperature increases on a temperate phytoplankton community—a mesocosm climate change scenario. *Journal of Experimental Marine Biology and Ecology*, 383(1), 79-88.
- Lavoie, P. A., Bonn, F., Dubois, J. M. M., and El-Sabh, E. M. (1985). Structure thermique et variabilité du courant de surface de l'estuaire maritime du Saint-Laurent à l'aide d'images du satellite HCMM. *Canadian journal of remote sensing*, 11(1), 70-84.
- Levasseur, M., Thompson, P. A., and Harrison, P. J. (1993). Physiological acclimation of marine phytoplankton to different nitrogen sources. *Journal of Phycology*, 29(5), 587-595.
- Lebaron, P., Parthuisot, N., and Catala, P. (1998). Comparison of blue nucleic acid dyes for flow cytometric enumeration of bacteria in aquatic systems. *Applied and environmental microbiology*, 64(5), 1725-1730.
- Levasseur, M. E., and Therriault, J. C. (1987). Phytoplankton biomass and nutrient dynamics in a tidally induced upwelling: the role of the NO_3^- : SiO_4 ratio. *Mar. Ecol. Prog. Ser.*, 39, 87-97.
- Li, W. K., McLaughlin, F. A., Lovejoy, C., and Carmack, E. C. (2009). Smallest algae thrive as the Arctic Ocean freshens. *Science*, 326(5952), 539-539.
- Long, R. A., and Azam, F. (1996). Abundant protein-containing particles in the sea. *Aquatic Microbial Ecology*, 10, 213.
- Longhurst, A., Sathyendranath, S., Platt, T., & Caverhill, C. (1995). An estimate of global primary production in the ocean from satellite radiometer data. *Journal of plankton Research*, 17(6), 1245-1271.

- Mahadevan, A., and Archer, D. (2000). Modeling the impact of fronts and mesoscale circulation on the nutrient supply and biogeochemistry of the upper ocean. *Journal of Geophysical Research: Oceans*, 105(C1), 1209-1225.
- Mahadevan, A., and Tandon, A. (2006). An analysis of mechanisms for submesoscale vertical motion at ocean fronts. *Ocean Modelling*, 14(3), 241-256.
- Mari, X., Torréton, J. P., Trinh, C. B. T., Bouvier, T., Van Thuoc, C., Lefebvre, J. P., and Ouillon, S. (2012). Aggregation dynamics along a salinity gradient in the Bach Dang estuary, North Vietnam. *Estuarine, Coastal and Shelf Science*, 96, 151-158.
- Mari, X., and Robert, M. (2008). Metal induced variations of TEP sticking properties in the southwestern lagoon of New Caledonia. *Marine Chemistry*, 110(1), 98-108.
- Mari, X., and Rassoulzadegan, F. (2004). Role of TEP in the microbial food web structure. I. Grazing behavior of a bacterivorous pelagic ciliate. *Marine Ecology Progress Series*, 279, 13-22.
- Mari, X., Beauvais, S., Lemée, R., Pedrotti, M.L. (2001). Non-Redfield C:N Ratio of Transparent Exopolymeric Particles in the Northwestern Mediterranean Sea. *Limnol.Oceanogr.*, 46(7): 1831-1836
- Mari, X. (1999). Carbon content and C:N ratio of transparent exopolymeric particles (TEP) produced by bubbling exudates of diatoms. *Mar. Ecol. Progr. Ser.*, 183: 59-71.
- Mari, X. Kiørboe., T. (1996). Abundance, size distribution and bacterial colonization of transparent exopolymeric particles (TEP) during spring in the Kattegat. *Journal of plankton research* 18:969–986
- Marie, D., Partensky, F., Jacquet, S., and Vaulot, D. (1997). Enumeration and cell cycle analysis of natural populations of marine picoplankton by flow cytometry using the nucleic acid stain SYBR Green I. *Applied and Environmental Microbiology*, 63(1), 186-193.
- Marra, J. (1978). Phytoplankton photosynthetic response to vertical movement in a mixed layer. *Marine biology*, 46(3), 203-208.
- Mecozzi, M., Acquistucci, R., Di Noto, V., Pietrantonio, E., Amici, M., and Cardarilli, D. (2001). Characterization of mucilage aggregates in Adriatic and Tyrrhenian sea: structure similarities between mucilage samples and the insoluble fractions of marine humic substance. *Chemosphere*, 44, 711–722.
- Menden-Deuer, S., and Lessard, E. J. (2000). Carbon to volume relationships for dinoflagellates,

- diatoms, and other protist plankton. Limnology and Oceanography, 45(3), 569-579.
- Montagnes, D. J., & Franklin, M. (2001). Effect of temperature on diatom volume, growth rate, and carbon and nitrogen content: reconsidering some paradigms. Limnology and Oceanography, 46(8), 2008-2018.
 - Mooers, C. N., and Maul, G. A. (1998). Intra-Americas sea circulation. The sea, 11, 183-208.
 - Morán, X. A. G., López-Urrutia, Angel, Calvo-Díaz., Alejandra., and Li, W. K. (2010). Increasing importance of small phytoplankton in a warmer ocean. Global Change Biology, 16(3), 1137-1144.
 - Mopper, K., Schultz, C. A., Chevrolot, L., Germain, C., Revuelta, R., and Dawson, R. (1992). Determination of sugars in unconcentrated seawater and other natural waters by liquid chromatography and pulsed amperometric detection. Environmental science & technology, 26(1), 133-138.
 - Mopper, K., Zhou, J., Sri Ramana, K., Passow, U., Dam, H. G., and D.T. Drapeau. (1995). The role of surface-active carbohydrates in the flocculation of a diatom bloom in a mesocosm. Deep-Sea Res. Part II, 42(1): 47-73.
 - Moreau, S., Mostajir, B., Almandoz, G. O., Demers, S., Hernando, M., Lemarchand, K., and Thyssen, M. (2014). Effects of enhanced temperature and ultraviolet B radiation on a natural plankton community of the Beagle Channel (southern Argentina): a mesocosm study. Aquatic Microbial Ecology, 72(2), 155-173.
 - Motwani, N. H., and Gorokhova, E. (2013). Mesozooplankton grazing on picocyanobacteria in the Baltic Sea as inferred from molecular diet analysis. PLoS One, 8(11), e79230.
 - Mucci, A., Starr, M., Gilbert, D., and Sundby, B. (2011). Acidification of lower St. Lawrence Estuary bottom waters. Atmosphere-Ocean, 49(3), 206-218.
 - Mucci, A., Levasseur, M., Gratton, Y., Martias, C., Scarratt, M., Gilbert, D., and Lansard, B. (2017). Tidally-induced variations of pH at the head of the Laurentian Channel. Canadian Journal of Fisheries and Aquatic Sciences, (ja).
 - Myklestad, S., and Haug, A. (1972). Production of carbohydrates by the marine diatom *Chaetoceros affinis* var. *willei* (Gran) Hustedt. I. Effect of the concentration of nutrients in the culture medium. Journal of Experimental Marine Biology and Ecology, 9(2), 125-136.
 - Myklestad, S. M. (1995). Release of extracellular products by phytoplankton with special emphasis on polysaccharides. Science of the total Environment, 165(1), 155-164.

 - Orellana, M. V., and Verdugo, P. (2003). Ultraviolet radiation blocks the organic carbon exchange between the dissolved phase and the gel phase in the ocean. Limnology and oceanography, 48(4), 1618-1623.
 - Ortega-Retuerta, E., Reche, I., Pulido-Villena, E., Agustí, S., and Duarte, C. M. (2009). Uncoupled distributions of transparent exopolymer particles (TEP) and dissolved carbohydrates in the Southern Ocean. Marine chemistry, 115(1), 59-65.

 - Panagiotopoulos, C., and Sempéré, R. (2005). Analytical methods for the determination of sugars in marine samples: A historical perspective and future directions. Limnology and Oceanography: Methods, 3(10), 419-454.
 - Passow, U., and Carlson, C. A. (2012). The biological pump in a high CO₂ world. Marine Ecology Progress Series, 470, 249-271.
 - Passow, U. (2012). The abiotic formation of TEP under different ocean acidification scenarios. Mar. Chem., 128-129(0): 72-80.
 - Passow U. (2002a). Production of transparent exopolymer particles (TEP) by phyto and bacterioplankton. Marine ecology-progress series 236:1-12
 - Passow U. (2002b). Transparent exopolymer particles (TEP) in aquatic environments. Progress in Oceanography 55:287-333

- Passow, U. (2000). Formation of Transparent Exopolymer Particles, TEP, from dissolved precursor material. *Marine Ecology Progress Series*, 192, 1–11.
- Passow, U., and Alldredge, A. L. (1999). Do transparent exopolymer particles (TEP) inhibit grazing by the euphausiid *Euphausia pacifica*? *Journal of Plankton Research*, 21(11), 2203-2217.
- Passow, U., and Alldredge, A. L. (1995). A dye-binding assay for the spectrophotometric measurement of transparent exopolymer particles (TEP). *Limnology and Oceanography*, 40(7), 1326-1335.
- Passow, U., and Alldredge, A. L. (1994). Distribution, size, and bacterial colonization of transparent exopolymer particles (TEP) in the ocean. *Marine Ecology Progress Series*, 113, 185–198.
- Passow, U., Alldredge, A. L., and Logan, B. E. (1994). The role of particulate carbohydrate exudates in the flocculation of diatom blooms. *Deep Sea Research Part I: Oceanographic Research Papers*, 41(2), 335-357
- Passow, U., and Wassmann, P. (1994). On the Trophic Fate of *Phaeocystis-Pouchetii* (Hariot). 4. the Formation of Marine Snow by P-Poucheti. *Marine Ecology Progress Series*, 104(1-2), 153-161.
- Peter, K. H., and Sommer, U. (2013). Phytoplankton cell size reduction in response to warming mediated by nutrient limitation. *PloS one*, 8(9), e71528.
- Pingree, R. D., Pugh, P. R., Holligan, P. I., and Forster, G. R. (1975). Summer phytoplankton blooms and red tides along tidal fronts in the approaches to the English Channel. *Nature*, 258(5537), 672-677.
- Piontek, J., Händel, N., Langer, G., Wohlers, J., Riebesell, U., and Engel, A. (2009). Effects of rising temperature on the formation and microbial degradation of marine diatom aggregates. *Aquatic Microbial Ecology*, 54, 305-318.
- Pocklington, R., and Tan, F. C. (1987). Seasonal and annual variations in the organic matter contributed by the St Lawrence River to the Gulf of St. Lawrence. *Geochimica et Cosmochimica Acta*, 51(9), 2579-2586.
- Pocklington, R. (1988). Organic matter in the Gulf of St. Lawrence. *Canadian Bulletin of Fisheries and Aquatic Science CBFSDB*, 220.
- Polyakov, I. V., Timokhov, L. A., Alexeev, V. A., Bacon, S., Dmitrenko, I. A., Fortier, L., and Laxon, S. (2010). Arctic Ocean warming contributes to reduced polar ice cap. *Journal of Physical Oceanography*, 40(12), 2743-2756.
- Quiroz, N. G. A., Hung, C. C., & Santschi, P. H. (2006). Binding of thorium (IV) to carboxylate, phosphate and sulfate functional groups from marine exopolymeric substances (EPS). *Marine Chemistry*, 100(3), 337-353.
- Ramos, J. B., Müller, M. N., & Riebesell, U. (2010). Short-term response of the coccolithophore *Emiliania huxleyi* to an abrupt change in seawater carbon dioxide concentrations. *Biogeosciences*, 7, 177.
- Redfield, A. C. (1963). The influence of organisms on the composition of seawater. *The sea*, 2, 26-77.
- Riebesell, U., Schulz, K. G., Bellerby, R. G. J., Botros, M., Fritsche, P., Meyerhöfer, M., and Zöllner, E. (2007). Enhanced biological carbon consumption in a high CO₂ ocean. *Nature*, 450(7169), 545-548.
- Reinfelder, J. R. (2010). Carbon concentrating mechanisms in eukaryotic marine phytoplankton.
- Reinfelder, J. R. (2012). Carbon dioxide regulation of nitrogen and phosphorus in four species of marine phytoplankton. *Marine Ecology Progress Series*, 466, 57-67.
- Riebesell, U., Czerny, J., Bröckel, K. V., Boxhammer, T., Büdenbender, J., Deckelnick, M., and Ludwig, A. (2013). A mobile sea-going mesocosm system—new opportunities for ocean change research. *Biogeosciences*, 10(3), 1835-1847.

- Rich, J. H., Ducklow, H. W., and Kirchman, D. L. (1996). Concentrations and uptake of neutral monosaccharides along 140°W in the equatorial Pacific: Contribution of glucose to heterotrophic bacterial activity and the DOM flux. *Limnology and Oceanography*, 41, 595-604.
- Riebesell, U., Zondervan, I., Rost, B., Tortell, P. D., Zeebe, R. E., and Morel, F. M. (2000). Reduced calcification of marine plankton in response to increased atmospheric CO₂. *Nature*, 407(6802), 364-367.
- Riebesell, U., Schulz, K. G., Bellerby, R. G. J., Botros, M., Fritsche, P., Meyerhofer, M., Neill, C., Nondal, G., Oschlies, A., Wohlers, J., and E. Zollner. (2007). Enhanced biological carbon consumption in a high CO₂ ocean. *Nature*, 450(7169): 545-548.
- Robert-Baldo, G. L., Morris, M. J., and Byrne, R. H. (1985). Spectrophotometric determination of seawater pH using phenol red. *Analytical Chemistry*, 57(13), 2564-2567.
- Robitaille, J. (2015). Affaiblissement filamentaire dans l'Estuaire du Saint-Laurent: modèles quasi-géostrophiques vs observations (Doctoral dissertation, Université du Québec à Rimouski).
- Rost, B., Zondervan, I., and Wolf-Gladrow, D. (2008). Sensitivity of phytoplankton to future changes in ocean carbonate chemistry: current knowledge, contradictions and research directions. *Marine Ecology Progress Series*, 373, 227-237.
- Rost, B., Riebesell, U., Burkhardt, S., and Sultemeyer, D. (2003). Carbon acquisition of bloom-forming marine phytoplankton. *Limnol. Oceanogr.*, 48, 55-67.
- Sambrotto, R. N., Savidge, G., Robinson, C., Boyd, P., Takahashi, T., Karl, D. M., and Codispoti, L. (1993). Elevated consumption of carbon relative to nitrogen in the. *Nature*, 363, 20.
- Sebah, S., Fairfield, C., Ullrich, M. S., and Passow, U. (2014). Aggregation and sedimentation of Thalassiosira weissflogii (diatom) in a warmer and more acidified future ocean. *PloS one*, 9(11), e112379.
- Skoog, A., and Benner, R. (1997). Aldoses in various size fractions of marine organic matter: Implications for carbon cycling. *Limnology and Oceanography*, 42(8), 1803-1813.
- Smith, D. J., and Underwood, G. J. (2000). The production of extracellular carbohydrates by estuarine benthic diatoms: the effects of growth phase and light and dark treatment. *Journal of Phycology*, 36(2), 321-333.
- Solomon, S. (Ed.). (2007). Climate change 2007-the physical science basis: Working group I contribution to the fourth assessment report of the IPCC (Vol. 4). Cambridge University Press.
- Staats, N., Stal, L. J., and Mur, L. R. (2000). Exopolysaccharide production by the epipelagic diatom *Cylindrotheca closterium*: effects of nutrient conditions. *Journal of Experimental Marine Biology and Ecology*, 249(1), 13-27.
- Stammerjohn, S. E., Martinson, D. G., Smith, R. C., and Iannuzzi, R. A. (2008). Sea ice in the western Antarctic Peninsula region: Spatio-temporal variability from ecological and climate change perspectives. *Deep Sea Research Part II: Topical Studies in Oceanography*, 55(18), 2041-2058.
- Stammerjohn, S., Massom, R., Rind, D., and Martinson, D. (2012). Regions of rapid sea ice change: An inter-hemispheric seasonal comparison. *Geophysical Research Letters*, 39(6).
- Stoderegger, K. E., and Herndl, G. J. (1999). Production of exopolymer particles by marine bacterioplankton under contrasting turbulence conditions. *Marine Ecology Progress Series*, 189, 9-16.
- Stordal, M.C., Santschi, P.H., and Gill, G.A. (1996). Colloidal pumping: evidence for the coagulation process using natural colloids tagged with ²⁰³Hg. *Environ. Sci. Technol.*, 30, 3335 – 3340.
- Sun, H., Xia, Y., Paudel, O., Yang, X. R., and Sham, J. S. (2012). Chronic hypoxia-induced upregulation of Ca²⁺ activated Cl⁻ channel in pulmonary arterial myocytes: a mechanism contributing to enhanced vasoreactivity. *The Journal of physiology*, 590(15), 3507-3521.

- Tang, C. L. (1980). Mixing and circulation in the northwestern Gulf of St. Lawrence: A study of a buoyancy-driven current system. *Journal of Geophysical Research: Oceans*, 85(C5), 2787-2796.
- Tan, F. C., and Strain, P. M. (1983). Sources, sinks and distribution of organic carbon in the St. Lawrence Estuary, Canada. *Geochimica et Cosmochimica Acta*, 47(1), 125-132.
- Tanaka T. (1992). Phase transitions of gels. *ACS Symp. Ser.* 480 :1-21
- Taucher, J., Jones, J., James, A., Brzezinski, M. A., Carlson, C. A., Riebesell, U., and Passow, U. (2015). Combined effects of CO₂ and temperature on carbon uptake and partitioning by the marine diatoms *Thalassiosira weissflogii* and *Dactyliosolen fragilissimus*. *Limnology and Oceanography*, 60(3), 901-919.
- Taucher, J., Schulz, K. G., Dittmar, T., Sommer, U., Oschlies, A., and Riebesell, U. (2012). Enhanced carbon overconsumption in response to increasing temperatures during a mesocosm experiment. *Biogeosciences*, 9(9), 3531.
- Therriault, J. C., and Levasseur, M. (1985). Control of phytoplankton production in the lower St. Lawrence Estuary: Light and freshwater runoff. *Naturaliste Canadien*. 1985.
- Therriault, J. C., Legendre, L., and Demers, S. (1990). Oceanography and ecology of phytoplankton in the St. Lawrence Estuary. In *Oceanography of a Large-Scale Estuarine System*, 269-295. Springer, New York, NY.
- Thoisen, C., Riisgaard, K., Lundholm, N., Nielsen, T. G., and Hansen, P. J. (2015). Effect of acidification on an Arctic phytoplankton community from Disko Bay, West Greenland. *Marine Ecology Progress Series*, 520, 21-34.
- Thornton, D. (2002). Diatom aggregation in the sea: mechanisms and ecological implications. *European Journal of Phycology*, 37(2), 149-161.
- Thornton, D. C., and Thake, B. (1998). Effect of temperature on the aggregation of *Skeletonema costatum* (Bacillariophyceae) and the implication for carbon flux in coastal waters. *Marine Ecology Progress Series*, 223-231.
- Tortell, P. D., Payne, C., Gueguen, C., Li, Y., Strzepek, R. F., Boyd, P. W., and Rost, B. (2008a). Uptake and assimilation of inorganic carbon by Southern Ocean phytoplankton. *Limnology and Oceanography*, 53 (4) 1278, 53(4), 1266-1278.
- Tortell, P. D., Payne, C. D., Li, Y., Trimborn, S., Rost, B., Smith, W. O., and DiTullio, G. R. (2008b). CO₂ sensitivity of Southern Ocean phytoplankton. *Geophysical Research Letters*, 35(4).
- Tortell, P. D., DiTullio, G. R., Sigman, D. M., and Morel, F. M. (2002). CO₂ effects on taxonomic composition and nutrient utilization in an Equatorial Pacific phytoplankton assemblage. *Marine Ecology Progress Series*, 236, 37-43.
- Traganza, E. D., Redalje, D. G., and Garwood, R. W. (1987). Chemical flux, mixed layer entrainment and phytoplankton blooms at upwelling fronts in the California coastal zone. *Continental Shelf Research*, 7(1), 89-105.
- Tyler, M. A., and Seliger, H. H. (1978). Annual subsurface transport of a red tide dinoflagellate to its bloom area: water circulation patterns and organism distributions in the Chesapeake Bay. *Limnology and Oceanography*, 23(2), 227-246.
- Underwood, G. J., Boulcott, M., Raines, C. A., and Waldron, K. (2004). Environmental effects on exopolymer production by marine benthic diatoms: dynamics, changes in composition, and pathways of production1. *Journal of Phycology*, 40(2), 293-304.
- Urbani, R., Magaletti, E., Sist, P., and Cicero, A. M. (2005). Extracellular carbohydrates released by the marine diatoms *Cylindrotheca closterium*, *Thalassiosira pseudonana* and *Skeletonema costatum*: Effect of P-depletion and growth status. *Science of the Total Environment*, 353(1), 300-306.
- Van Oostende, N., Moerdijk-Poortvliet, T. C., Boschker, H. T., Vyverman, W., and Sabbe, K. (2013). Release of dissolved carbohydrates by *Emiliania huxleyi* and formation of transparent

exopolymer particles depend on algal life cycle and bacterial activity. *Environmental microbiology*, 15(5), 1514-1531.

- Verdugo, P., Alldredge, A. L., Azam, F., Kirchman, D. L., Passow, U., and Santschi, P. H. (2004). The oceanic gel phase: a bridge in the DOM–POM continuum. *Marine Chemistry*, 92(1), 67-85.
- Verdugo, P., 2012. *Marine Microgels*. *Ann. Rev. Mar. Sci.*, 4(1): 375-400.
- Verdugo, P., and Santschi, P. H. (2010). Polymer dynamics of DOC networks and gel formation in seawater. *Deep Sea Research Part II: Topical Studies in Oceanography*, 57(16), 1486-1493.
- Verdugo, P., Alldredge, A. L., Azam, F., Kirchman, D. L., Passow, U., and Santschi, P. H. (2004). The oceanic gel phase: a bridge in the DOM–POM continuum. *Marine Chemistry*, 92(1), 67-85.
- Villacorte, L. O., Kennedy, M. D., Amy, G. L., and Schippers, J. C. (2009). The fate of transparent exopolymer particles (TEP) in integrated membrane systems: removal through pre-treatment processes and deposition on reverse osmosis membranes. *Water research*, 43(20), 5039-5052.
- Villacorte, L. O., Ekowati, Y., Winters, H., Amy, G. L., Schippers, J. C., and Kennedy, M. D. (2013). Characterisation of transparent exopolymer particles (TEP) produced during algal bloom: a membrane treatment perspective. *Desalination and Water Treatment*, 51(4-6), 1021-1033.
- Wedborg, M., Persson, T., & Larsson, T. (2007). On the distribution of UV-blue fluorescent organic matter in the Southern Ocean. *Deep Sea Research Part I: Oceanographic Research Papers*, 54(11), 1957-1971.
- Wells, M. L., and Goldberg, E. D. (1992). Marine submicron particles. *Marine Chemistry*, 40(1-2), 5-18.
- Wells, M.L., Goldberg, E. (1992). Occurrence of small colloids in seawater. *Nature* 353, 342–344.
- Wetz, M. S., Robbins, M. C., and Paerl, H. W. (2009). Transparent exopolymer particles (TEP) in a river-dominated estuary: spatial-temporal distributions and an assessment of controls upon TEP formation. *Estuaries and coasts*, 32(3), 447-455.
- Wetz, M. S., and Wheeler, P. A. (2007). Release of dissolved organic matter by coastal diatoms. *Limnology and Oceanography*, 52(2), 798-807.
- White, P. A., Kalf, J., Rasmussen, J. B., and Gasol, J. M. (1991). The effect of temperature and algal biomass on bacterial production and specific growth rate in freshwater and marine habitats. *Microbial ecology*, 21(1), 99-118.
- Wotton, R. S. (2004). The ubiquity and many roles of exopolymers (EPS) in aquatic systems. *Scientia marina*, 68(S1), 13-21.
- Wurl, O., and Holmes, M. (2008). The gelatinous nature of the sea-surface microlayer. *Marine Chemistry*, 110(1), 89-97.
- Yang, L., and Zhang, L. M. (2009). Chemical structural and chain conformational characterization of some bioactive polysaccharides isolated from natural sources. *Carbohydrate polymers*, 76(3), 349-361.
- Yang, G., and Gao, K. (2012). Physiological responses of the marine diatom *Thalassiosira pseudonana* to increased pCO₂ and seawater acidity. *Marine Environmental Research*, 79, 142-151.
- Zhou, J., Mopper, K., and Passow, U. (1998). The role of surface-active carbohydrates in the formation of transparent exopolymer particles by bubble adsorption of seawater. *Limnol.Oceanogr.*,43(8):1860-1871.

